

TECHNISCHE UNIVERSITÄT MÜNCHEN

Lehrstuhl II des Instituts für Organische Chemie und Biochemie
und Institute for Advanced Study at the Department Chemie

**Characterization of breast cancer cell lines overexpressing the urokinase
receptor splice variant uPAR-del4/5 or the GTP binding protein rab31**

Bettina Grismayer

Vollständiger Abdruck der von der Fakultät für Chemie der Technischen
Universität München zur Erlangung des akademischen Grades eines

Doktors der Naturwissenschaften (Dr. rer. nat.)

genehmigten Dissertation.

Vorsitzender: Univ.-Prof. Dr. S. Glaser

Prüfer der Dissertation:

1. Univ.-Prof. Dr. Dr. h.c. H. Kessler
2. apl. Prof. Dr. V. Magdolen

Die Dissertation wurde am 08.03.2012 bei der Technischen Universität München
eingereicht und durch die Fakultät für Chemie am 19.04.2012 angenommen.

Meinen Eltern

Abbreviations

Ab	antibody
AGO	Arbeitsgemeinschaft Gynaekologische Onkologie
APS	ammonium persulfate
ASCO	American Society for Clinical Oncology
ATF	amino-terminal fragment
ATP	adenosine triphosphate
bak	bcl-2 homologous antagonist killer
bax	bcl-2-associated X protein
bp	base pairs
BLAST	basic local alignment search tool
BSA	bovine serum albumin
Ca ²⁺	calcium
Cat	catching Ab
CD	cation-dependent
Cdc42	cell division control protein 42
cDNA	complementary DNA
CI	cation-independent
CLSM	confocal laser-scanning microscopy
Col I	collagen type I
Col IV	collagen type IV
D1	domain I of uPAR
D2	domain II of uPAR
D3	domain III of uPAR
Det	detection Ab
DMEM	Dulbecco's modified eagle medium
DMFS	distant metastasis free survival
DMSO	dimethylsulfoxide
DNA	deoxyribonucleic acid
dNTP	deoxyribonucleic triphosphate
ECM	extracellular matrix

EDTA	ethylenediaminetetraacetic acid
EEA1	early endosome antigen 1
EGF	epidermal growth factor
EGFR	epidermal growth factor receptor
ELISA	enzyme-linked immunosorbent assay
ER	endoplasmatic reticulum
ER-positive	estrogen receptor positive
Erk1/2	extracellular signal regulated kinases 1/2 (MAPK)
FACS	fluorescence-activated cell sorting
FAK	tyrosine kinase focal adhesion kinase
FCS	foetal calf serum
Fig	figure
FN	fibronectin
G418	geneticin
GAM	growth arrest medium
GAP	GTPase activating proteins
GAPDH	glyceraldehyde 3-phosphate dehydrogenase
GDI	GDP-dissociation inhibitor
GDP	guanosine diphosphate
GEF	GDP-GTP exchange factors
Gly	glycine
GPI	glycosylphosphatidylinositol
GST	glutathione S-transferase
GTP	guanosine triphosphate
HB region	helical bundle region
HEPES	(4-(2-hydroxyethyl)-1-piperazineethanesulfonic acid
His	histidine
HPRT	hypoxanthine-guanine-phosphoribosyl-transferase
HRP	horse radish peroxidase
IgG	immunoglobulin G

IgY	immunoglobulin Y
h	hour
ICC	immunocytochemistry
IGF-II	insulin-like growth factor II
JAK	janus kinase
kDa	kilo Dalton
LNN	lymphnode-negative
LRP1	LDL receptor related protein 1
Lys	lysine
Ln	laminin
LZ	<i>lacZ</i> -gene tag
mAb	monoclonal antibody
Man-6-P	mannose-6-phosphate
MAPK	mitogen-activated protein kinase
Mg ²⁺	magnesium
mM	milli Molar
MMP	matrixmetalloprotease
MPR	mannose-6-phosphate receptor
mRNA	messenger ribonucleic acid
NGF	nerve growth factor
nm	nanometer
nM	nano Molar
OD	optical density
OS	overall survival
p	phosphate group
pAb	polyclonal antibody
PAI-1	plasminogen activator inhibitor 1
PAI-2	plasminogen activator inhibitor 2
PBS	phosphate-buffered saline
PCR	polymerase chain reaction
PDGF	platelet-derived growth factor
PFA	paraformaldehyde

PI3K	phosphatidylinositol 3-kinase
PVDF	polyvinylidene difluoride
QPCR	quantitative real time PCR
REP	Rab escort proteins
RIN	Ras and Rab interactor
RT	room temperature
SDS	sodium dodecyl sulfate
SDS-PAGE	sodium dodecyl sulfate polyacrylamide gel electrophoresis
SMB	somatomedin B domain
STAT	signal transducer and activator of transcription
TBS	Tris-buffered saline
TIMP	tissue inhibitor of metalloproteases
TMB	3,3',5,5'-Tetramethylbenzidine
tPA	tissue-type plasminogen activator
TGN	trans-Golgi network
Tris	Tris-(hydroxymethyl)-aminomethan
uPA	urokinase-type plasminogen activator
uPAR	urokinase receptor
uPAR-del4/5	urokinase receptor splice variant with deletion of exon 4 and 5
uPAR-del5	urokinase receptor splice variant with deletion of exon 5
VN	vitronectin
v/v	volume/volume
WT	wild type
w/v	weight/volume
XGal	5-bromo-4-chloro-3-indolyl-beta-D-galactopyranoside

1 Abstract	1
2 Introduction	3
2.1 Cancer.....	3
2.2 Cancer metastasis.....	4
2.3 The urokinase-system	5
2.4 The urokinase receptor uPAR (CD87).....	6
2.4.1 uPAR and cell signaling.....	9
2.4.2 Interaction of uPAR with integrins	10
2.4.3 uPAR expression and disease	11
2.5 uPAR mRNA variants and uPAR-del4/5.....	12
2.6 uPAR-del4/5 as a prognostic marker for breast cancer.....	13
2.7 Rab31 as a prognostic marker for breast cancer.....	15
2.8 Rab GTPases.....	17
2.8.1 Rab GTPases in membrane trafficking.....	17
2.8.2 Regulation of Rab proteins	18
2.8.3 Structure of Rab proteins.....	20
2.8.4 Rab proteins and cancer	23
2.9 Rab31 (rab22B).....	24
2.9.1 Rab31 structure and intracellular localization	24
2.9.2 Rab31 interacting proteins.....	25
2.9.3 Rab31 functions	27
3 Aims of the study	29
4 Material	30
4.1 Eukaryotic cell lines.....	30
4.2 Growth media for eukaryotic cells	30
4.3 Enzymes, proteins and electrophoresis ladders	31

4.4 Antibodies.....	32
4.5 Technical devices.....	33
4.6 Expendable materials.....	35
4.7 Chemicals and reagents.....	36
4.8 Buffers and solutions.....	38
4.9 Kits.....	40
4.10 Primer.....	40
5 Methods.....	41
5.1 Cell culture.....	41
5.1.1 Cultivation of eukaryotic cells.....	41
5.1.2 Storing and thawing.....	41
5.1.3 Stable transfection and selection of single clones.....	42
5.1.4 Detection of mycoplasma contamination.....	43
5.2 Cellular assays in vitro.....	44
5.2.1 Cell proliferation.....	44
5.2.2 Cellular adhesion.....	45
5.2.3 Cellular invasion through matrigel™.....	46
5.3 Xenograft mouse model.....	46
5.4 Immunocytochemical staining.....	47
5.5 Flow cytometry.....	47
5.6 Western blot analysis.....	48
5.6.1 Cell lysis without phosphatase inhibitors.....	48
5.6.2 Cell lysis with phosphatase inhibitors.....	48
5.6.3 Western blot.....	48
5.7 Enzyme-linked immunosorbent assay (ELISA).....	49
5.8 Zymography of metalloproteases.....	50
5.9 Immunohistochemistry.....	51

5.10 Quantitative real time PCR	51
5.11 Statistical analysis	52
6 Results	53
6.1 Characterization of breast cancer cell lines overexpressing uPAR-del4/5	53
6.1.1 Stable transfection of breast cancer cell lines	53
6.1.2 Proliferation of breast cancer cell lines overexpressing uPAR-del4/5	61
6.1.3 Adhesion of uPAR-del4/5 overexpressing breast cancer cell lines to extracellular matrix proteins.....	63
6.1.4 Invasive capacity of breast cancer cells overexpressing uPAR-del4/5.....	68
6.1.5 Effects of uPAR-del4/5 overexpressing MDA-MB-231 cells on lung colonisation in a xenograft mouse model	70
6.2 Characterization of polyclonal antibodies directed against rab31	73
6.2.1 Specificity of rab31 directed antibodies in immunocytochemical (ICC) staining.....	73
6.2.2 Cross-reactivity of rab31 directed antibodies.....	75
6.2.3 Pre-selection of rab31 antibodies for the development of a rab31-ELISA format	77
6.2.4 Immunohistochemical staining of breast cancer tissue	79
6.3 Characterization of breast cancer cell lines overexpressing rab31.....	81
6.3.1 Selection of breast cancer cell lines	81
6.3.2 Stable transfection of breast cancer cell lines	81
6.3.3 Proliferation of breast cancer cell lines overexpressing rab31.....	87
6.3.4 Adhesion to extracellular matrix proteins.....	92
6.3.5 Matrigel™ invasion assay.....	99
6.3.6 Effects of rab31 overexpressing MDA-MB-231 cells on lung metastasis in a xenograft mouse model.....	101
6.4 Modulated matrixmetalloprotease (MMP) expression of MDA-MB-231 cells	102
6.5 The extracellular signal-regulated kinase 1 and 2 (Erk1/2).....	104
6.6 EGFR signaling in rab31 overexpressing MDA-MB-231 cells	106

7 Discussion	108
7.1 Characterization of breast cancer cell lines overexpressing uPAR-del4/5 ...	108
7.2 Characterization of breast cancer cell lines overexpressing rab31.....	115
7.3 Link between uPAR-del4/5 and rab31	121
7.4 Conclusion.....	123
8 References.....	124
9 Appendix.....	135

1 Abstract

The receptor for the tumor-associated serine protease uPA, uPAR consists of three structurally homologous domains (D1-D3). The splice variant uPAR-del4/5 is a urokinase receptor form which lacks domain D2. uPAR-del4/5 mRNA has been shown to be an independent prognostic factor for distant metastasis-free survival (DMFS) in node-negative breast cancer patients. Using microarray analysis, several genes, including rab31, were found to be up-regulated in breast tumor samples with high uPAR-del4/5 mRNA expression. Quantitative analysis of mRNA expression in 280 patients demonstrated that high rab31 mRNA values were significantly associated, independent from uPAR-del4/5, with a poor DMFS outcome in breast cancer. Rab31 is a member of the Rab family of small GTP-binding proteins involved in intracellular transport, signal transduction and receptor internalization / recycling.

To analyze *in vitro* the effects of uPAR-del4/5 and rab31 overexpression, respectively, three different breast cancer cell lines (MDA-MB-231, CAMA-1 and MDA-MB-435) were stably transfected with expression plasmids encoding uPAR-del4/5 or rab31, respectively. In addition, single clones with high, medium or low expression levels of both proteins were selected to check whether the observed effects are dose-dependent.

The stably transfected cell lines were analyzed *in vitro* regarding proliferation, invasive capacity through matrigelTM and cell adhesion on several extracellular matrix proteins. Furthermore, metastatic behavior was analyzed in a xenograft mouse model. In two out of three investigated breast cancer cells lines no significant changes in proliferation were monitored when uPAR-del4/5 was overexpressed. Only stably transfected MDA-MB-435 cells showed enhanced proliferation upon overexpression of the splice variant. In contrast to this, all breast cancer cell lines overexpressing rab31 displayed a significantly increased proliferation rate. The adhesive capacity to extracellular matrix proteins turned out to be reduced in a dose-dependent manner in all investigated breast cancer cell lines overexpressing uPAR-del4/5 or rab31. Further experiments with MDA-MB-

231 cells, revealed that the overexpression of the uPAR splice variant as well as the overexpression of rab31, causes a reduction of invasive capacity through matrigelTM in a dose-dependent manner. These results are in line with the obtained *in vivo* data. MDA-MB-231 cells stably transfected with uPAR-del4/5 or rab31, respectively were injected into the tail vein of immunodeficient nude mice in order to investigate the spreading of cancer cells to the lungs. In both cases, the number of lung metastasis was significantly reduced upon overexpression of uPAR-del4/5 or rab31.

These results demonstrate that uPAR-del4/5 and rab31 not only represent independent prognostic markers in breast cancer, but affect tumor-biologically relevant processes in a similar manner. Thus, these factors may be components of different, but possibly associated, tumor-relevant signaling pathways.

2 Introduction

2.1 Cancer

Cancer is the leading cause of death worldwide. In 2008, 7.6 million people died from cancer, this are about 13 % of all deaths worldwide (www.who.int). There are more than 100 distinct types of cancer, and subtypes of tumors can be found within specific organs.

Hanahan and Weinberg described six essential alterations in cell physiology that collectively dictate malignant growth, as the hallmarks of cancer.

- self-sufficiency in growth signals
- insensitivity to anti-growth signals
- evasion of programmed cell death (apoptosis)
- limit-less replicative potential
- sustained angiogenesis
- tissue invasion and metastasis (Hanahan et al. 2000).

Recently, two new aspects were added. These are the ability of cells, to re-program their energy metabolism, and to evade destruction by immune cells (Hanahan et al. 2011).

In addition to cancer cells, tumors exhibit another dimension of complexity. They contain a repertoire of recruited, apparent normal cells that contribute to the acquisition of hallmark traits by creating the “tumor microenvironment” (Hanahan et al. 2011).

Breast cancer is the most common cancer in women and the entity with the highest mortality rate (www.rki.de). Breast cancer strikes one out of 8-10 women once in her life. Well known prognostic factors for breast cancer include the hormone receptor status (estrogen receptor, progesterone receptor), the oncoprotein Her2, and the metastasis status of the lymphnodes (de Bock et al. 2004). By the end of 2007, components of the urokinase-system, uPA and PAI-1 were recommended for clinical utility by the American Society for Clinical Oncology (ASCO) and the German Arbeitsgemeinschaft Gynaekologische

Onkologie (AGO) (Mengele et al. 2010). Now, in addition to the conventional prognostic/predictive biomarkers (estrogen receptor, progesterone receptor and Her2), uPA and PAI-1 are highly recommended for assessment of the risk of breast cancer patients to disease recurrence and to predict response to systemic adjuvant chemotherapy (Schmitt et al. 2010).

2.2 Cancer metastasis

Cancer metastasis results from a number of interdependent events. First of all, the cancer cells have to detach from their original localization and start to migrate. This is accompanied by concurrent invasion of the cancer cells into the surrounding tissue. This process requires adhesion to and subsequent degradation of extracellular matrix (ECM) components. In the following steps of cancer metastasis, the cells enter the blood and lymphatic vessels and spread through out the whole body. In order to form metastasis at distant sites of the organism, the cancer cells have to adhere to and invade through the endothelium (Andreasen et al. 1997).

Extracellular proteolytic enzymes like serine proteinases and metalloproteinases are major players in cancer metastasis. The release of proteolytic enzymes into the tumor environment leads to the degradation of the basement membrane and the extracellular matrix. This enables cancer cells to invade into the surrounding normal tissue (Andreasen et al. 1997). The analysis of many different human cancers has shown that high levels of uPA and/or PAI-1 in tumor tissue is correlated with a poor prognosis of the patients in a variety of cancer types including breast cancer (Andreasen et al. 1997; Duffy et al. 2004).

2.3 The urokinase-system

The urokinase-system plays an important role in thrombolysis, inflammation, fertility, cell migration, tissue re-modelling and in cancer invasion, and vascularisation (Montuori et al. 2005). The relationship between the urokinase-system and tumor biology is complex. It involves several important steps like cell proliferation, apoptosis, cell migration, invasion, and angiogenesis. In all these steps, one or more components of the urokinase-system are involved (McMahon et al. 2008).

There are two types of plasminogen activators, the urokinase-type (uPA) and the tissue-type (tPA). Both can catalyze the conversion of plasminogen into plasmin. But each of them has a distinct site of operation. The primary function of tPA is to generate plasmin for thrombolysis, while uPA mainly generates plasmin for matrix degradation (Andreasen et al. 1997).

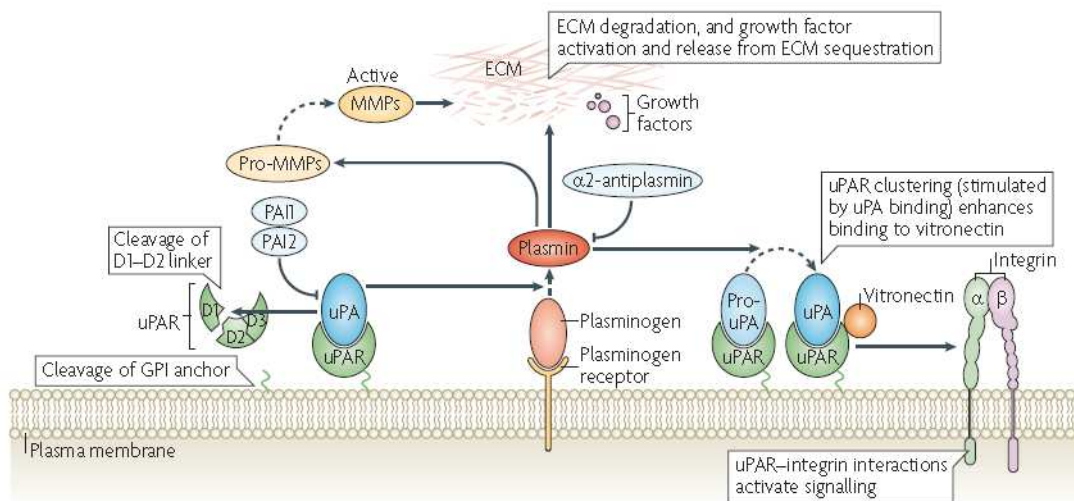


Fig. 1 Scheme of the urokinase-system

The urokinase receptor uPAR binds uPA in its active and zymogen form. uPA (receptor bound or secreted) catalyzes the conversion of plasminogen into plasmin, which in turn can activate pro-uPA. Furthermore plasmin cleaves and activates metalloproteases (MMPs). Plasmin and MMPs degrade many extracellular matrix (ECM) components but also activate proliferation signaling cascades like TGF- β 1 (Duffy et al. 2004). The activity of uPA and plasmin are antagonized by PAI-1, PAI-2 and α 2-antiplasmin. uPA binding stimulates clustering of uPAR in the plasma membrane and increases its ability to bind vitronectin (VN). The receptor uPAR can be cleaved by uPA in the linker between D1 and D2, generating a soluble D1 fragment and a membrane bound D2-D3 fragment. uPA can no longer bind the receptors, thereby inactivating the function of uPAR in proteolysis and cell signaling. Both full-length uPAR and D2-D3 can be shed through removal of the GPI-anchor by proteases or phospholipases (Smith et al. 2010).

The urokinase receptor uPAR can bind both, the serine protease uPA and its zymogen form, pro-uPA. Activated uPA cleaves the zymogen plasminogen, converting it into the active proteinase plasmin. Plasmin cleaves a range of ECM components, and is essential for the degradation and clearance of fibrin clots (fibrinolysis). Fibrinolytic functions of plasmin are mainly activated by tPA. Furthermore, it activates matrixmetalloproteases (MMPs) such as MMP3, MMP9, MMP12 and MMP13, leading to the degradation of proteins in basement membranes and the ECM. This facilitates cancer cell invasion into the surrounding tissue. Because uPAR is associated with the external surface of the plasma membrane by a glycosylphosphatidylinositol (GPI)-anchor, the receptor focuses the proteolytic activity to the cell surface. In addition to MMP activation and matrix degradation, plasmin can act in a positive feedback loop and cleave pro-uPA into its active form uPA. The plasminogen activation system is negatively regulated by the plasminogen activator inhibitor 1 (PAI-1) and PAI-2, which inhibit uPA, and by α 2-antiplasmin and α 2-macroglobulin, which inhibit plasmin (Smith et al. 2010; Andreasen et al. 2000; Mengele et al. 2010).

2.4 The urokinase receptor uPAR (CD87)

The urokinase receptor (CD87) is a 50-60 kDa, highly glycosylated protein linked to the cell membrane *via* its GPI-tail. Deglycosylation decreases its molecular weight to 35 kDa (Ploug et al. 1994).

uPAR is synthesized as a single polypeptide chain of 335 amino acids containing 28 cysteine residues, with a 22 amino acids signal peptide. Posttranslational events lead to the cleavage of the last 30 carboxy-terminal residues and to the attachment of a GPI-tail to Gly283, that anchors the receptor to the cell surface (Montuori et al. 2005; Ploug et al. 1991).

The receptor is composed of three similarly sized (about 90 residues each), homologous domains. The domains are designated D1, D2 and D3, as numbered from the N-terminus. The three domains are connected by short linker regions (Montuori et al. 2005; Behrendt et al. 1991).

Due to its cysteine pattern, the receptor was ascribed to the Lys6/uPAR/ α -neurotoxin protein domain family, which adopt a so called three-finger fold (Ploug et al. 1994; Llinas et al. 2005). In uPAR, each of the three-finger fold domains forms a globular structure with 5-6 antiparallel β -strands linked by 4-5 disulphide bonds (Smith et al. 2010).

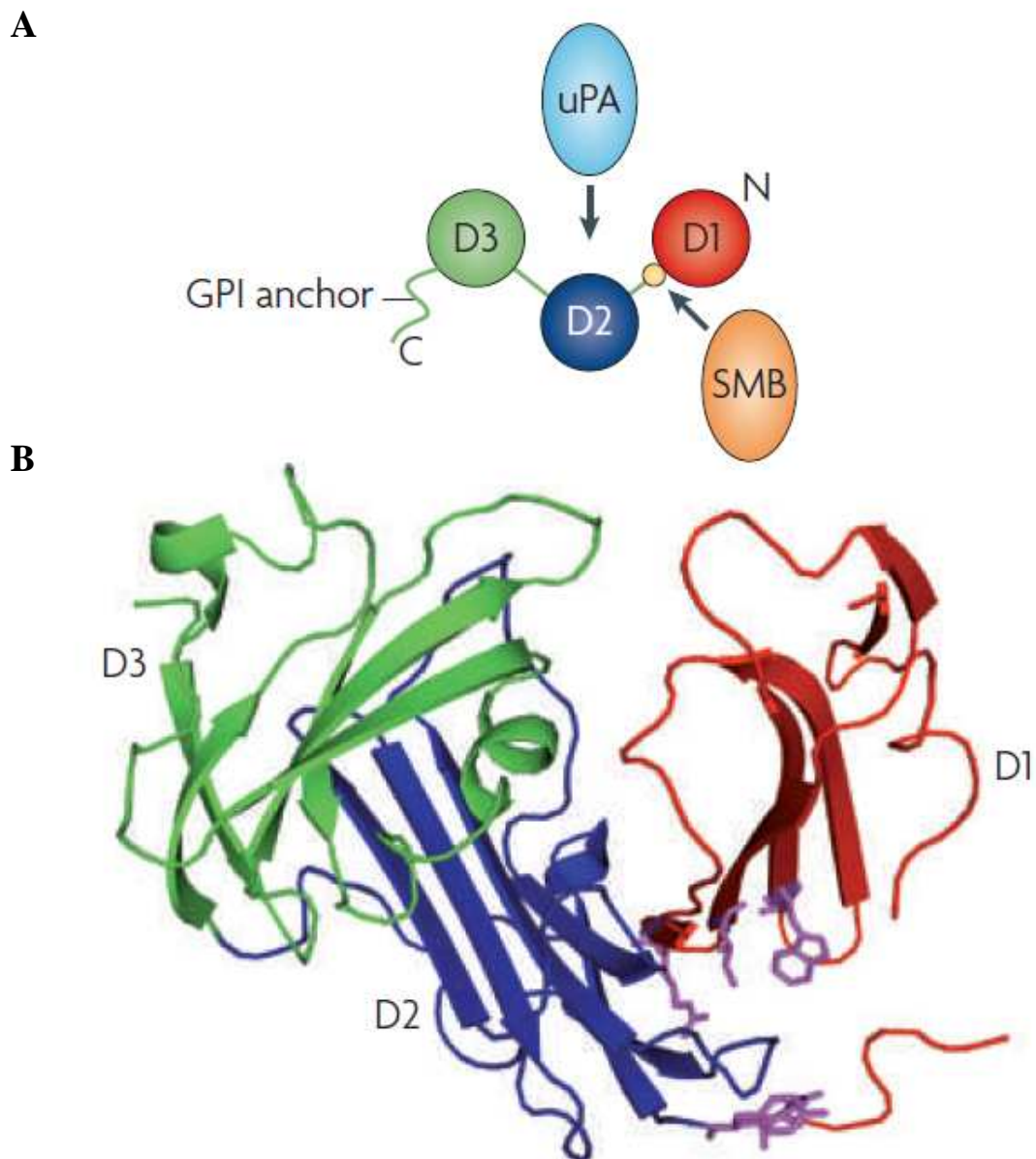


Fig. 2 Structure of uPAR

A Scheme of the uPAR structure indicating the C-terminal GPI-anchor and the three three-finger-fold domains (D1-D3). The binding sites for uPA *via* its amino-terminal fragment (ATF) and the vitronectin binding site *via* its somatomedin B (SMB) domain are indicated by arrows. **B** The three-dimensional structure of uPAR, domains D1-D3 are indicated in the same color like in A. Residues for vitronectin binding are coloured in purple. The uPA binding site is within the concave structure formed by the three globular β -sheet containing domains D1-D3 (Smith et al. 2010).

Llinas et al. solved the crystal structure of a soluble form of human uPAR at 2.7Å resolution with an inhibitory peptide of uPA-uPAR interaction (Llinas et al. 2005). This structure shows, how the three domains pack together into a concave structure (Fig. 2). The domains are organized in a circular manner. This generates a deep internal cavity and a large external surface (Tang et al. 2008). uPAR binds uPA at its amino-terminal growth factor domain in the central cavity, this binding includes residues from all three domains (Smith et al. 2010). The vitronectin-binding site of uPAR is found in D1 and in the D1-D2 linker. uPAR binds to vitronectin in its N-terminal somatomedin B (SMB) domain (Smith et al. 2010; Madsen et al. 2008).

Because vitronectin and uPA have diverse binding sites, uPAR can simultaneously bind both ligands. Furthermore, interaction of uPA with uPAR increases vitronectin binding by uPAR. This allows the coordinated regulation of proteolysis, cell adhesion and signaling (Smith et al. 2010).

Up to now many variants of the urokinase receptor have been described. Soluble uPAR variants, lacking the GPI-anchor, have been detected in conditioned medium from some cell lines and in ascites from ovarian cancer patients (Andreasen et al. 1997).

The three uPAR domains are connected by short linker regions. The D1-D2 linker region exhibits a high proteolytic sensitivity. *In vitro*, uPAR was shown to be cleaved by several enzymes, such as trypsin, chymotrypsin, elastase, cathepsin-G, metalloproteases, and by plasmin and uPA itself (Ragno 2006; Beaufort et al. 2004). Cleavage in the D1-D2 linker region creates a soluble D1 fragment and a D2-D3 fragment that can be either membrane associated or shed (Hoyer-Hansen et al. 1992). Full-length or cleaved uPAR is released from the membrane as a consequence of GPI-anchor removal by glycosylphosphatidyl-inositol-specific phospholipase C or D, or through extracellular proteolytic cleavage (Smith et al. 2010; Montuori et al. 2005).

uPAR is efficiently internalized *via* clathrin coated pits. PAI-1 binds covalently to urokinase receptor bound uPA, this inhibits the enzymatic activity of urokinase. This ternary complex uPAR:uPA:PAI-1 associates with LDL receptor related

protein 1 (LRP1) or other members of the LDL receptor family, and is sequestered into clathrin coated pits. This leads to the degradation of the uPA:PAI-1 complexes in the lysosome and the subsequent recycling of at least parts of uPAR to the cell surface (Czekay et al. 2001). Cortese et al. describe another uPA:PAI-1 and LDL receptor independent mechanism of uPAR internalization which is similar to macropinocytosis. This process, which leads to a rapid recycling of the urokinase receptor to the plasma membrane, does not require ligand binding and LRP-1 association. Moreover, it is independent from the activity of regulatory proteins such as members of the Rho GTPase family (RhoA, Rac1 and Cdc42) and phosphatidylinositide3-kinase (PI3K), which are usually involved in macropinocytosis. Constitutively endocytosed uPAR is found in early endosome antigen 1 (EEA1) positive early/recycling endosomes but does not reach lysosomes in the absence of ligands (Cortese et al. 2008).

2.4.1 uPAR and cell signaling

In addition to its proteolytic properties uPA also exerts several other important biological effects in a non-proteolytic manner. These functions are largely related to the regulation of the interactions between the cell and the surrounding matrix. uPAR can act as a signaling receptor that modulates cell adhesion, migration, and proliferation through interactions with other membrane proteins like integrins, epidermal growth factor receptor (EGFR), G protein-coupled receptors and the extracellular matrix protein vitronectin (Tang et al. 2008; Blasi et al. 2010). Its molecular properties and structure are largely responsible for conferring this versatile role. The active molecular complex may be a trimeric uPA-uPAR₂ complex (Blasi et al. 2002). Also, uPAR signaling can be induced by uPA binding to uPAR, it is independent of the proteolytic activity of uPA (Smith et al. 2010).

As already mentioned, uPAR is a receptor for uPA and VN. As a GPI-anchored receptor, uPAR lacks transmembrane and intracellular domains and is therefore incapable of transducing intracellular signals on its own (Tang et al. 2008). Like other GPI-anchored proteins, uPAR associates with cholesterol- and sphingolipid-rich membrane microdomains named 'lipid rafts'. These are important platforms for

signal transduction. Accumulation of the receptor in lipid rafts might increase protein-protein interactions with its co-receptors and intracellular effectors. This can lead to an enhanced downstream signaling (Smith et al. 2010).

Signaling through uPAR and its interacting proteins activates the Ras-mitogen-activated protein kinase (MAPK) pathway, the tyrosine kinases focal adhesion kinase (FAK also known as PTK2), Src and the small GTPase Rac, which belongs to the Rho family (Smith et al. 2010). Other pathways such as janus kinase (JAK)-signal transducer and activator of transcription (STAT) as well as PI3K-Akt, have also been implicated in uPAR signaling (Smith et al. 2010).

2.4.2 Interaction of uPAR with integrins

Integrins are hetero-dimeric cell surface receptors that interact for example with fibronectin, vitronectin, laminin, fibrin and collagens (Reuning et al. 2003). Binding of integrins to these proteins anchors the cells to the ECM. As a membrane-spanning receptor integrins harbor a cytoplasmic-domain. The cytoplasmic-tail is linked to the cytoskeleton and can transduce signals between the extracellular environment and the cell interior (Reuning et al. 2003; Blasi et al. 2002). The interaction of integrins with molecules which regulate cytoskeletal organization as well as signal transduction has influence on cell shape, cell migration and intracellular signaling (Blasi et al. 2002). Therefore, direct integrin signaling and indirect modulation of integrin signaling pathways can alter ECM re-modelling, which can contribute to tumorigenesis (Tang et al. 2008).

Matrix-degradation by components of the urokinase-system alters the integrin-mediated interaction of ECM with the cytoskeleton (Bass et al. 2009). In addition to this, uPAR can affect ECM-integrin-interaction directly by binding to this cell surface receptor (Bass et al. 2009). As already mentioned, integrins are important proteins in the process of cellular migration. There are several studies indicating that uPA:uPAR interaction with integrins is necessary for cell migration. uPA-bound uPAR co-localizes/interacts with integrins which leads to enhanced migration of the cell. Furthermore, the interaction with uPAR was shown to alter phagocytosis, adhesion, protease secretion and proliferation (Chaurasia et al.

2006; Blasi et al. 2002). Direct interaction of uPAR with integrins is described for several members of the integrin subfamily, like for example $\alpha_5\beta_1$, $\alpha_v\beta_3$ and, $\alpha_v\beta_5$ (Bass et al. 2009; Blasi et al. 2010).

Only little is known about how the interaction between uPAR and integrins is regulated. Some reports indicate the necessity of the intact three domain structure of uPAR. Furthermore it was shown, that the interaction is enhanced by ligand binding to integrins as well as by uPA binding to uPAR (Blasi et al. 2010).

2.4.3 uPAR expression and disease

In the healthy organism, uPAR is moderately expressed in various tissues including lungs, kidney, spleen, vessels, uterus, bladder, thymus, heart, liver and testis. Strong uPAR expression is observed in organs undergoing extensive tissue re-modelling, such as trophoblast cells and migrating, but not resting, keratinocytes at the edge of wounds (Blasi et al. 2010). uPAR is expressed during ECM re-modelling, for example in gestational tissues during embryo implantation and placental development (Smith et al. 2010). The expression of uPAR is increased in many pathological conditions, in particular cancer, inflammation and infections (Blasi et al. 2002).

For instance, uPAR is expressed in the kidney during chronic proteinuric disease and in the central nervous system following ischaemia or trauma. uPAR expression is strongly induced during leukocyte activation and differentiation, suggesting a role in inflammatory and immune responses (Smith et al. 2010).

uPAR is overexpressed in human tumors including leukemias, breast cancer, lung, bladder, colon, liver, pleura, pancreas, and brain (Sidenius et al. 2003). Beside of uPA and PAI-1, an increase of uPAR is associated with tumor progression and with shortened disease-free and/or overall survival of patients with malignant solid tumors (Schmitt et al. 1997).

The expression of uPAR in normal breast tissue has been found to be either completely absent or at extremely low levels. In contrast to this, many tumor tissues have a high expression of uPAR. Furthermore, high expression of uPAR is found particularly at the advancing fronts of invasive breast carcinoma tumors and

in those epithelial cells protruding into the stroma. The presence of uPAR on the invasive front of breast cancer cells suggests that uPAR is the decisive feature for the role of the uPA-system in cancer cell invasion (de Bock et al. 2004).

2.5 uPAR mRNA variants and uPAR-del4/5

The human uPAR gene is located on the long arm of chromosome 19 (19q13). It is encoded by seven exons and six introns extending over 23 kb of genomic DNA (Ragno 2006). Exon 2/3, 4/5 and 6/7 encode for domain D1-D3 (Fig. 3). The 30 carboxy-terminal aminoacids are cleaved off posttranslationally, and the GPI-tail is linked at Gly283 (Ploug et al. 1991).

The presence of more than one mRNA variant, derived from the same gene is a common observation for a growing number of proteins (Mercatante et al. 2001). These variants can result either from alternative splicing or sustained intronic sequences. Furthermore, the utilization of alternative transcription initiation or polyadenylation sites can cause mRNA variants. During tumor progression, alterations of the splicing process can occur. Therefore, alternative splicing may play a major role in tumorigenesis. Especially for many cancer-associated genes, such as CD44, WT-1, survivin, mdm2, MUC-1, and VEGF a broad spectrum of alternatively and/or aberrantly spliced variants with different and often oncogenic functions have been identified. However, it is often unknown whether these mRNA variants are translated into protein (Luther et al. 2003).

Alternatively spliced forms of human uPAR mRNA lacking exon5 (uPAR-del5) were described by Casey et al. (Casey et al. 1994). Others describe the exchange of exon 7 for another final exon (Pyke et al. 1993). Whether some of these different uPAR fragments exert a tumor-associated biological role *in vivo* is still unknown (Luther et al. 2003).

Luther and coworkers analyzed non-malignant and malignant human cells, as well as breast cancer tissue with respect to the expression of alternatively spliced uPAR mRNA variants. Two splice variants were detected with high frequency. The exon 5 deletion variant uPAR-del5 and a variant, lacking both exon 4 and 5 named

uPAR-del4/5. Exon 4 and 5 encode for domain II of the urokinase receptor (Luther et al. 2003).

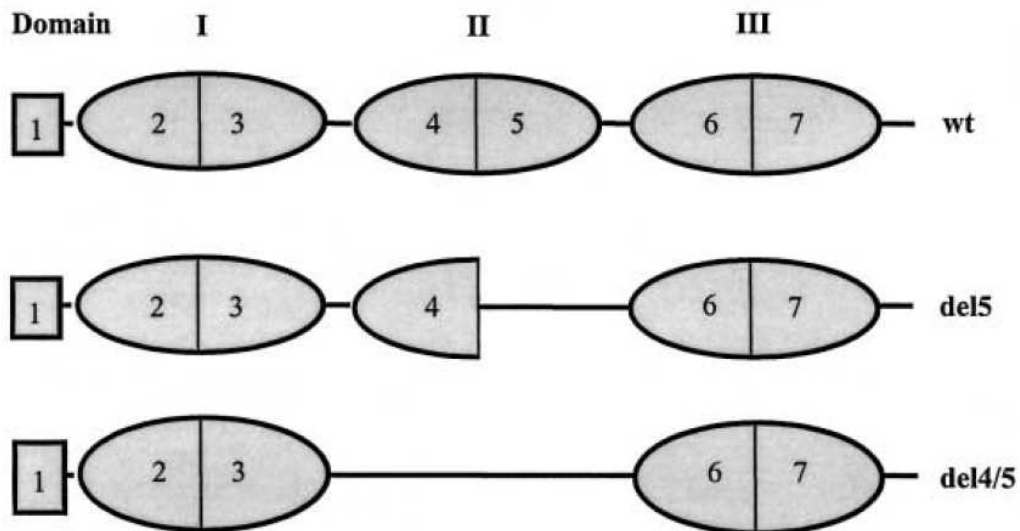


Fig. 3 Exon organization of different uPAR splice variants

The wt-receptor is composed of three homologous domains, each encoded by 2 exons. Exon 1 encodes for signal peptide sequence. Variant del5 is missing exon 5. del4/5 is missing exon 4 and 5, encoding D2 (Luther et al. 2003).

uPAR-del4/5 was found to be frequently present in cultured malignant human cells as well as in breast cancer tissue. The expression of soluble and GPI-linked uPAR-del4/5 in CHO cells, demonstrated that this splice variant is translated and posttranslationally processed (Luther et al. 2003).

2.6 uPAR-del4/5 as a prognostic marker for breast cancer

The splice variant uPAR-del4/5 was found to be overexpressed in tissue of breast cancer patients. uPAR-del4/5 is expressed independently of other uPAR variants and full-length uPAR. Up to now it can not be excluded that low levels of uPAR-del4/5 mRNA are also present in non-malignant cells. The first study of Luther et al., regarding expression and correlation of uPAR-del4/5 with the patients outcome, included node-negative and node-positive patients, many of them treated with adjuvant systemic therapy. In this study they could show, that a high

expression of uPAR-del4/5 mRNA is significantly associated with a short disease free survival of breast cancer patients (Luther et al. 2003).

In the second study the mRNA expression of uPAR-del4/5 was analyzed in a cohort of 280 tumor tissues from lymphnode-negative (LNN) breast cancer patients, who did not receive adjuvant systemic therapy.

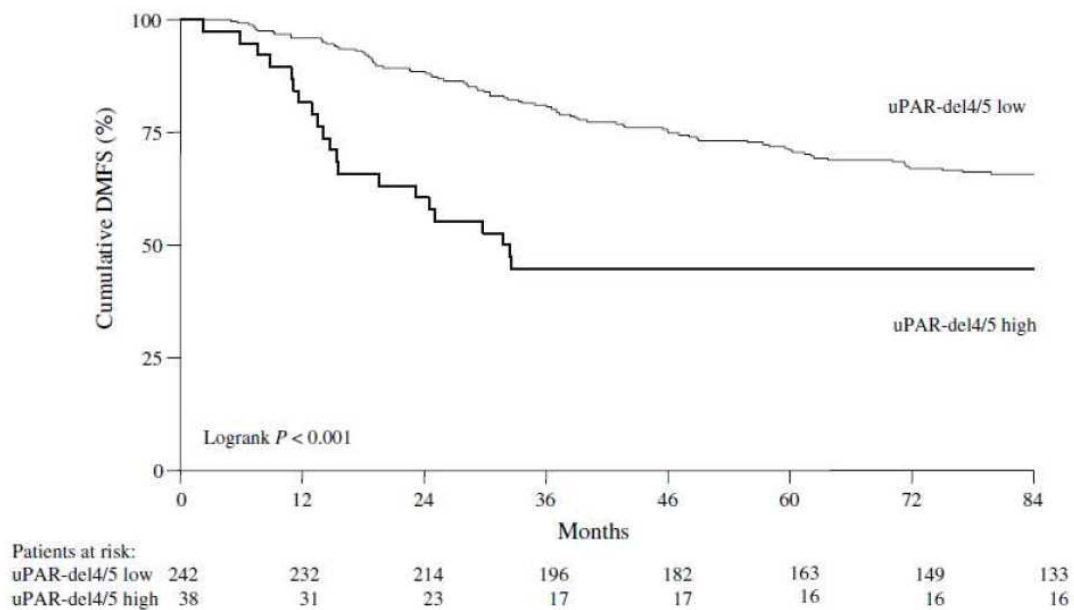


Fig. 4 Distant metastasis free survival as a function of uPAR-del4/5 expression levels

uPAR-del4/5 mRNA expression analysis of 280 LNN, untreated breast cancer patients reveals a significant shorter distant metastasis free survival of patients expressing uPAR-del4/5 at high levels (Kotzsch et al. 2008).

Patients with high mRNA levels of uPAR-del4/5 show a significantly shorter distant metastasis free survival (DMFS) and overall survival, compared to patients with low uPAR-del4/5 expression levels (Kotzsch et al. 2008). Furthermore, in multivariate regression analysis uPAR-del4/5 mRNA values significantly contributed to the base model of traditional prognostic factors for DMFS. This shows that uPAR-del4/5 mRNA is an independent, pure prognostic factor in breast cancer (Kotzsch et al. 2008). Interestingly, recently Kotzsch et al. could show that uPAR-del4/5 has no prognostic significance in advanced ovarian cancer (Kotzsch et al. 2011).

2.7 Rab31 as a prognostic marker for breast cancer

The tumorbiological role of uPAR-del4/5 is still unclear. To further explore the potential function of uPAR-del4/5, Kotzsch et al. analyzed two different breast cancer cohorts by microarray analysis, in order to find differentially expressed genes, in breast cancer tissue with high versus low uPAR-del4/5 mRNA expression levels. Only seven genes were found to overlap in both groups. These genes are dermatopontin, cadherin-11, homeo box B6, TIMP-3, tropomyosin-1, olfactomedin-like protein, and rab31. Rab31 was selected for further analysis since other Rab proteins have been shown to be involved in breast and other types of cancer (Kotzsch et al. 2008).

Analysis of 280 LNN breast cancer patients for rab31 mRNA expression revealed a significant relation between high rab31 mRNA values and a worse outcome of the patients (Fig. 5).

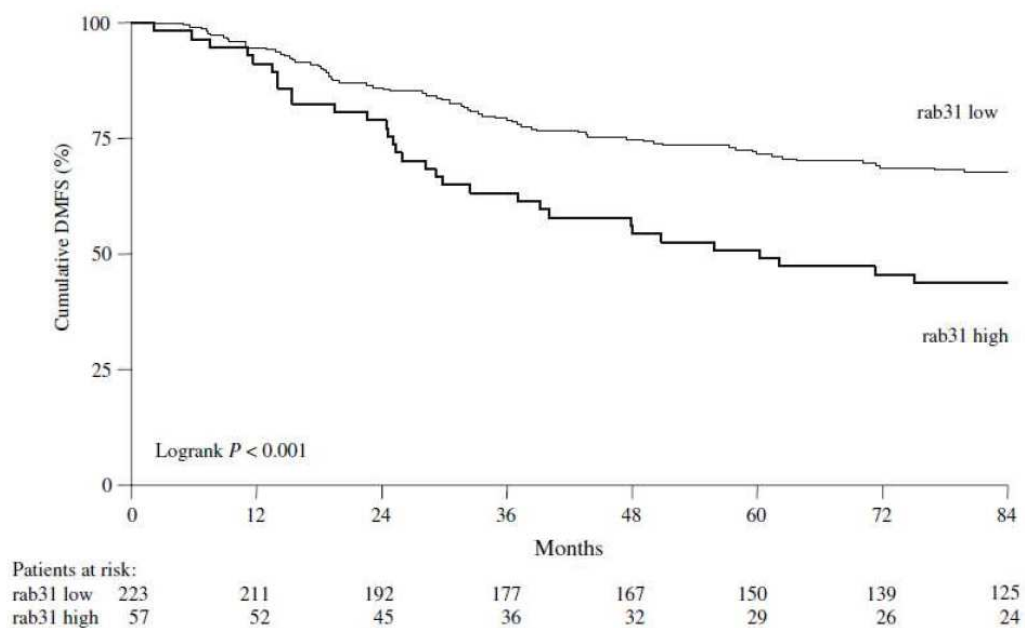


Fig. 5 Distant metastasis free survival as a function of rab31 expression levels

Rab31 mRNA expression analysis of 280 LNN, untreated breast cancer patients reveals a significant shorter distant metastasis free survival of patients expressing rab31 at high levels (Kotzsch et al. 2008).

Like uPARdel4/5, rab31 mRNA values contribute significantly to the base multivariate model. Therefore, rab31 can be considered as an independent

prognostic marker for breast cancer (Kotzsch et al. 2008). An independent study identified rab31 as one out of 11 genes that is overexpressed in ER-positive breast cancer patients (Abba et al. 2005). In ovarian cancer, Kotzsch et al. demonstrated – similar to the situation with uPAR-del4/5 - that rab31 mRNA has no prognostic significance in advanced ovarian cancer (Kotzsch et al. 2011).

Interestingly, patients expressing both proteins at high levels show a significantly worse DMFS and overall survival (OS) compared to patients expressing both proteins at low levels. Rab31 and uPAR-del4/5 mRNA values have independent but additive pure prognostic relevance in lymphnode-negative breast cancer patients (Kotzsch et al. 2008).

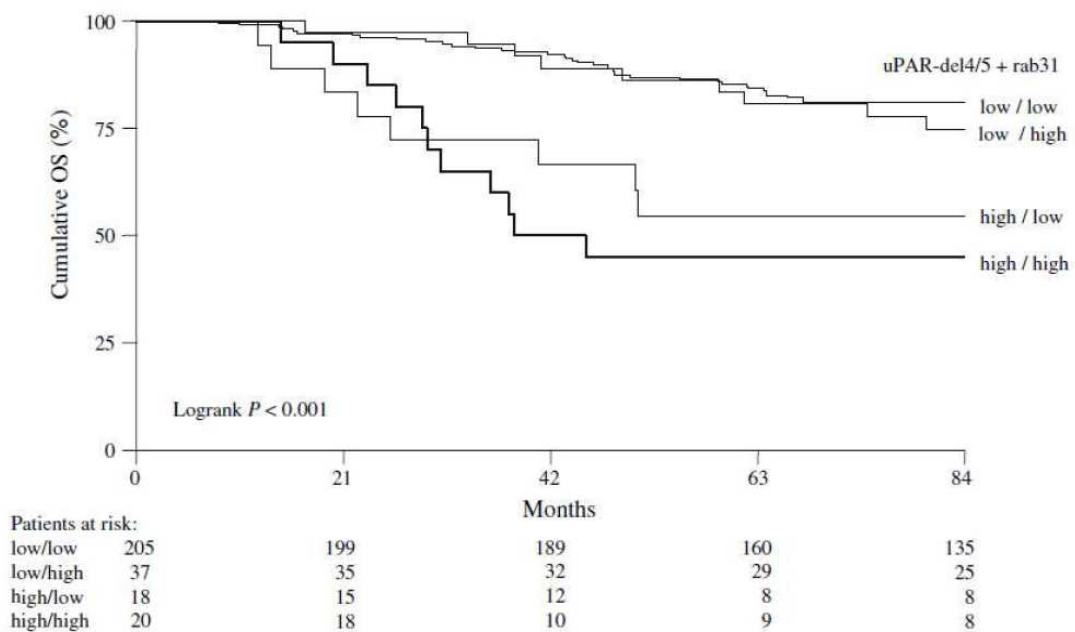


Fig. 6 Overall survival as a function of the combined mRNA expression of uPAR-del4/5 and rab31

The subgroup of patients expressing uPAR-del4/5 and rab31 at high levels show a significant shorter overall survival compared to patients expressing both proteins at low levels (Kotzsch et al. 2008).

2.8 Rab GTPases

2.8.1 Rab GTPases in membrane trafficking

The compartmentalization of eukaryotic cells requires the transport of lipids and proteins between distinct membrane-bound organelles. Rab GTPases, which belong to the Ras superfamily of small GTPases, have emerged as key regulators of membrane trafficking in eukaryotic cells. Each Rab protein is specifically localized to a particular membrane within this pathway. Up to now, almost 70 different human Rab proteins have been identified (Stenmark et al. 2001; Goud et al. 2010; Subramani et al. 2010). Some Rabs are localized to the endoplasmic reticulum (ER) regulating the transport of cargo from ER to the Golgi apparatus. Others can be found in endosomes, clathrin-coated vesicles, the plasma membrane, membrane ruffles and secretory granules. Described functions of Rab proteins include trafficking between the Golgi apparatus and endosomes, phagocytosis, the assembly of adherens junctions, trafficking of sonic hedgehog signaling components, mitochondrial dynamics and neuroendocrine secretion (Subramani et al. 2010).

Rab proteins are recruited and activated at the donor membrane. After vesicle budding from the donor membrane, Rab proteins facilitate the transport along the cytoskeleton and are involved in docking and fusion with the acceptor membrane. The key to this function and to membrane specificity of each Rab protein is the recruitment of effector molecules that bind exclusively GTP-bound Rabs. An abundance of different Rab effector proteins are described and a single Rab protein can have several effectors which confer the capability to the Rab, of regulating several molecular events at a restricted membrane location. For example rab5 can regulate endocytic vesicle tethering and fusion, and in addition it can control vesicle formation at the plasma membrane and microtubule-dependent motility of endocytic structures (Subramani et al. 2010; Stenmark et al. 2001). Figure 7 gives an example on the multiple trafficking events Rab proteins are involved in, like endocytosis, recycling, biosynthesis, exocytosis and degradation (Agola et al. 2011).

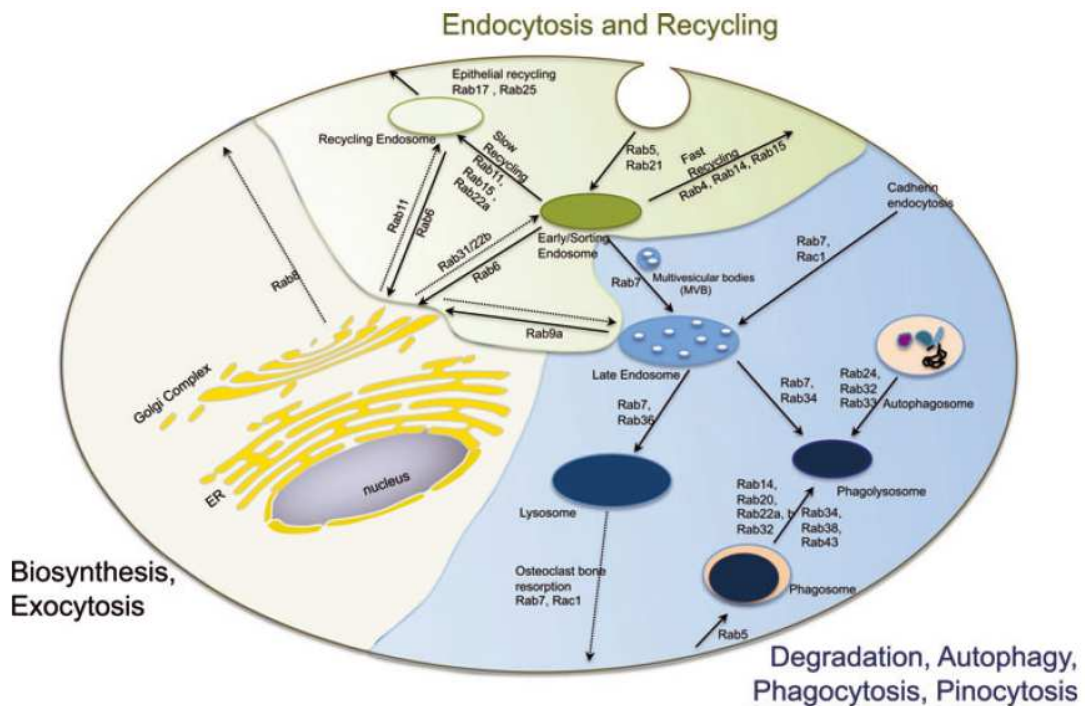


Fig. 7 Rab proteins in endocytosis, recycling, and degradative pathways

Receptor mediated endocytosis occurs *via* clathrin-coated vesicles and is regulated by rab5 and rab21. Internalized protein is delivered to early/sorting endosomes. From here molecules can return to the plasma membrane *via* fast or slow recycling routes. Newly synthesized plasma membrane proteins are delivered from the trans-Golgi network to recycling endosomes, while lysosomal hydrolases are delivered to early and late endosomes *via* two mannose 6-phosphate receptors. Recycling from early endosomes to the Golgi depends on rab6, while rab9 controls transport from the late endosome to the trans-Golgi. Light green overlay encompasses endocytic and recycling circuits; light blue overlay encompasses degradative circuits; and neutral overlay encompasses the biosynthetic/exocytic routes (Agola et al. 2011).

2.8.2 Regulation of Rab proteins

The function of Rab GTPases depends on their ability to alternate between two conformational states, the inactive (GDP-bound) and the active (GTP-bound) form. Furthermore, their function depends on their capacity to associate reversibly with specific membrane compartments (Rodriguez-Gabin et al. 2001).

Specific regulators promote the switch between these two states. GDP-GTP exchange factors (GEFs) promote the exchange of GDP for GTP, turning the GTPase into the on-state. GTPase activating proteins (GAPs) promote GTP hydrolysis, and turn the GTPase off. Rab GTPases are typically in their on-state when they are bound to the membrane, and promote the assembly of effector

complexes at membrane surfaces. The effectors are cytosolic or membrane proteins and can display a diverse range of biological functions important for cell signaling, vesicle formation and fusion. The vesicle and its target are endowed with a unique set of GTPases, this ensures specific recognition (Barr 2009; Lodhi et al. 2007).

The reversible membrane localization of Rab proteins depends on the post-translational modification of a cysteine motif at the carboxyl-terminus, with one or more often, two highly hydrophobic geranylgeranyl groups. This post-translational modification requires the initial recognition of the newly synthesized Rab protein by a Rab escort protein (REP), which presents the Rab protein to the geranylgeranyl transferase. The REP then functions as a chaperone that keeps the hydrophobic, geranylgeranylated Rab in a soluble form and delivers it to the appropriate membrane (Stenmark et al. 2001).

The functional state of Rab GTPases depends on the structural conformation, which is determined by binding to guanine nucleotides. Rab GTPases associated to REP are thought to be in the GDP-bound state, whereas membrane delivery is accompanied by the exchange of GDP with GTP, catalyzed by GEFs, and the release of REP. Upon GTP-hydrolysis, which is catalyzed by GAPs, the GDP bound form of Rab becomes a target for Rab GDP-dissociation inhibitor (GDI), which extracts the GDP-Rab - including its very hydrophobic geranylgeranyl groups - from the membrane, allowing it to return *via* the cytosol to its membrane of origin (Armstrong 2000; Stenmark et al. 2001).

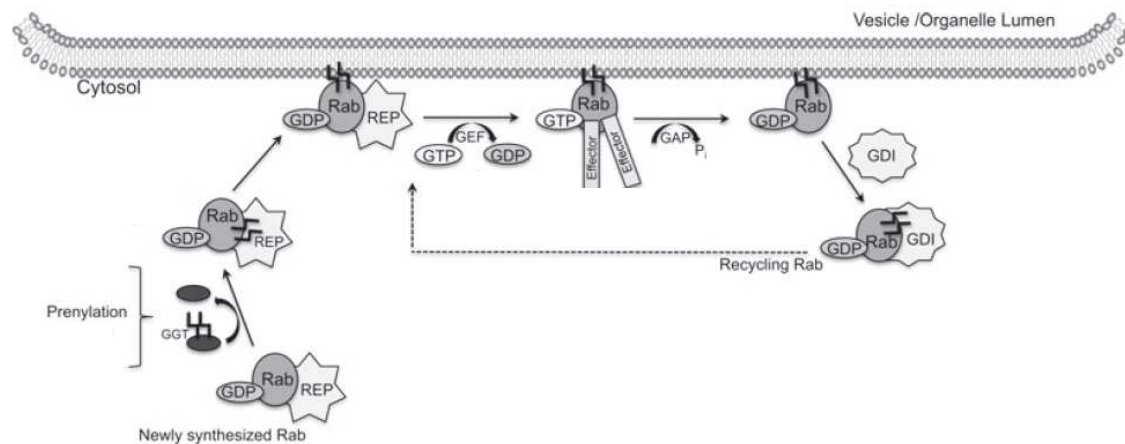


Fig. 8 Scheme of the guanine-nucleotide and membrane cycles of Rab GTPases

Newly synthesized Rabs are recognized by Rab escort protein (REP) which presents it to the geranylgeranyl transferase. This leads to prenylation of the C-terminal cysteine motif. REP can act as a chaperone and keeps the highly hydrophobic geranylgeranylated Rab in solution. The geranylgeranylated Rab is inserted into the membrane. GDP/GTP exchange factors (GEFs) activate the Rab protein. Effector proteins bind the GTP-bound Rab. GTPase activating proteins (GAPs) promote GTP-hydrolysis, and turn the GTPase off. GDP-dissociation inhibitors (GDIs) extract the Rab from the membrane and escort it back to the donor membrane (modified according to Agola et al. 2011).

2.8.3 Structure of Rab proteins

Rab GTPases generally differ most in their C-terminus, which has been implicated in subcellular targeting, whereas regions involved in guanine-nucleotide binding are most conserved (Stenmark et al. 2001).

The Rabs share a fold that is common to all small GTPases of the Ras superfamily. The basic structure of the GTPase domain consists of a central 6-stranded mixed β -sheet (comprising five parallel strands and one antiparallel) surrounded by five α -helices. In these structures, the elements responsible for guanine nucleotide and Mg^{2+} binding, as well as GTP-hydrolysis, are located in five loops (G1-G5) with conserved sequence motifs. These five loops connect the α -helices and β strands. The amino-acid residues that come together in the active site are closely associated with either the phosphate-groups of the bound nucleotide and Mg^{2+} , or the guanine base and are highly conserved within the entire Ras superfamily (Itzen et al. 2011). Numerous mutagenesis studies have shown that the putative Rab switch regions (G2 and G3) are crucial for the interaction

of Rab proteins with regulatory protein partners such as GEFs and GAPs (Stenmark et al. 2001). GTP-binding induces conformational changes in the switch I loop and the switch II region, resulting in the modulation of binding affinities for the regulatory and effector proteins (Agarwal et al. 2009). The designation as switch region comes from a comparison of the structures of Rabs in the GTP- and GDP-bound form, where it was seen that these are the areas which change most significantly upon GTP-hydrolysis. These regions are also directly involved in the GTPase reaction. G1 is often referred to as the P-loop. G1 is involved in a number of interactions of the backbone with nucleotide phosphatases. G4 and G5 are involved in the interactions with the guanine base and are responsible for the discrimination against other nucleotides such as ADP/ATP (Itzen et al. 2011).

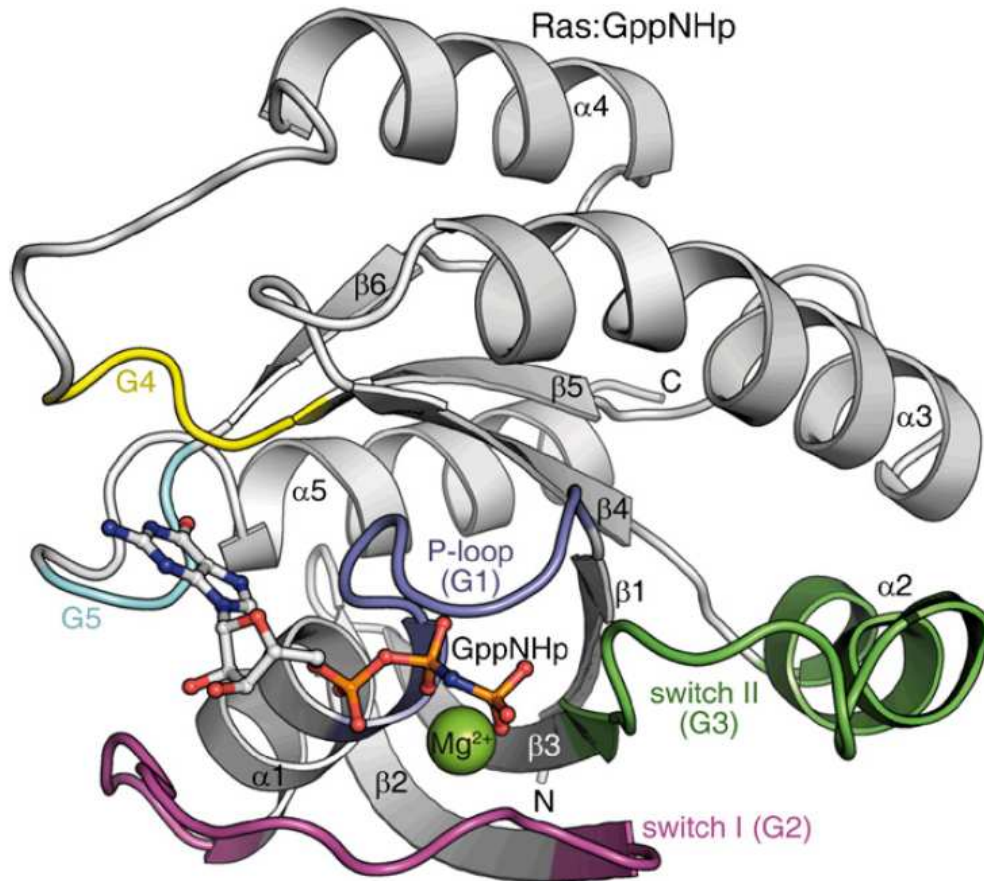


Fig. 9 Structure of Rab proteins

Overview of the 3-D structure of H-Ras in complex with the non-cleavable GTP analog GppNHp. Conserved sequence motifs (G1-G5) involved in nucleotide binding connect the six β -sheets and five α -helices. Furthermore, these linker regions are responsible for guanine nucleotide and Mg^{2+} -binding, as well as for GTP-hydrolysis. The P-loop interacts with nucleotide phosphatases. Conformational changes in the switch I (G2) and switch II (G3) region upon GTP-binding induce the interaction with effectors and GAPs. G4 and G5 interact with the guanine base and discriminate against binding of other nucleotides (Itzen et al. 2011).

As already mentioned, Rab proteins are post-translationally modified with one or two geranylgeranyl groups. This modification appears in most human Rabs at two cysteine residues, but a few Rabs have only one prenylatable cysteine. In the case of Rab proteins, there is no conserved carboxy-terminal motif, with sequences such as XCCXX, XXCCX, XXXCC, CCXXX or XXCXC as well as XCXXX all occurring. Geranylgeranylation of this carboxy-terminal cysteine allows for anchoring of the Rab to the plasma membrane or to a vesicular membrane (Itzen et al. 2011).

2.8.4 Rab proteins and cancer

Mutations in Rab proteins and altered GTPase expression or activity were shown to be involved in neurologic and neurodegenerative diseases, lipid storage disorders and cancer (Agola et al. 2011). Up to now the best characterized Rab protein involved in cancer progression is rab25. It was shown to be involved in cell proliferation and the protection from apoptosis. Rab25 is highly expressed in ovarian and breast cancer and correlates with a poor outcome in both diseases. Furthermore, rab25 expression is increased in prostate cancer, and in transitional cell carcinoma of the bladder. Rab25 has been shown to increase cell survival by decreasing the levels of the proapoptotic molecules bax and bak. In addition, rab25 expression increases the proliferation and aggressiveness of ovarian and breast cancer cells by increasing Akt-phosphorylation, which in turn activates the phosphoinositide-3-kinase pathway (Cheng et al. 2005; Subramani et al. 2010).

To give some more examples beside of rab25, a series of Rab proteins was shown to be involved in cancer *in vivo* and *in vitro*. Rab5a is associated with the axillary lymphnode metastasis of breast cancer patients (Yang et al. 2011), rab27a acts as a mediator of invasion and metastasis in human breast cancer cells (Wang et al. 2008) and the presence of rab27b protein proved to be associated with a low degree of differentiation and the presence of lymphnode metastasis in ER-positive breast cancer patients (Hendrix et al. 2010). As already mentioned, rab31 was shown to be a prognostic factor in lymphnode-negative breast cancer patients. High rab31 RNA expression correlated significantly with a poor prognosis of the patients (Kotzsch et al. 2008).

2.9 Rab31 (rab22B)

2.9.1 Rab31 structure and intracellular localization

After the initial cloning of rab31 (also known as rab22B) from human melanocytes in 1996, a BLAST analysis revealed that the most closely related Rab protein, with 71 % amino-acid identity was canine rab22 (rab22A) (Chen et al. 1996). Because the accepted guideline for the use of the next available Rab numbers was at that time, an identity less than 85 %, the new protein was named rab31 instead of rab22B (Chen et al. 1996; Bao et al. 2002). Rodriguez-Gabin et al. identified a Rab sequence (rrab22B) expressed in rat oligodendrocytes with a high identity to human rab31. A comparison of the rrab22B sequence with human rab31 showed 88 % identity, the predicted amino acid sequence had 94 % identity. These results show that rrab22b encodes the rat homolog of human rab31. In view of the fact that a segment of the carboxy-terminal domain shows 9 differences among the 14 residues, one must consider that rrab22B still may very well encode a new member of the Rab family, especially, because the carboxy-terminal end is part of the motif responsible for the targeting of Rab proteins to specific membrane compartments (Rodriguez-Gabin et al. 2001). Despite of this fact the authors refer to rrab22B as rab31 (Rodriguez-Gabin et al. 2009).

The coding sequence of human rab31 corresponds to a 194 amino acid protein with a nominal molecular mass of 21.6 kDa and a pI of 6.7. Rab31 was mapped to chromosome 18 (Chen et al. 1996). It is expressed fairly ubiquitously in human tissue. The transcript is found in spleen, thymus, prostate, testis, ovary, small intestine, colon, leukocytes, heart, brain, placenta, lung, liver, muscle, kidney, pancreas, melanoma cells and fibroblasts (Chen et al. 1996; Bao et al. 2002). Within the cells, rab31 was shown to be localized to the trans-Golgi, the trans-Golgi network (TGN) and to endocytic compartments (Rodriguez-Gabin et al. 2001).

Phylogenetic analysis suggests that rab21, rab22A and rab31 are grouped within the rab5 subfamily. All three can be co-localized with rab5 and its effectors on early endocytic compartments, and mutants of these Rabs disrupt trafficking through the endocytic pathway. In contrast to rab5, rab21, rab22a and rab31 have

also been localized to the trans-Golgi and rab22A and rab31 have been implicated in regulating endosome-to-Golgi and Golgi-to-endosome trafficking (Goud et al. 2010).

2.9.2 Rab31 interacting proteins

GEFs promote the exchange of GDP for GTP, keeping Rab proteins in the active state. Most GEFs share a region of homology known as the Vps9 domain (Goud et al. 2010). The Vps9 domain, together with an upstream tandem helical bundle (HB) region, is a GEF domain for the rab5 subfamily of G proteins. Up to now a couple of Vps9 domain containing GEFs, were shown to interact with rab31. Gapex-5 is one example for a Vps9 domain-containing protein. Lodhi et al. could show that Gapex-5 is a GEF for rab31 (Lodhi et al. 2007). Lysates of Cos-1 cells overexpressing rab31 were incubated with GDP or GTP γ S. Using pull-down assays with a GST-tagged HB-Vps9 domain of Gapex-5, interaction of Gapex-5 with rab31 *via* its Vps9 domain was confirmed (Lodhi et al. 2007).

Another study by Kajihho et al. demonstrated the interaction of RIN proteins, ALS2CL, and ALS2 with rab31 (Kajihho et al. 2011). The RIN (Ras and Rab interactor, or Ras interaction/interference) family is composed of RIN1, RIN2 and RIN3. In mock-transfected HEK293T cells, only 5 % of rab31 is present in the GTP-bound active form. The expression of RIN proteins or rabex-5 increased the formation of GTP-bound rab31 in HEK293T cells. The biggest effect was observed for RIN2 and RIN3. Experiments with Vps9 mutant RIN proteins show, that the interaction *via* the Vps9 domain is responsible for the increase in GTP-bound rab31. Additional experiments with HEK293T cells overexpressing ALS2 and ALS2CL revealed similar results as monitored for RIN2 and RIN3. This data indicate, that RIN2, RIN3 and ALS2, ALS2CL are capable of acting as GEFs for rab31 (Kajihho et al. 2011).

Another well described rab5 GEF is EEA1, a multidomain tethering factor involved in the fusion of endosomes. EEA1 has two Rab-binding domains, one close to the amino-terminus and another at the carboxy-terminus. Lodhi et al. (2007) could show that GTP-bound rab31 interacts strongly with both domains, whereas rab5

displays stronger affinity for the amino-terminal domain. Interestingly, EEA1 shows higher affinity to rab31 than to rab5. In contrast to this another rab5 GEF, rabaptin-5 failed to interact with rab31 (Lodhi et al. 2007).

GEF	Rab31 interaction	Reference
Gapex-5	yes	(Lodhi et al. 2007)
RIN-1	slight	(Kajiho et al. 2011)
RIN-2	medium	(Kajiho et al. 2011)
RIN-3	high	(Kajiho et al. 2011)
ALS2 and ALS2CL	yes	(Kajiho et al. 2011)
rabex-5	slight	(Kajiho et al. 2011)
EEA1	yes	(Lodhi et al. 2007)
rabaptin-5	no	(Lodhi et al. 2007)

Table 1 GEFs investigated for rab31 interaction

In order to identify more proteins that interact with rab31, Rodriguez-Gabin et al. used the yeast two-hybrid system to screen a mouse brain cDNA library. In this study, rab31 was found to interact with ORCL-1 (Rodriguez-Gabin et al. 2010). ORCL-1 is a member of group II inositol polyphosphate 5-phosphatases. It acts as a phosphatidyl inositol 4,5 diphosphate 5 phosphatase [PI(4,5)P₂ 5-phosphatase] that plays a key role in the regulation of the levels of PI(4)P and PI(4,5)P₂, two signaling molecules involved in membrane trafficking and Golgi/TGN organization. GST-rab31 pull-down experiments and co-immunoprecipitation confirmed interaction of rab31 and ORCL-1. Furthermore, co-localization of ORCL-1 and rab31 was observed in the TGN, endosomes and in carriers budding from the TGN (Rodriguez-Gabin et al. 2010).

Another protein interacting with rab31 is the mRNA-binding protein HuR. It is a member of the Hu/ELAV-family and is ubiquitously expressed. The protein shuttles between the nucleus and the cytoplasm. In the cytoplasm HuR stabilizes its target transcripts and/or regulates the translation of the transcript. Aberrant expression of HuR was shown to be associated with a reduced survival of patients suffering from several cancers types, including breast cancer. In invasive breast cancer elevated

cytoplasmic HuR expression is associated with an aggressive form of the disease (Heinonen et al. 2005). In addition, cytoplasmic HuR expression was shown to be associated with tamoxifen resistance of MCF7 breast cancer cells. Cytoplasmic HuR is thought to be the functional pool of HuR with respect to mRNA stabilization and it reflects the carcinogenic properties of this protein. HuR directly binds rab31 mRNA in 184B5Me and MCF7 cells. Silencing of HuR leads to the downregulation of rab31 protein. Interestingly HuR silencing has effects on several tumor relevant signaling pathways such as p53, MAPK and TGF- β signaling pathways in breast epithelial cells. Furthermore, HuR silencing altered the expression of several genes related to cell transformation (Heinonen et al. 2011).

2.9.3 Rab31 functions

Only little is known about the function of rab31. Rodriguez-Gabin et al. showed that rab31 functions in a vesicular transport route from TGN to the endosomes and may be somehow involved in the formation of transport intermediates from the TGN. The authors localized rab31 in tubulo vesicular carriers that bud from the TGN, travel along microtubules towards the cell periphery, and fuse with endocytic compartments (Rodriguez-Gabin et al. 2001).

Rab31 is involved in both the Golgi/TGN organization and in the transport of mannose-6-phosphate (Man-6-P) receptors from TGN to endosomes (Rodriguez-Gabin et al. 2009). This transport connects biosynthetic pathways to endocytic pathways and plays an essential role in the biology of the cells, as it is involved in the biogenesis of endosomes, lysosomes and the plasma membrane (Rodriguez-Gabin et al. 2010). Kajihio et al. further elucidated the regulation of MPRs transport from TGN to early endosomes. They could show that the rab31-GEF, RIN3 regulates MPRs transport (Kajihio et al. 2011). Furthermore, rab31 regulates the formation of MPRs containing carriers at the TGN. This is in agreement with reports that Rab proteins participate in each of the four main events of membrane trafficking namely, carrier budding, carrier delivery, carrier tethering and fusion of the carrier with the target compartment (Rodriguez-Gabin et al. 2010). Similar results were shown by Ng et al. (Ng et al. 2009).

In addition, Ng et al. showed another function of rab31 in intracellular trafficking. In the epidermoid carcinoma cell line A431, rab31 modulates the internalization of the EGFR. The effect on EGFR appears rather specific, as rab31 associates with EGFR in a GTP-dependent manner (Ng et al. 2009).

3 Aims of the study

The aim of this study is to clarify the tumorbiological role of the urokinase receptor splice variant uPAR-del4/5 and of the GTP binding protein rab31 with respect to their functional activity *in vitro* and *in vivo*.

In detail the following topics are investigated:

A In order to characterize the function of rab31, the human protein is expressed in *E. coli*, purified from the cell lysate and used as immunogen to assemble specific antibodies directed to rab31. The generated antibodies are tested for specificity in immunocytochemistry, Western blot analysis and ELISA.

B What effects does the overexpressing of uPAR-del4/5 in breast cancer cells have on tumor-biologically relevant processes like proliferation, adhesion and invasion? Do high levels of uPAR-del4/5 in breast cancer cells result in alterations of the tumorigenic properties in an experimental metastasis model?

C Beside of batch-transfected cells (this cells typically display a heterogeneous expression pattern within the cell population), cell clones with high, medium or low expression of the splice variant are isolated and analyzed in order to answer the question, are the observed effects in uPAR-del4/5 overexpressing cells dependent on the level of uPAR-del4/5 expression?

D Breast cancer cells are transfected with an expression plasmid encoding rab31. Batch-transfected cells, as well as cell clones expressing high, medium or low levels of rab31 are isolated and analyzed. Does the overexpression of rab31 have effects on tumorbiologically relevant processes like proliferation, adhesion and invasion? Do high levels of rab31 in breast cancer cells result in alterations of the tumorigenic properties in an experimental metastasis model?

4 Material

4.1 Eukaryotic cell lines

The eukaryotic human breast cancer cell lines MDA-MB-231, MDA-MB-435 and CAMA-1 were used for stable transfection. In addition, ZR 75 and adriamycin-resistant MCF-7 cells (a-MCF-7) were analyzed. All cell lines were purchased from American Type Culture Collection [ATCC] (Manassas, VA, USA).

4.2 Growth media for eukaryotic cells

Growth medium for human breast cancer cell lines MDA-MB-231, MDA-MB-435, CAMA-1, ZR 75 and a-MCF-7:

Composition	Cat. #	Company
500 ml DMEM + GlutaMAX™	61965	Invitrogen Gibco, San Diego, USA
10 mM Hepes (1M)	15630	Invitrogen Gibco, San Diego, USA
550 mM L-arginine	A8094	Sigma, Saint Louis, USA
272 mM L-asparagine	A4159	Sigma, Saint Louis, USA
10 % (v/v) FCS	10270	Invitrogen Gibco, San Diego, USA

Selection of stably transfected cell clones occurred under antibiotic selection pressure by usage of 1 g/l Geneticin G418 (Invitrogen Gibco, San Diego, USA).

Cell culture solutions	Composition
Cell freezing medium	90 % (v/v) FCS 10 % (v/v) DMSO
Splitting solution	0.2 % (v/v) EDTA in PBS
Adhesion medium	DMEM + GlutaMAX™ 0.5 % (w/v) BSA 20 mM Hepes
Invasion medium	DMEM 0.1 % (w/v) BSA
Blocking solution (sterile)	PBS 2 % (w/v) BSA

4.3 Enzymes, proteins and electrophoresis ladders

Appellation	Cat.#	Company
1 kb DNA ladder peqGOLD	25-2150	PeqLab, Erlangen, Germany
Collagen type I	C1809	Sigma, Saint Louis, USA
Collagen type IV, from human placenta	C5533	Sigma, Saint Louis, USA
Epidermal growth factor, human, recombinant	9644	Sigma, Saint Louis, USA
Fibronectin from human plasma	354008	Becton Dickinson BD, Bedford, USA
Growth factor reduced matrigel™	356230	Becton Dickinson BD, Bedford, USA
Laminin from human placenta	L6274	Sigma, Saint Louis, USA
Prestained protein marker	SM0671	Fermentas Life Science, St. Leon-Rot, Germany
Rab22A	ab90109	Abcam, Cambridge, UK
Rab5	ab62956	Abcam, Cambridge, UK
Taq DNA Polymerase, recombinant	10342-020	Invitrogen Gibco, San Diego, USA
Unstained protein marker	SM0431	Fermentas Life Science, St. Leon-Rot, Germany
Vitronectin from human plasma	354238	Becton Dickinson BD, Bedford, USA

4.4 Antibodies

Primary antibodies:

Antibody	Epitope	Company	Application
Anti-rab31 (C-15), rabbit pAb	Human rab31 near C-terminus	Santa Cruz Cat.# sc-85111	ICC
Anti-uPAR (IIIF10), mouse mAb	D1 uPAR	(Luther et al. 2003)	WB, ICC, FACS
Anti-uPAR (IID7), mouse mAb	D2 uPAR	(Luther et al. 2003)	WB
EGF-receptor (C74B9), rabbit mAb	Total EGF receptor	Cell Signaling Cat. # 2646	WB
anti-phospho-tyrosine (PY20)	Phospho-tyrosine	Invitrogen Cat. #03-7799	WB
p44/42 MAPK (Erk1/2)	Erk1/2	Cell Signaling Cat. # 9102S	WB
Phospho-p44/42 MAPK (Erk1/2)	Erk1/2 Thr202/Tyr204	Cell Signaling Cat. # 9101S	WB
anti-proMMP9 (E9)	proMMP9	Provided by Dr. Christian Ries	WB
MAB 374/ clone 6C5, mouse mAb	GAPDH	Millipore	WB
RT1-IgG rab31, rabbit pAb	Human rab31	In house	WB, ELISA, ICC
RT2-IgG rab31, rabbit pAb	Human rab31	In house	ICC
RT3-IgG rab31, rabbit pAb	Human rab31	In house	WB, ELISA, ICC
RT4-IgG rab31, rabbit pAb	Human rab31	In house	WB, ELISA
ChT1 rab31, chicken pAb	Human rab31	In house	WB, ELISA
ChT4 rab31, chicken pAb	Human rab31	In house	WB, ELISA

Secondary antibodies:

Source	Antigen	Conjugation	Application Dilution	Company
Goat	Mouse IgG	Alexa Fluor® 488	ICC FACS	Invitrogen Gibco, San Diego, USA
Goat	Rabbit IgG	Alexa Fluor® 488	ICC FACS	Invitrogen Gibco, San Diego, USA
Goat	Chicken IgY (IgG)	Alexa Fluor® 488	ICC	Invitrogen Gibco, San Diego, USA
Goat	Mouse IgG	HRP	WB ELISA	Jackson Immuno Research, West Grove, USA
Goat	Rabbit IgG	HRP	WB ELISA	Jackson Immuno Research, West Grove, USA
Rabbit	Chicken IgY	HRP	WB ELISA	Sigma, Saint Louis, USA

4.5 Technical devices

Appellation	Application	Company
Polymax 2040	Platform shaker	Heidolph, Schwabach, Germany
Sartorius BP1200	Scale	Sartorius, Göttingen, Germany
IKAMAG®	Magnetic stirrer	IKA Labtech, Staufen, Germany
Axiovert 25	Microscope	Zeiss, Jena, Germany
Axiovert 35 Laser device	Confocal laser scanning microscope	Zeiss, Jena, Germany Leica, Wetzlar, Germany
Blaubrand® counting chamber	Cell counting	Brand GmbH, Wertheim , Germany
Cawomat 2000 IR	X-ray film processor	CAWO, Schrobenhausen, Germany
Centrifuge 5415C	Centrifugation	Eppendorf, Hamburg, Germany

Centrifuge 5417R	Centrifugation	Eppendorf, Hamburg, Germany
Centrifuge Labofuge 400R	Centrifugation	Heraeus, Hanau, Germany
Compact XS/S gel electrophoresis	DNA-electrophoresis	Biometra, Göttingen, Germany
ELISA Reader	Photospectrometer	SLT Spectra, Crailsheim, Germany
FACS Calibur	Flowcytometrie	BD Biosciences, Franklin Lakes, NJ, USA
Fast Blot	Semi-dry Western blot	Biometra, Göttingen, Germany
Heracell Incubator-CO ₂	Cell incubator	Heraeus Instruments, Hanau, Germany
Herasafe biological safety cabinet	Laminar flow	Heraeus Instruments, Hanau, Germany
Labcycler	PCR	Sensoquest, Göttingen, Germany
Mini Protean B	Protein-elektrophoresis	Bio-Rad, Hercules, CA, USA
pH-Meter	pH adjustment	Schott, Mainz, Germany
Power supply Blue Power 500	Elektrophoresis	Serva, Heidelberg, Germany
Power supply EV231	Elektrophoresis Western blot	Consort, Turnhout, Belgium
Purelab classic	VE water	Elga GmbH, Wien, Austria
REAXtop	Shaker	Heidolph, Schwabach, Germany
Rotator	Rotator	Brand, Wertheim, Germany
Thermomixer 5436	Heating block	Eppendorf, Hamburg, Germany
UV Transiluminator	Gel documentation	Biometra, Göttingen, Germany
XCell Sure Lock	Protein-electrophoresis	Invitrogen Gibco, Carlsbad, USA

4.6 Expendable materials

Cell culture flasks, 15ml and 50ml tubes, serological pipettes (2/5/10/25/50ml), all pipette tips, 1.5/ 2 ml reaction tubes, 0.2 ml PCR tubes were purchased from Sarstedt, Nümbrecht, Germany.

Cell culture plates and cell scrapers were obtained from BD Biosciences, Franklin Lakes, NJ, USA.

CEA RP-new	Ernst Christiansen GmbH, Planegg, Germany
Combitips [®] plus 2.5 /5 ml	Eppendorf AG, Wesseling-Berzdorf, Germany
Cryogenic vials	NALGENE [®] Labware, Thermo Fisher Scientific, Roskilde, Denmark
FACS tubes conical 4.5 ml	Greiner Bio-One, Frickenhausen, Germany
Immobilon [™] PVDF Transfer Membrane	Millipore, Schwalbach, Germany
Lab-Tek [™] Chamber Slides	Nunc Thermo Fisher Scientific, Roskilde, Denmark
Minisart [®] sterile filter 0.1 /0.2 µm	Sartorius, Aubagne, France
Novex [®] 10 % zymogram gelatine gel	Invitrogen Gibco, Carlsbad, USA
Nunc-immuno [™] 96 well plates	Nunc Thermo Fisher Scientific, Roskilde, Denmark
Pasteur pipette glass 120 mm	Hirschmann Laborgeräte, Eberstadt, Germany
Sterile syringe and injection needles	Braun, Melsungen, Germany
Transwell [®] permeable support (8µm, 24 well (#3422))	Costar Corning, Amsterdam, Netherlands
Whatman [®] paper	Macherey-Nagel, Düren, Germany

4.7 Chemicals and reagents

Appellation	Application	Company
Aceticacid	Coomassie stain	CarlRoth, Karlsruhe, Germany
Albumin Bovine Serum (BSA) $\geq 98\%$	Cell culture	Sigma, St.Louis, USA
Albumin Bovine Serum 96 %	Western blot	Sigma, St.Louis, USA
Ammonium persulfate (APS)	SDS-PAGE	CarlRoth, Karlsruhe, Germany
Boricacid	Western blot	Sigma, St.Louis, USA
Bromphenolblue	Sample buffer	CarlRoth, Karlsruhe, Germany
CaCl ₂	Zymogram	Sigma, St.Louis, USA
Complete™ + EDTA Protease Inhibitor Cocktail	Cell lysis	Roche Diagnostics GmbH, Mannheim, Germany
Coomassie Brilliantblue R250	Coomassie stain	CarlRoth, Karlsruhe, Germany
Developing buffer	Zymogram	Invitrogen Gibco, Carlsbad, USA
Dimethylsulfoxide	Cell culture	Sigma, St.Louis, USA
Dulbecco's Modified Eagle Medium (DMEM) + GlutaMAX	Cell culture	Invitrogen Gibco, Carlsbad, USA
EDTA	Adhesion Assay	Sigma, St.Louis, USA
Ethanol 99.9 %	Western blot	Merck, Darmstadt, Germany
Ethidiumbromide	DNA electrophoresis	CarlRoth, Karlsruhe, Germany
Ethylenediaminetetraacetic acid (EDTA)	Cell culture	Biochrom AG, Berlin, Germany
FACS clean	FACS	BD Biosciences, Franklin Lakes, NJ, USA
FACS flow	FACS	BD Biosciences, Franklin Lakes, NJ, USA
Foetal calf serum (FCS)	Cell culture	Invitrogen Gibco, Carlsbad, USA
Geneticin® G 418 Sulfate	Cell culture	Invitrogen Gibco, Carlsbad, USA
Glycerol	Coomassie stain	CarlRoth, Karlsruhe, Germany
Glycine	Buffers	CarlRoth, Karlsruhe, Germany
HCl	pH adjustment	CarlRoth, Karlsruhe, Germany

Hepes	Cell lysis	CarlRoth, Karlsruhe, Germany
Hepes 1M	Cell culture	Invitrogen Gibco, Carlsbad, USA
Isopropanol	Cell culture	Merck, Darmstadt, Germany
L-Arginine	Cell culture	Sigma, St.Louis, USA
L-Asparagine	Cell culture	Sigma, St.Louis, USA
Lipofectin® Reagent	Cell culture	Invitrogen Gibco, Carlsbad, USA
Mycoplasma decontamination antibiotics	Cell culture	Applichem, Gatersleben, Germany
N,N,N',N', Tetramethylethyldiamin (TEMED)	SDS-PAGE	Sigma, St.Louis, USA
Na ₂ HPO ₄	PFA fixation	Merck, Darmstadt, Germany
NaCl	Buffers	CarlRoth, Karlsruhe, Germany
NaF	Cell lysis	CarlRoth, Karlsruhe, Germany
Na ₂ CO ₃	ELISA	Merck, Darmstadt, Germany
NaHCO ₃	ELISA	Merck, Darmstadt, Germany
NaH ₂ PO ₄	PFA fixation	Sigma, St.Louis, USA
NaOH	pH adjustment	Merck, Darmstadt, Germany
Paraformaldehyde (PFA)	ICC FACS	Serva, Heidelberg, Germany
Phosphate buffered saline (PBS)	Cell culture	Invitrogen Gibco, Carlsbad, USA
p-Nitrophenyl N-Acetyl-β-D-Glucosaminide	Adhesion Assay	Sigma, St.Louis, USA
Renaturing buffer	Zymogram	Invitrogen Gibco, Carlsbad, USA
Roti®-Load 1 reducing, 4x	SDS-PAGE	CarlRoth, Karlsruhe, Germany
Roti®-Load 2 non-reducing, 4x	Zymogram	CarlRoth, Karlsruhe, Germany
Rotiphorese 40 (Acrylamide)	SDS-PAGE	CarlRoth, Karlsruhe, Germany
Saponin	ICC / FACS	CarlRoth, Karlsruhe, Germany
Skimmed milk powder	Western blot	Sigma, St.Louis, USA
Sodium dodecyl sulfate (SDS) Pellets	SDS-PAGE Buffers	CarlRoth, Karlsruhe, Germany
Sodium orthovanadate	Cell lysis	Sigma, St.Louis, USA
Sodium citrate	Adhesion Assay	Merck, Darmstadt, Germany

Sodium pyrophosphate	Cell lysis	Sigma, St.Louis, USA
β -glycerol phosphate	Cell lysis	Sigma, St.Louis, USA
β -mercaptoethanol	Sample buffer	Merck, Darmstadt, Germany
Tris-Ultra Pure	SDS-PAGE Buffers	CarlRoth, Karlsruhe, Germany
Triton [®] X-100	Cell lysis Buffers	Sigma, St.Louis, USA
Trypan blue solution 0.4 %	Cell culture	Sigma, St.Louis, USA
Trypsin	Cell culture	Invitrogen Gibco, Carlsbad, USA
Tween [®] -20	Buffers	Applichem, Gatersleben, Germany
Universal Agarose peqGOLD	DNA electrophoresis	PeqLab, Erlangen, Germany

4.8 Buffers and solutions

Appellation	Composition	Application
PFA 4 %, pH 7.4	Solution 1: 0.1 M Na ₂ HPO ₄ Solution 2: 0.1 M NaH ₂ PO ₄ Mix solution 1 and 2 until pH 7.4 4 % (w/v) PFA solved in solution 1+2	ICC FACS
Agarosegel 1 %	1 % agarose in 40 ml TAE	DNA electrophoresis
Anode buffer	50 mM boric acid pH 8.5 20 % (v/v) ethanol	Western blot
Blocking buffer	1x TBS pH 7.4 0.1 % Tween-20 5 % (w/v) skimmed milk powder	Western blot
Carbonate-buffer, pH 9.6	Solution 1: 50 mM Na ₂ CO ₃ pH 11 Solution 2: 100 mM NaHCO ₃ pH 8 Mix both solutions until pH 9.6	ELISA
Cathode buffer	50 mM boric acid pH 8.5 5 % (v/v) ethanol	Western blot
Coomassie staining solution	0.1 % (w/v) Coomassie brilliant blue R250 10 % (v/v) aceticacid	Coomassie stain
Destaining solution	10 % (v/v) aceticacid	Coomassie stain

DNA-loading buffer	30 % (v/v) glycerol 0.24 % (w/v) bromphenolblue	DNA electrophoresis
Electrophoresis buffer 10x	0.25 M Tris 1 % (w/v) SDS 1.9 M glycine	SDS-PAGE
Fixation buffer	45 % (v/v) ethanol 10 % (v/v) aceticacid	Coomassie stain
Glycerol buffer	5 % (v/v) glycerol 25 % (v/v) ethanol	Coomassie stain
Hexosaminidase substrate	100 mM sodium citrate buffer pH 5.0 0.5 % (v/v) Triton X-100 15 mM p-nitrophenyl N-acetyl- β -D-glucosaminide	Adhesion Assay
Saponin solution	0.025 % saponin in PBS	ICC
Separating gel 12 %	375 mM Tris 1.5M pH 8.8 0.1 % (w/v) SDS 12 % (v/v) acrylamide 0.1 % (w/v) APS 0.1 % (v/v) TEMED	SDS-PAGE
Stacking gel	129 mM Tris 0.5M pH 6.8 0.1 % (w/v) SDS 5 % (v/v) acrylamide 0.1 % (w/v) APS 0.1 % (v/v) TEMED	SDS-PAGE
Stop solution	0.2 N NaOH 5 mM EDTA	Adhesion Assay
Stripping solution pH 2.2	160 mM glycine 0.1 % (w/v) SDS 1 % (v/v) Tween-20	Western blot
TAE	40 mM Tris-Acetate 1 mM EDTA pH 8.0	DNA-electrophoresis
TBS 10x (pH 7.4)	1.4 M NaCl 0.1 M Tris-HCl	Western blot Cell lysis
TBST	TBS 1x pH 7.4 0.1 (v/v) Tween-20	Western blot

Triton-lysisbuffer	1x TBS pH 7.4 1 % (v/v) Triton X-100 0.1 % (w/v) Complete™ + EDTA	Cell lysis
Triton-lysisbuffer + phosphatase inhibitors	TBS 1x pH 7.4 1 % Triton X-100 0.1 % (w/v) Complete™ + EDTA 1 mM sodium orthovanadate 1 mM β-glycerol-phosphate 50 mM NaF 10 mM sodium pyrophosphate	Cell lysis

4.9 Kits

Appellation	Application	Company
BCA™ Protein Assay Kit	Protein determination	Thermo Fisher Scientific, Rockford, IL, USA
DNA High Pure PCR Template Preparation Kit	Mycoplasma detection	Roche Diagnostics GmbH, Mannheim, Germany
Hemacolor Staining Kit	Invasion assay	Merck, Darmstadt, Germany
Pierce ECL Substrate	Western blot	Thermo Fisher Scientific, Rockford, IL, USA
TMB Microwell Peroxidase Substrate System	ELISA	KPL, Gaithersburg MD, USA
RNeasy Mini Kit	RNA preparation	Qiagen, Hilden, Germany
Cloned AMV first-strand cDNA Synthesis Kit	cDNA synthesis	Invitrogen Gibco, Carlsbad, USA

4.10 Primer

Application	5'	3'
Mycoplasma-PCR	5'- CGC CTG AGT AGT ACG TTC GC- 3'	5'- GCG GTG TGT ACA AGA CCC GA- 3'

5 Methods

5.1 Cell culture

5.1.1 Cultivation of eukaryotic cells

All cell lines were cultivated at 37 °C, 5 % (v/v) CO₂ in water saturated atmosphere. Cells were sub cultivated into new cell culture flasks every 3-4 days. For this, adherent breast cancer cells were detached from the cell culture flask by incubation with PBS, 0.02 % (v/v) EDTA at 37°C for 5 min. Cells were washed off the flask using 5 ml PBS, transferred into 10 ml Falcon tubes and centrifuged at 300 x g for 3 min. The supernatant was aspirated and cells were resuspended in growth medium. One fourth to one fifth of the detached cells was passed into a new cell culture flask.

5.1.2 Storing and thawing

For storage, cells were detached from the culture flasks with PBS containing 0.02% (v/v) EDTA at 37 °C for 5 min, washed with 5 ml PBS and centrifuged down. PBS was aspirated completely. The cell pellet was quickly resuspended in freezing medium containing FCS and 10 % DMSO and transferred into cryogenic vials. Slow freezing of the cells was ensured by using a NALGENE® freezing container at -80 °C. For long-term storage cell stocks were transferred to fluid nitrogen at -196 °C.

After thawing cells were washed in 5 ml of cold cell culture medium. After centrifugation at 300 x g for 3 min, cells were resuspended in medium and transferred into cell culture flasks. The culture medium was renewed after 4 to 5 hours of incubation to remove dead cells. Cells were passed into new cell culture flasks at least twice, before experimental usage.

5.1.3 Stable transfection and selection of single clones

MDA-MB-231, MDA-MB-435 and CAMA-1 cells were stably transfected with expression plasmids (pRcRSV) carrying the human cDNA for full-length uPARwt or the splice variant uPAR-del4/5 as previously described (Lutz et al. 2001; Luther et al. 2003). In addition, cells were transfected with pRcRSV plasmids encoding the human full-length rab31 cDNA.

For stable transfection, breast cancer cells were seeded on 6 well cell culture plates one day prior to transfection, to reach a confluence of approximately 70 %. At the day of transfection cells were washed once with PBS and recovered with cell culture medium free of FCS (GAM). Lipofectin[®] Reagent (Invitrogen) was used for stable transfection of breast cancer cells. 300 µl GAM were incubated together with 10 µl Lipofectin[®] reagent in transfection vials (solution A) for 45 min at RT. 2 µg of DNA was dissolved in 300 µl GAM in a second transfection vial (solution B). Solution A and B were mixed and incubated at RT for 15 min. Afterwards, medium was aspirated from each well and the DNA/ Lipofectin[®] solution was pipetted slowly onto the cells and incubated for 6 h at 37 °C in the cell incubator. Transfection medium was carefully aspirated and standard growth medium was applied to the wells. When cells were grown to 80 % confluence, cells were detached from the wells and transferred into small cell culture flasks. Successful transfection of cells with vector pRcRSV enables the cells with a resistance to geneticin (G418). Selection of stably transfected cells was performed by supplementation of 1 g/l (w/v) G418 into the cell culture medium. About 10 days post addition of the antibiotics all non resistant cells were dead.

Separation of single cell clones was conducted by limited dilution. Highly diluted cells were seeded on Ø 10 cm cell culture petri dishes. Colonies, which develop from single cell clones were picked and transferred into 96 well plates for further growth. This process had to be repeated at least twice. Expression of uPAR-del4/5 or rab31 was checked by immunocytochemistry and Western blot after each round of subcloning, to get cell lines with a homogeneous high, medium or low expression.

In order to investigate the effects of uPAR-del4/5 or rab31 on metastasis *in vivo*, MDA-MB-231 cells were transfected with the bacterial *lacZ*-gene (MDA-MB-231-LZ). This transfection was accomplished in the laboratory of Prof. Dr. Achim Krüger (Experimentelle Onkologie, TUM). The *lacZ*-gene encodes the β -galactosidase which converts the substrate 5-bromo-4-chloro-3-indolyl-beta-D-galactopyranoside (XGal). XGal cleavage by active β -galactosidase results in an insoluble indigo blue product. This effect was used to trace injected cancer cells in a xenograft mouse model (Kruger et al. 1998).

5.1.4 Detection of mycoplasma contamination

Mycoplasma contamination of the cells was regularly checked using a mycoplasma detecting polymerase chain reaction (PCR). For this, cellular DNA was obtained by using the DNA High Pure PCR Template Preparation Kit by Roche Diagnostics according to the manufacturers' recommendations. PCR products were analysed by agarose gel electrophoresis. Amplified mycoplasma-DNA PCR product was detected at 500 bp.

Protocol:

10x PCR reaction buffer	5 μ l
dNTPs	0.15 mM
3' Primer	1.2 μ M
5' Primer	1.2 μ M
DNA template	1 μ g
Taq Polymerase	1 unit
H ₂ O	ad 50 μ l

PCR cycles:

Temperature [°C]	Time	Cycles
94	5 min	
94	30 sec	30x
60	1 sec	
72	30 sec	
72	5 min	
4	∞	

5.2 Cellular assays *in vitro*

For all cellular assays cells were seeded 48 to 72 h before the experiment to 6 well culture plates. To reach a comparable growing density of about 70 % for all cell lines.

5.2.1 Cell proliferation

The proliferative activity of cells was determined using manual counting. MDA-MB-231, MDA-MB-435 and CAMA-1 cell transfectants were seeded in triplicates on 24 well cell culture plates. Starting with 20 000 cells per well of MDA-MB-231 and MDA-MB-435 cells and 30 000 CAMA-1 cells. Every 24 hours cells were detached in a defined volume PBS + 0.05 % EDTA.

Time	Volume
24 h	200 µl
48 h	300 µl
72 h	400 µl
96 h	500 µl

After addition of 50 µl trypan blue solution, cell number per well was determined in duplicates using a Blaubrand[®] counting chamber. The cell number of each cell lines after 24 h was set as 100 %. Proliferation was illustrated as % of increase in cell number relative to the 24 h value.

5.2.2 Cellular adhesion

To determine cellular adhesion of the transfected cells towards extracellular matrix proteins, each protein was diluted in PBS. 100 μ l protein-solution was added to 96 well culture plates and incubated as follows.

Protein	Concentration	Incubation
Vitronectin	2 μ g/ml	1 h, RT
Fibronectin	5 μ g/ml	1 h, RT
Collagen type I	5 μ g/ml	3 h, 37 $^{\circ}$ C
Collagen type IV	5 μ g/ml	3 h, 37 $^{\circ}$ C
Laminin	5 μ g/ml	3 h, 37 $^{\circ}$ C

After incubation, wells were washed with 100 μ l PBS per well and blocked with 200 μ l of 2 % (w/v) BSA/PBS for 1 h at RT, followed by additional washes with PBS. Solution was aspirated completely right before addition of the cells to avoid exsiccation.

Cells were detached and resuspended in adhesion medium. After cell counting in a Blaubrand[®] counting chamber, 20 000 cells per 100 μ l were added to the plate in triplicates. In addition a standard curve, starting with 25 000 cells in PBS was applied to the 96 well plate. After adhering to the plate for 2 h at 37 $^{\circ}$ C, medium and non adherent cells were aspirated. Plates were washed gently with PBS twice. Wells containing the standard curve remained untouched. For cell number determination of adherent cells, 50 μ l PBS and 50 μ l hexosaminidase substrate were applied to each well. Hexosaminidase substrate without PBS was added to the standard curve. After incubation for 90 min at 37 $^{\circ}$ C, the reaction was stopped by addition of 100 μ l stop solution. Optical density was recorded at 405 nm by a SLT Spectra ELISA Reader. Cell number in each well was calculated using the standard curve. Adherent cell number of vector control cells on each coating was set as 100 %.

5.2.3 Cellular invasion through matrigel™

Studies on the invasive capacity of transfected MDA-MB-231 cells were performed using the 24 well Costar Transwell chamber system. Membrane filters with a pore size of 8 µm and a diameter of 6.5 mm were coated with 30 µg growth factor reduced matrigel™ (BD) diluted in 100 µl invasion medium. The coated transwells were incubated for 3 h at 37 °C and dried overnight under the laminar flow (without a lid). Prior to the experiment, inserts were reconstituted with 200 µl invasion medium for 2 h at 37 °C.

The lower compartment of the invasion chamber was filled with 600 µl of DMEM containing 10 % FCS as a source of chemoattractant. 40 000 cells were suspended in 200 µl serum-free invasion medium and seeded into the upper compartment of the invasion chamber. The inserts were placed into the wells, avoiding bubbles between the two compartments. After 24 h incubation at 37 °C, cells and matrigel™ on the top surface of the filter were wiped off with a cotton swab. Cells that had migrated into the lower compartment and attached to the lower surface of the filter were fixed and stained using the Hemacolor staining kit (Merck). Purple cells on the dried membrane were counted under the light microscope. Cell number of invaded vector control cells was set to 100 %.

5.3 Xenograft mouse model

The xenograft mouse experiment was performed in collaboration with Prof. Dr. Achim Krüger (Experimentelle Onkologie, TUM). Pathogen-free female CD1 nu/nu mice (8-10 weeks old) were obtained from Charles River (Sulzfeld, Germany). On day one, 1.0×10^6 cells diluted in 200 µl PBS were injected into the tail vein of each mouse. 35 days post injection mice were sacrificed, lungs were prepared, fixed and XGal stained as described by Krüger et al. (Krüger et al. 1998). Blue colonies were counted on the surface of the lung.

5.4 Immunocytochemical staining

Cell culture microchamber slides were coated with 5 µg/ml fibronectin for 1 hour at RT. For each cell line, 40 000 cells per well were seeded on the microchamber slide and cultured over night. Cells were fixed in 4 % (w/v) paraformaldehyde (PFA) for 15 min at RT, washed with PBS, and permeabilized in PBS, 0.025 % (w/v) saponin for 5 min at RT. After blocking with 2 % (w/v) BSA in PBS, for 30 min at RT, antibodies directed to uPAR or rab31 respectively, were incubated with the cells for 1.5 h at RT followed by secondary Alexa 488-conjugated antibody for 45 min at RT, in the dark. Slides were mounted in PBS and fluorescence intensity was determined by confocal laser scanning microscopy (CLSM). In order to convert fluorescence staining intensity into colours of a glow scale, the look-up table “glowOv/Un LUT” provided with the CLSM scanning software was applied: low intensity (red), medium intensity (yellow), and high intensity (white). Staining procedures in the absence of any Ab as cell autofluorescence or in the presence of the secondary Alexa-488-conjugated IgG alone, served as controls and did not result in noticeable fluorescence signals.

5.5 Flow cytometry

Cells were cultivated in T25 cell culture flasks for 2-3 days. Cells were detached and resuspended in growing medium. For each preparation $1 \cdot 10^5$ cells were transferred to conic FACS vials. After washing with PBS, cells were fixed using 4% (w/v) PFA solution, permeabilized with 0.025 % (w/v) saponin and blocked in PBS, 2 % (w/v) BSA. Immunostaining was performed by incubating with Ab diluted in PBS, 1 % (w/v) BSA for 1h, RT followed by detection with Alexa-488-conjugated goat-anti-mouse IgG for 45 min at RT in the dark.

All experiments were performed with a FACS Calibur (Becton Dickinson) and data was analyzed using the *CellQuest™* software from Becton Dickinson.

5.6 Western blot analysis

5.6.1 Cell lysis without phosphatase inhibitors

For whole cell lysates, cells were cultured in small cell culture flasks until about 70% of the growing surface is covered. Detached cells were washed with PBS, centrifuged and the supernatant was aspirated. The cell pellet was lysed in 70 μ l TBS containing 1 % (v/v) Triton-X-100 and CompleteTM proteases inhibitor cocktail with EDTA. After incubation for 1 h at 4°C on a wheel, lysates were cleared by centrifugation. The total protein content was determined using the BCATM Protein Assay Kit according to the manufacturers' recommendations.

5.6.2 Cell lysis with phosphatase inhibitors

For analysis of phosphorylated proteins cells were seeded on 6 well plates pre-treated with collagen type IV (5 μ g/ml, 3 h 37 °C) or left untreated. After 0, 24, 48, 72 or 96 h medium was removed and cells were washed with PBS. Cells were scraped off the plate and transferred to a tube. Post centrifugation, supernatant was removed and the pellet was lysed using TBS containing 1 % Triton-X-100, 1mM sodium orthovanadate, 1 mM glycerol phosphate, 50 mM NaF, 10 mM sodium pyrophosphate and CompleteTM proteases inhibitor cocktail with EDTA. After incubation for 1 h at 4 °C on a wheel, lysates were cleared by centrifugation. The total protein content was determined using the BCATM Protein Assay Kit according to the manufacturers' recommendations.

5.6.3 Western blot

20 μ g total protein of each sample were mixed with reducing sample buffer and boiled for 5 min at 95 °C. Acrylamide content of the gel was used according to the expected size of the investigated protein. Proteins were separated in a SDS-PAGE and transferred onto a polyvinylidene difluoride (PVDF) membrane using a semi-dry Blotting device. The anode buffer contained 20 % (v/v) ethanol and 50 mM boric acid pH 8.8. The cathode buffer was composed of 5 % (v/v) ethanol and 50mM boric acid pH 8.8. The Blotting device was supplied with 75 mA for each

membrane for 2h. Membranes were blocked in TBS, 5 % (w/v) skimmed milk powder, and 1 % (v/v) Tween-20 for 1 h at RT. After washing with TBST the respective antibody was applied diluted in 5 % (w/v) skimmed milk powder, and 1% (v/v) Tween-20 overnight at 4 °C. Antibodies directed against phosphorylated proteins (PY20, p-p44/42 Erk1/2) were diluted in TBST containing 2 % (w/v) BSA. The horse radish peroxidase-conjugated secondary antibody was diluted in TBST 1 % (w/v) skimmed milk powder and applied for 1 h at RT followed by several washes with TBST. Proteins were visualized using the ECLTM chemiluminescent substrate according to the manufacturers' recommendations. In order to normalise differences in protein loading and blotting efficiency, membranes were subsequently stripped, blocked over night with 5 % (w/v) skimmed milk powder in TBST and reprobed with mAb directed to the endogenous control GAPDH.

5.7 Enzyme-linked immunosorbent assay (ELISA)

Generated rab31 directed antibodies were tested for specificity in an enzyme-linked immunosorbent assay (ELISA) setup. For this experiment 96 well microtiter plates (Nunc) were coated with 100 µl of detection antibody diluted in carbonate-buffer pH 9.6 and incubated over night at 4 °C. After three washes with TBS + 0.05 % Tween-20, 100 µl of determined amounts of recombinant protein, diluted in 0.5 % (w/v) BSA in TBS + 0.05 % Tween-20 were applied to the wells and incubated for 1 h at RT. In the next step plates were washed using TBS + 0.05 % Tween-20 followed by incubation with 100 µl of a primary detection antibody diluted in 0.5 % (w/v) BSA in TBS + 0.05 % Tween-20 for 1 h at RT. Subsequently plates were washed and incubated with a secondary, horse-radish peroxidase conjugated antibody for 1 h at RT. After three additional washes, 3,3',5,5'-Tetramethylbenzidine (TMB) substrate (Pierce) was applied to the wells due to manufacturers' instructions. The signal was enhanced using 50 µl 0.5 M H₂SO₄. Absorbance at 450 nm was subsequently recorded using an ELISA Reader (SLT Spectra).

5.8 Zymography of metalloproteases

In order to analyse gelatine metalloprotease activity of transfected MDA-MB-231 cells, the conditioned medium of the cells was analyzed using zymography. Activity of the gelatinases MMP9 and MMP2 can be monitored by usage of acrylamide gels incorporated with the substrate gelatine. Proteins in the conditioned serumfree medium were denatured by SDS, but not boiled or reduced. After electrophoresis, SDS was removed from the gel, replacing the SDS with a non-ionic detergent like Triton-X 100 (renaturing buffer). The gel was then incubated in a buffer suitable for enzymatic activity, allowing the renatured MMPs to digest the gel-bound gelatine in an area around their electrophoresed position. These digested areas were visualized by coomassie stain, with the areas of digestion appearing clear against a blue-stained background of undigested protein (Troberg et al. 2004).

MDA-MB-231 cells, stably transfected with the empty vector, uPAR-del4/5 or rab31 were seeded on collagen type IV pre-treated, or untreated 6 well plates. For each cell line 8×10^5 cells in 1 ml serum-free growing medium (DMEM) was applied to the wells. After cultivating for 48 h, supernatant was collected and stored at -20 °C.

After thawing, supernatant was centrifuged for 2 min at 4 °C at maximum speed. Gel apparatus (XCell SureLock Mini-Cell, Invitrogen) was filled with ice cold SDS-runningbuffer. For each condition, 30 µl supernatant (+ non-reducing loading buffer) was applied to a precasted 10 % gelatine gel (Novex, Invitrogen). After separation, SDS was removed from the gel washing twice with Novex Zymogram Renaturing Buffer for 1 h at RT. Prior to the addition of the developing buffer, gels were washed with dH₂O. Novex Zymogram Developing buffer was supplemented with 10 mM CaCl₂. Gels were incubated for 30 min at RT, buffer was refreshed and gels were incubated again for 72 h at 37 °C. The zymogram was stained using 0.1 % Coomassie solution, followed by destaining in 10 % aceticacid. Degraded gelatine appeared as white bands in front of the blue stained gelatine background.

5.9 Immunohistochemistry

Immunohistochemical-analysis was conducted in collaboration with the *Institut für Pathologie, der Technischen Universität Dresden*. Conventional sections from two samples of invasive ductal breast cancer were selected for immunostaining with pAb RT3. Immunohistochemistry was performed as described previously (Luther et al. 1996). Conventional sections from samples of invasive ductal breast cancer were selected for immunostaining with pAb RT3-IgG and pAb from animal #4 (RT4-IgG). Immunohistochemistry was performed as described previously (Luther et al. 1997). Briefly, formalin-fixed, paraffin-embedded sections of tumour tissue were dewaxed, rehydrated, and irradiated for antigen retrieval in a microwave oven in 100 mM citrate buffer, pH 6.0, at 750 W. After several washes with PBS, sections were treated with 0.3 % H₂O₂ for 30 min. Normal horse serum diluted in PBS was applied for 20 min to block endogenous peroxidase activity as well as nonspecific antibody binding. Subsequently, primary antibodies were allowed to react overnight at 4 °C followed by incubation with biotinylated horse anti-mouse IgG (DAKO, Hamburg, Germany) for 15 min at 37 °C. After washing, the Vectastain Elite ABC-reagent (Vector Laboratories, Burlingame, CA) was applied for 15 min at 37 °C, and the washing steps were repeated. The peroxidase reaction was developed with 3,3'-diaminobenzidine (Sigma-Aldrich) for 10 min at RT. Finally, counterstaining of sections was performed with haematoxylin. As a negative control, the primary antibody was omitted and replaced by PBS or by an irrelevant antibody.

5.10 Quantitative real time PCR

RNA of breast cancer cells was isolated using the RNeasy Mini kit (Qiagen, Hilden, Germany) according to manufacturers' recommendations. Reverse transcription of the RNA was conducted using the cloned AMV first-strand cDNA Synthesis Kit (Invitrogen, Carlsbad, USA), due to manufacturers' instructions. For quantification of uPAR-del4/5 and rab31 mRNA, quantitative real time PCR (QPCR) was accomplished using the LightCycler[®] system (Roche Diagnostics GmbH, Mannheim, Germany) as described previously (Luther et al. 2003; Kotsch

et al. 2008). All QPCR assays were conducted in collaboration with the *Institut für Pathologie, der Technischen Universität Dresden*.

5.11 Statistical analysis

Data was analyzed for statistical significance using the Mann-Whitney u-test supported by the software StatView. Differences with a p value ≤ 0.05 were appointed as statistically significant.

6 Results

6.1 Characterization of breast cancer cell lines overexpressing uPAR-del4/5

6.1.1 Stable transfection of breast cancer cell lines

The urokinase receptor splice variant uPAR-del4/5 is an independent, pure prognostic factor in breast cancer (Kotzsch et al. 2008). The tumor biological role of uPAR-del4/5 is rather unclear. Therefore, we started to investigate the effects of uPAR-del4/5 overexpression in different breast cancer cell lines *in vitro* and *in vivo*. Furthermore, the effect of different uPAR-del4/5 levels on tumor-relevant processes was investigated in this study.

Three different breast cancer cell lines MDA-MB-231, MDA-MB-435 and CAMA-1 were stably transfected with the eukaryotic expression plasmid pRcRSV harboring the cDNA of the urokinase receptor splice variant uPAR-del4/5. Cloning of the pRcRSV-derived expression plasmid encoding the full-length membrane-bound uPAR has been described by Lutz et al. (Lutz et al. 2001). Luther et al. used this plasmid as template for reverse long range PCR in order to delete the DNA sequences encoding exon 4 and exon 5 (Luther et al. 2003). Additionally, cells were stably transfected with the membrane-bound full-length receptor uPARwt. As a control, cell lines were transfected with the empty expression vector pRcRSV (vector control).

The pRcRSV plasmid carries a resistance gene for geneticin. Therefore, stable transfected cell clones were selected by supplementation of the growth medium with G418. Despite of their resistance, many cells showed no or very low expression of uPAR-del4/5 leading to a heterogeneous expression pattern of batch-transfected cell lines (Fig. 10). For this reason, single cell clones were isolated in order to generate cell lines with a homogeneous high, medium or low expression level of the splice variant. To achieve this, two rounds of subcloning were conducted to obtain a cell population derived from a single cell clone.

The human breast cancer cell line MDA-MB-231 is an epithelial cell line originating from a pleural effusion of a 51 year old caucasian women suffering from breast

adenocarcinoma in 1973 (Cailleau et al. 1974). This highly metastatic cell line was stably transfected with an expression plasmid encoding uPAR-del4/5 as described before.

uPARwt and uPAR-del4/5 expression was analyzed by immunocytochemical staining followed by CLSM analysis (Fig. 10). The monoclonal antibody IIIIF10 detects domain D1 of the urokinase receptor (Luther et al. 1997). Hence, this antibody can not distinguish between the wildtype and the splice variant. Nevertheless, the immunocytochemical staining showed an enhanced D1 staining in cells stably transfected with the uPAR-del4/5 plasmid, compared to vector control cells. Moreover, these cells showed an enhanced membrane staining, indicating the correct integration of the receptor into the cell membrane (Fig. 10). As already mentioned, batch-transfected cells showed a heterogeneous expression pattern of the receptor. After two rounds of subcloning cell lines with homogeneous high (#2-6-12), medium (#2-6-16) or low (#2-11-10) expression of the receptor were isolated (Fig. 10).

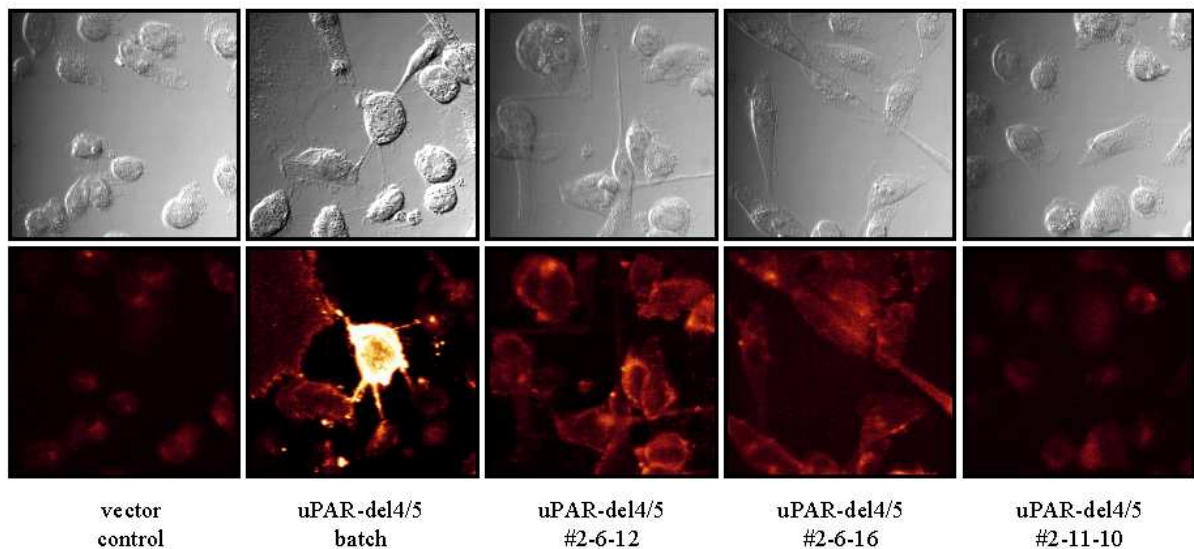


Fig. 10 Immunocytochemical staining of MDA-MB-231 cells overexpressing uPAR-del4/5

MDA-MB-231 human breast cancer cells, stably transfected with uPAR-del4/5 or vector control were seeded on fibronectin-coated cell culture chamber slides and cultured for 24 h. Cells were fixed with 4 % PFA solution and immunostained using a mAb directed against D1 of uPAR (IIIIF10 dilution 1:100). Signal was detected using a secondary Alexa488 conjugated goat anti-mouse IgG.

The overexpression was further analyzed by Western blot analysis. Cell lysates were prepared as described before, the total protein content was determined and

20 µg total lysate were applied under reducing conditions to the SDS gel. After electrophoresis, the proteins were transferred to a PVDF membrane by usage of a semi-dry blotting device. Immunostaining with the IIF10 antibody (Fig. 11) confirmed the expression levels observed by immunocytochemical staining (Fig. 10). Cell clone #2-6-12 represented the highest expression of the splice variant compared to the medium expression of clone #2-6-16 and the very low expression in clone #2-11-10. Batch-transfected cells exhibited an intermediate expression of uPAR-del4/5. As endogenous control the membrane was stained for the housekeeping protein GAPDH (Fig. 11).

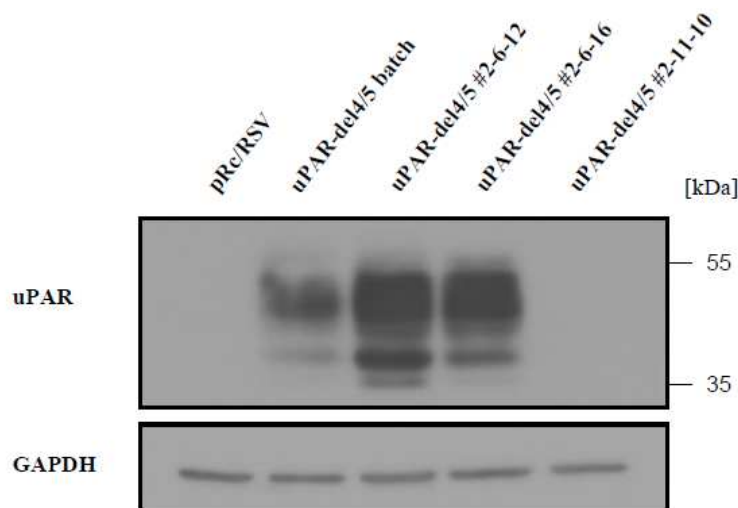


Fig. 11 Western blot of stably transfected MDA-MB-231 cells overexpressing uPAR-del4/5

MDA-MB-231 cells transfected with empty vector control or the uPAR-del4/5 expression plasmid were lysed and analyzed by Western blot. Membranes were stained using the mAb IIF10 (1:1000 in 5 % (w/v) skimmed milk powder in TBST), directed to D1 of uPAR. Reactive proteins were visualized by chemiluminescence as described before. For control of equal loading membranes were stripped and subsequently stained using a mAb detecting the endogenous housekeeping control protein GAPDH.

To distinguish between wildtype uPAR and uPAR-del4/5, membranes were stained with the monoclonal antibody IID7 directed against domain D2 of the receptor (Luther et al. 1997). Vector control cells showed a weak endogenous expression of D2. uPAR-del4/5 transfected cells, which exhibited a strong signal for D1, represented only faint reaction with the mAb directed to D2 indicating the expression of the splice variant uPAR-del4/5 (Fig. 12). In contrast to this, cells

transfected with a plasmid encoding the wildtype receptor showed a strong signal for D2. This confirms that cells transfected with the plasmid encoding the uPAR-del4/5 construct are expressing the splice variant.

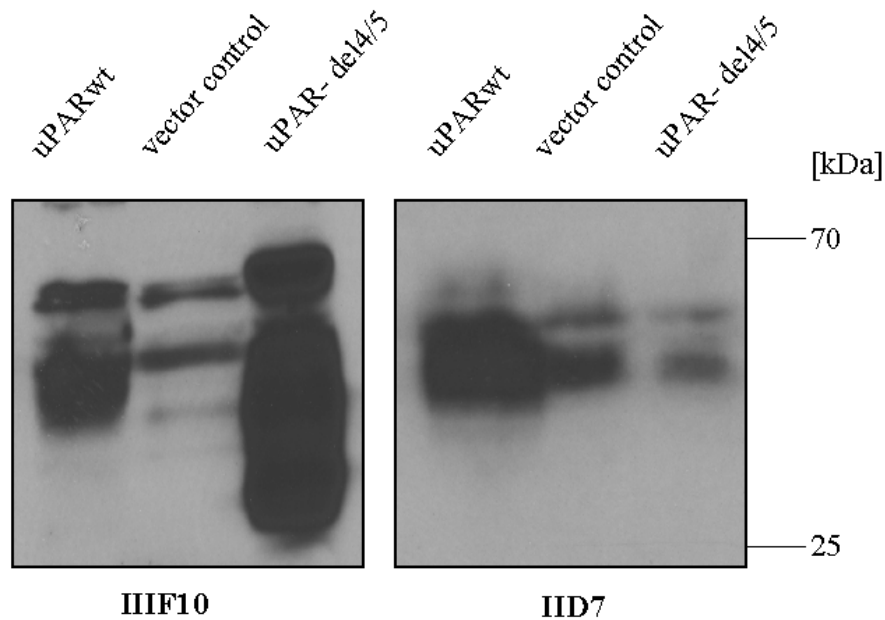


Fig. 12 Characterization of uPAR expression by D1-specific mAb IIF10 and D2-specific mAb IID7

To distinguish between different uPAR variants membranes were stained with antibodies directed against different domains of the receptor. MDA-MB-231 cells transfected with the wildtype uPAR, the splice variant uPAR-del4/5 or vector control were lysed and analyzed by western blot. **Left box** The membrane was stained using a monoclonal antibody IIF10 directed against D1 of uPAR (1:1000 in 5 % (w/v) skimmed milk powder /TBST). **Right box** The membrane was stripped and subsequently incubated with a mAb IID7 directed against D2 of uPAR (1:500 in 5 % (w/v) skimmed milk powder /TBST).

Expression of different uPAR-del4/5 overexpressing cells was additionally confirmed by flow cytometry. Cells were stained with mAb IIF10 as described before and analyzed by flow cytometry (Fig. 13). This data confirmed the results obtained by ICC and Western blot. The isolated cell clones showed differential expression levels of the splice variant. Cell clones #2-6-12 and #2-6-16 had very high levels of uPAR-del4/5 compared to vector control cells. In addition to this, a slightly elevated expression of the splice variant was detected in clone number #2-11-10 compared to vector control cells.

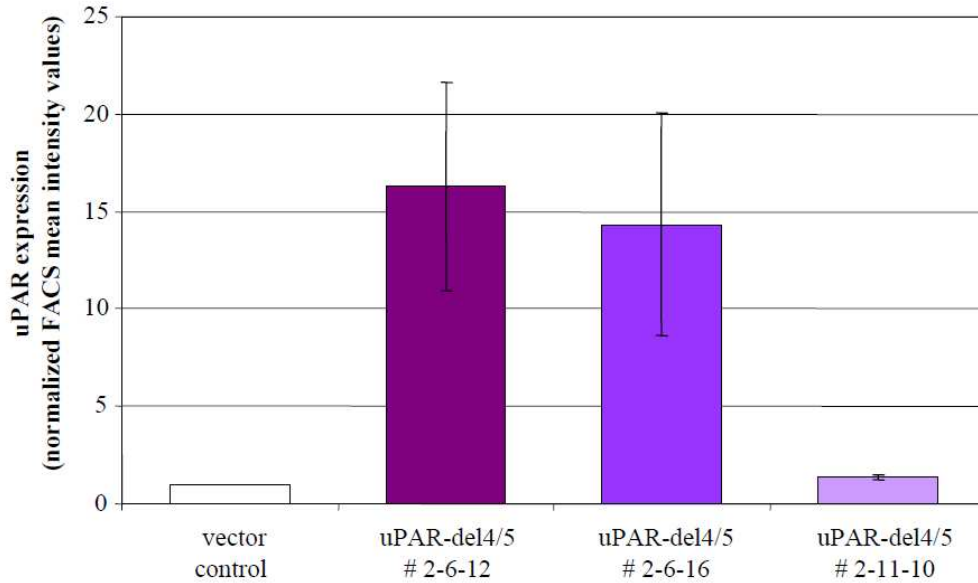


Fig. 13 Determination of uPAR-del4/5 expression by FACS analysis

Expression of uPAR-del4/5 in selected MDA-MB-231 cell clones was measured by FACS analysis. Normalised FACS mean fluorescence intensity values of 5 individual experiments are depicted as the mean \pm SEM.

The uPAR-del4/5 expression level of clone #2-11-10 was not distinctly different from vector control cells in ICC and Western blot analysis. Using quantitative PCR, however, we demonstrated a significantly upregulated uPAR-del4/5 mRNA expression compared to vector control cells (Fig. 14).

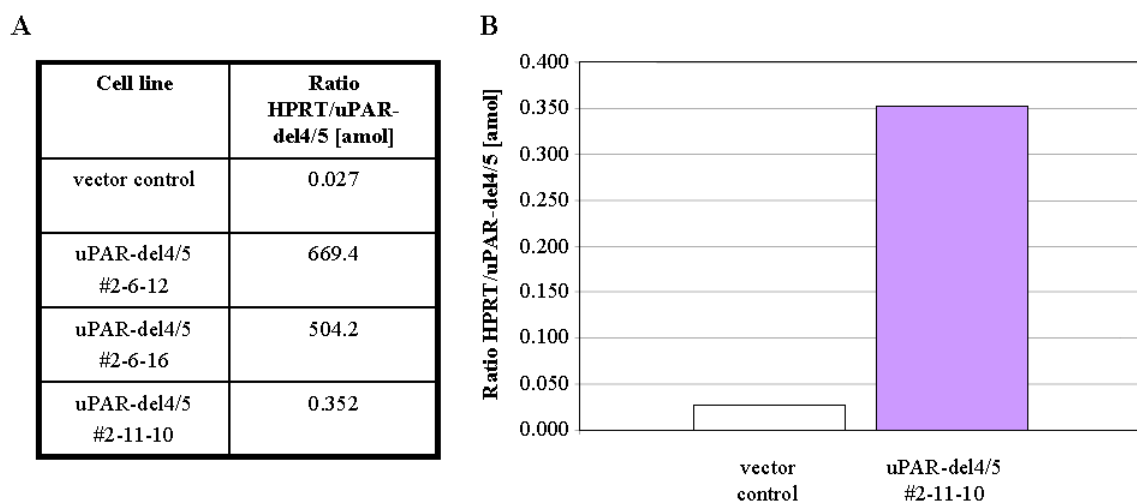


Fig. 14 Quantitative PCR analysis of MDA-MB-231 cells overexpressing uPAR-del4/5

uPAR-del4/5 mRNA expression of stably transfected MDA-MB-231 cells was determined using quantitative PCR as described before. **A** RNA content was calculated relative to the measured HPRT amount for each uPAR-del4/5 overexpressing cell clones. **B** mRNA expression of the low expressing cell clone #2-11-10 compared to the expression in vector control cells.

The non-invasive breast cancer cell line CAMA-1 was established from cells in the malignant pleural effusion of a patient with adenocarcinoma of the breast by J. Fogh et al. in 1975 (Fogh et al. 1977). CAMA-1 cells have no detectable endogenous uPAR mRNA expression (data not shown). Therefore, this cell line was selected for further analysis of the tumorbiological role of uPAR-del4/5. CAMA-1 cells were stably transfected with pRcRSV expression plasmids encoding uPAR-del4/5, or the empty vector respectively. Single cell clones were isolated and analyzed by immunocytochemical staining. Enhanced staining of the receptor was monitored at the cell membrane, indicating a correct membrane insertion of uPAR-del4/5 in stable transfected CAMA-1 cells (Fig. 15). Batch-transfected cell lines again showed a heterogeneous expression of uPAR-del4/5. After two rounds of subcloning, homogeneous cell lines with differential expression levels were isolated (Fig. 15). Vector control cells showed no endogenous expression of uPAR. The batch-transfected cell line represented a heterogeneous expression of uPAR-del4/5. In contrast to this, cell clone number #1-10-3 was characterized by a homogeneous medium expression of uPAR-del4/5.

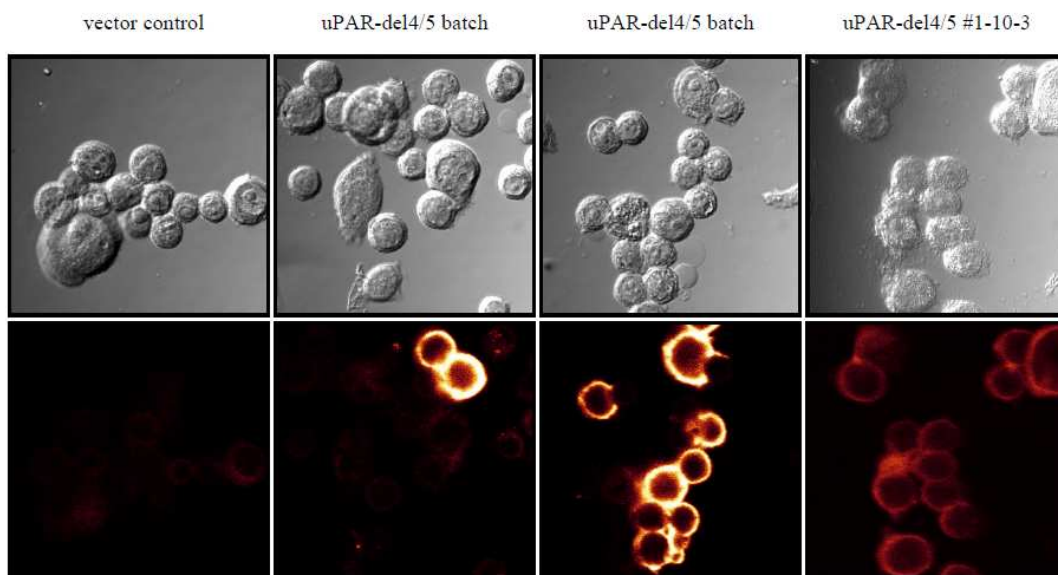


Fig. 15 Immunocytochemical staining of CAMA-1 cells overexpressing uPAR-del4/5

CAMA-1 human breast cancer cells, stably transfected with the uPAR-del4/5 plasmid or the empty vector, were seeded on fibronectin-coated cell culture chamber slides and cultured for 24 h. Cells were fixed with 4 % PFA solution and immunostained using a mAb IIIIF10, directed against D1 of uPAR (dilution 1:100). The signal was detected using a secondary Alexa488 conjugated goat anti-mouse IgG.

The expression level of different cell clones was determined by Western blot analysis using mAb IIF10, as described before. Cell clones with high (#1-10-19), medium (#1-10-3) or low (#1-10-5) expression of uPAR-del4/5, as well as batch-transfected cells were selected for further analysis (Fig. 16).

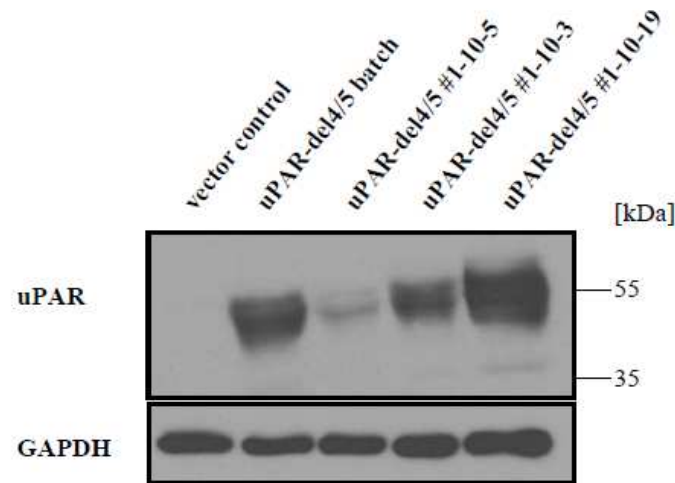


Fig. 16 Western blot analysis of stably transfected CAMA-1 cells overexpressing uPAR-del4/5

CAMA-1 cells transfected with empty vector control or the uPAR-del4/5 expression plasmid were lysed and analyzed by Western blot. Membranes were stained using the mAb IIF10 (1:1000 in 5 % (w/v) skimmed milk powder in TBST). Reactive proteins were visualized by chemiluminescence as described before. For control of equal loading membranes were stripped and subsequently stained using a mAb detecting the endogenous control GAPDH.

The human cell line MDA-MB-435 was derived from the pleural effusion of a female patient with breast cancer in the late 1970s (Cailleau et al. 1978). The metastatic cell line has been used in a large number of studies investigating the molecular mechanism of breast cancer. In the year 2000, speculations about the origin of this cell line arose. Expression array studies revealed a gene expression profile similar to melanoma cells. Additional studies supported the idea that MDA-MB-435 and the melanoma cell line M14 are identical, due to an early cross-contamination of both cell lines. Another study supported the idea of identical cell lines, but classified them as breast cancer cell lines. The most current study on this issue from Ann Chambers states that MDA-MB-435 and M14 cells are identical cell lines and originate from a breast cancer patient (Chambers 2009).

MDA-MB-435 cells were stably transfected with pRcRSV expression plasmids encoding uPAR-del4/5 or the empty vector. Western blot analysis revealed the overexpression of uPAR-del4/5 in two independent batch-transfected cell lines. Vector control cells showed no endogenous uPAR expression (Fig. 17).

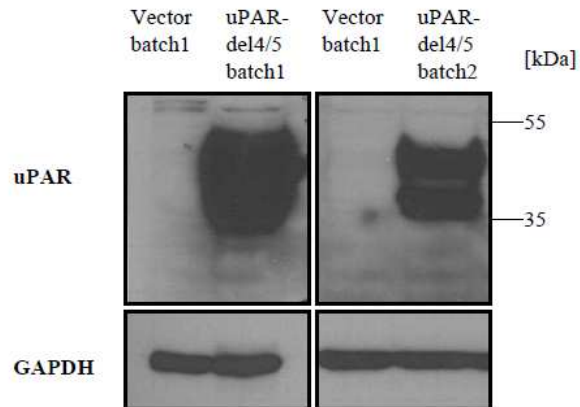


Fig. 17 Western blot analysis of stably transfected MDA-MB-435 cells overexpressing uPAR-del4/5

MDA-MB-435 cells transfected with empty vector control or the uPAR-del4/5 expression plasmid were lysed and analyzed by Western blot. Membranes were stained using the mAb IIF10 (1:1000 in 5 % (w/v) skimmed milk powder in TBST). Reactive proteins were visualized by chemiluminescence as described before. For control of equal loading membranes, were stripped and subsequently stained using a mAb detecting the endogenous control GAPDH.

Immunocytochemical staining of MDA-MB-435 cells indicated a membrane location of the receptor. uPAR-del4/5 expression in MDA-MB-435 cells was homogeneous without subcloning (Fig. 18). As already demonstrated by Western blot analysis, vector control cells showed no endogenous expression of uPAR. The batch-transfected cell lines, batch1 and batch2 represented a high expression of uPAR-del4/5.

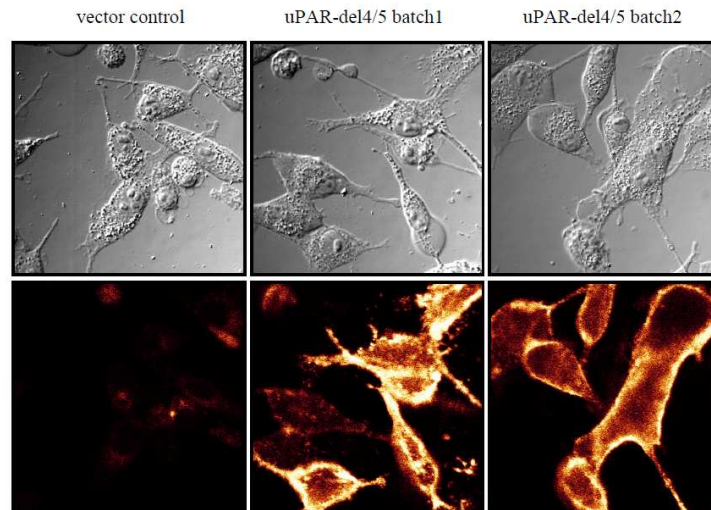


Fig. 18 Immunocytochemical staining of MDA-MB-435 cells overexpressing uPAR-del4/5

MDA-MB-435 human breast cancer cells, stably transfected with uPAR-del4/5 or vector control, were seeded on fibronectin-coated cell culture chamber slides and cultured for 24 h. Cells were fixed with 4 % PFA solution and immunostained using a mAb directed against D1 of uPAR (IIIIF10 dilution 1:100). The signal was detected using a secondary Alexa488 conjugated goat anti-mouse IgG.

6.1.2 Proliferation of breast cancer cell lines overexpressing uPAR-del4/5

The impact of uPAR-del4/5 overexpression on cell proliferation was analyzed using manual counting. Cells were seeded in 24 well plates, in triplicates for each time point. 24, 48, 72 and 96 h post seeding cells were detached from the well and counted in a Blaubrand[®] counting chamber under trypan blue exclusion.

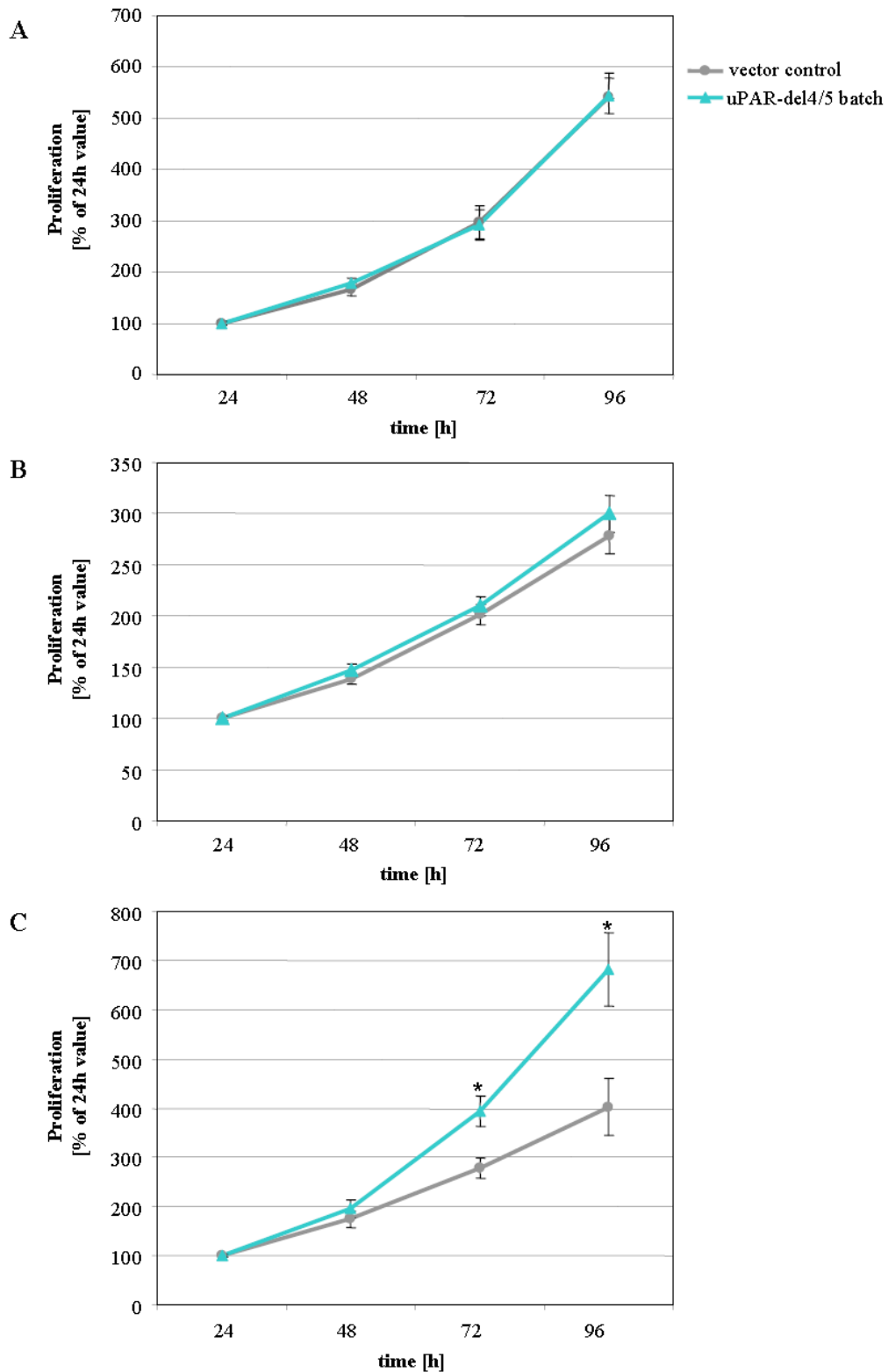


Fig. 19 Proliferation of cells over-expressing uPAR-del4/5

Cells were seeded to 24 well plates, detached with 0.05 % EDTA-solution after 24, 48, 72 and 96 h and counted with the help of a Blaubrand[®]-chamber under trypan blue exclusion. Proliferation curves of **A** MDA-MB-231, **B** CAMA-1 and, **C** MDA-MB-435 cells overexpressing uPAR-del4/5 (blue) or transfected with the empty vector (grey). Cell number at 24h was set to 100 %. Increase in cell number was expressed relative to the 24 h value in %. The Graph shows the mean value of at least three independent experiments. Statistically significant differences ($p < 0.05$) are indicated by an asterisk.

MDA-MB-231 and CAMA cells overexpressing uPAR-del4/5 showed no significant changes in proliferation after 96 h of incubation (Fig. 19 A and B). In contrast to this, batch-transfected MDA-MB-435 cells showed a significantly increased proliferation after 96 h when uPAR-del4/5 was overexpressed (Fig. 19 C).

6.1.3 Adhesion of uPAR-del4/5 overexpressing breast cancer cell lines to extracellular matrix proteins

In order to analyze the adhesive capacity of breast cancer cells overexpressing uPAR-del4/5, 96 well plates were coated with different extracellular matrix proteins. Equal number of cells were seeded and incubated for 2 h at 37 °C. After washing the plates with PBS, hexosaminidase substrate was added for 90 min at 37 °C, followed by addition of the stop solution. The chromogenic change was measured and the relative adhesion of the cell lines was normalized to the adhesion of vector control cells on each coating.

MDA-MB-231 cells showed a significantly reduced adhesion towards collagen type IV. The strongest effect was observed testing cell clones with a high (#2-6-12) expression of the splice variant, similar results were obtained testing cell clones with a medium (#2-6-16) expression level and batch-transfected cells. Cell clones with a low expression of the splice variant showed a slight but significant reduction of adhesion towards collagen type IV. As a positive control, cells overexpressing the wildtype receptor were analyzed. These cells are characterized by an enhanced adhesion to extracellular matrix proteins (Fig. 20).

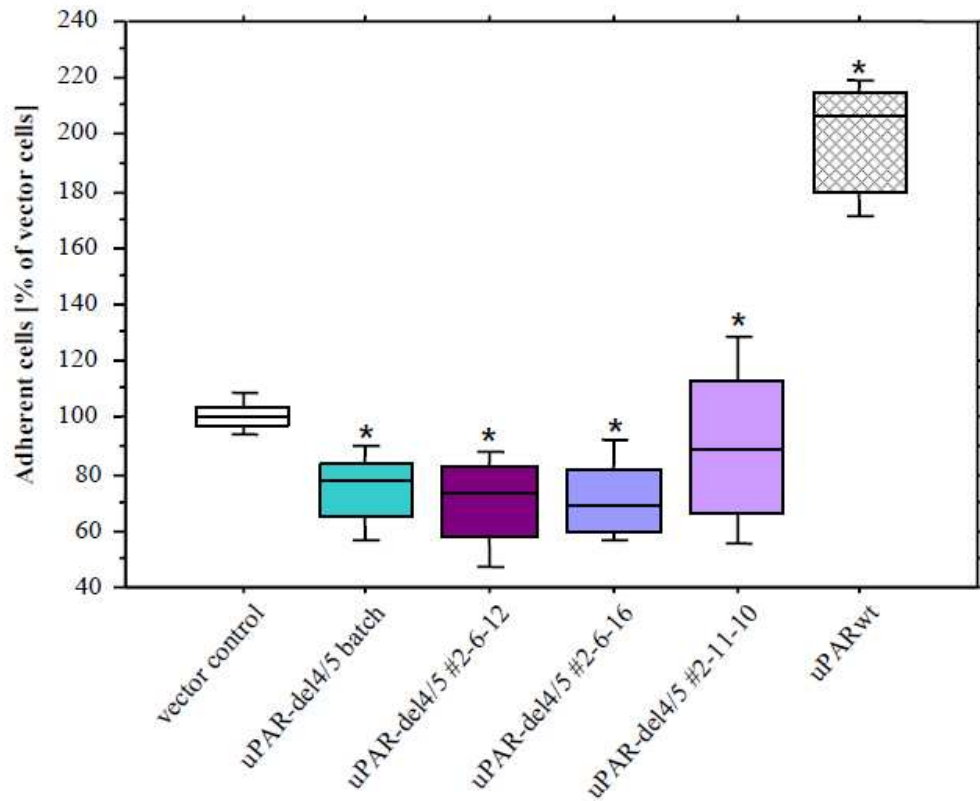


Fig. 20 Overexpression of uPAR-del4/5 reduces adhesion of MDA-MB-231 cells to collagen type IV

MDA-MB-231 cells were seeded on collagen type IV-coated 96 well plates. After 2 h of cell cultivation, the number of adherent cells was monitored by the hexosaminidase activity assay. Adhesion of vector control cells (white), batch-transfected uPAR-del4/5 overexpressing cells (green), as well as cell clones with a high (dark purple), medium (blue) or low expression (violet) of uPAR-del4/5 were analyzed. As a positive control cells overexpressing the wildtype receptor (checked) were included. At least 4 independent experiments were performed in triplicates each. The results are given in % relative to the cell number of adherent vector-transfected control cells. Whisker box plots indicate the 25th and 75th percentile, the vertical bars indicate the 10th and 90th percentile. The median is indicated by a bar within the box. Statistically significant differences ($p < 0.05$) are indicated by an asterisk.

Similar effects were observed with other protein coatings like fibronectin, vitronectin, laminin and collagen type I (Table 2).

	uPAR-del4/5 batch	uPAR-del4/5 #2-6-12	uPAR-del4/5 #2-6-16	uPAR-del4/5 #2-11-10	uPARwt batch
FN	86.4* +/- 3.6	70.6* +/- 4.8	70.9* +/- 5.3	85.2* +/- 6.7	196.3* +/- 3.9
VN	82.6* +/- 2.8	60.2* +/- 7.0	62.4* +/- 5.9	78.9* +/- 8.9	194.8* +/- 6.6
Ln	81.7* +/- 3.0	80.0* +/- 12.3	78.2* +/- 11.9	92.7 +/- 20.2	200.7* +/- 32.3
Col I	80.8* +/- 3.9	71.2* +/- 7.7	69.2* +/- 5.8	87.4 +/- 12.4	191.6* +/- 15.1
Col IV	74.7* +/- 4.2	70.6* +/- 7.9	72.0* +/- 6.1	89.7* +/- 13.8	200.3* +/- 11.4

Table 2 Adhesion of MDA-MB-231 cells to extracellular matrix proteins

Adhesion of MDA-MB-231 cells overexpressing uPAR-del4/5 towards fibronectin (FN), vitronectin (VN), laminin (Ln), collagen type I (Col I) and collagen type IV (Col IV). At least 4 independent experiments were performed in triplicates each. The results are given as the mean value in %, relative to the cell number of adherent vector-transfected control cells. Statistically significant differences ($p < 0.05$) are indicated by an asterisk.

Analysis of CAMA-1 cells revealed even stronger effects. Batch-transfected cells showed a moderate but significant reduction towards collagen type IV. Cell clones with high (#1-10-19) and medium (#1-10-5) expression showed a strong decrease of adhesion towards collagen type IV. The cell clone with low (#1-10-3) expression of uPAR-del4/5 showed a moderate but significant reduction of adhesive capacity (Fig. 21). The effect appeared dependent on the expression level of uPAR-del4/5. Adhesion of high and medium expressing cell clones was significantly reduced compared to the adhesion of cell clones expressing low levels of uPAR-del4/5 (Fig. 21).

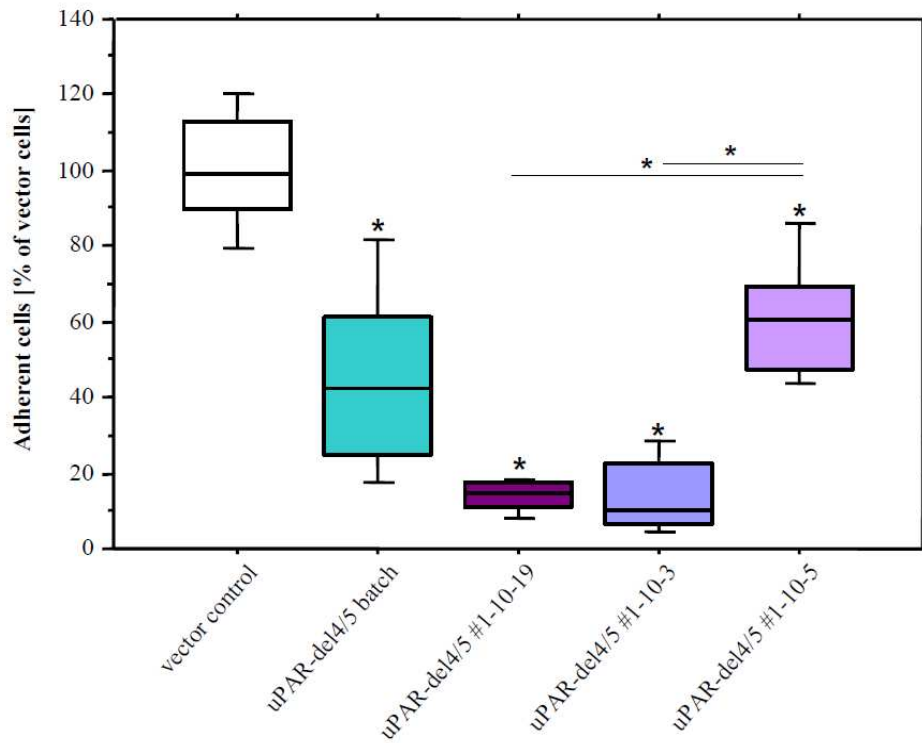


Fig. 21 Overexpression of uPAR-del4/5 reduces adhesion of CAMA-1 cells to collagen type IV

CAMA-1 cells were seeded on collagen type IV-coated 96 well plates. After 2 h of cell cultivation, the number of adherent cells was monitored by the hexosaminidase activity assay. Adhesion of vector control cells (white), batch-transfected uPAR-del4/5 overexpressing cells (green), as well as cell clones with a high (dark purple), medium (blue) or low expression (violet) of uPAR-del4/5 were analyzed. At least 4 independent experiments were performed in triplicates each. The results are given in % relative to the cell number of adherent vector-transfected control cells. Whisker box plots indicate the 25th and 75th percentile, the vertical bars indicate the 10th and 90th percentile. The median is indicated by a bar within the box. Statistically significant differences ($p < 0.05$) are indicated by an asterisk.

Testing adhesion of CAMA-1 cells towards other components of the extracellular matrix revealed similar results (Table 3).

	uPAR-del4/5 batch	uPAR-del4/5 #1-10-19	uPAR-del4/5 #1-10-3	uPAR-del4/5 #1-10-5
VN	73.0* +/- 6.8	84.1* +/- 6.2	69.1* +/- 7.0	81.1* +/- 4.2
Col I	36.0* +/- 7.8	20.9* +/- 5.4	20.1* +/- 7.2	56.2* +/- 14.4
Col IV	44.2* +/- 9.9	13.9* +/- 1.9	14.5* +/- 4.2	60.6* +/- 7.0

Table 3 Adhesion of CAMA-1 cell overexpressing uPAR-del4/5 to extracellular matrix proteins

Adhesion of CAMA-1 cells overexpressing uPAR-del4/5 towards vitronectin (VN), collagen type I (Col I) and collagen type IV (Col IV). At least 4 independent experiments were performed in triplicates each. The results are given as the mean value in %, relative to the cell number of adherent vector-transfected control cells. Statistically significant differences ($p < 0.05$) are indicated by an asterisk.

Analysis of batch-transfected MDA-MB-435 cells showed similar results. In this cell line, overexpression of uPAR-del4/5 caused a significantly decreased adhesive capacity towards collagen type I, fibronectin, vitronectin and laminin. Interestingly, adhesion to collagen type IV was not significantly altered in MDA-MB-435 cells (Fig. 22).

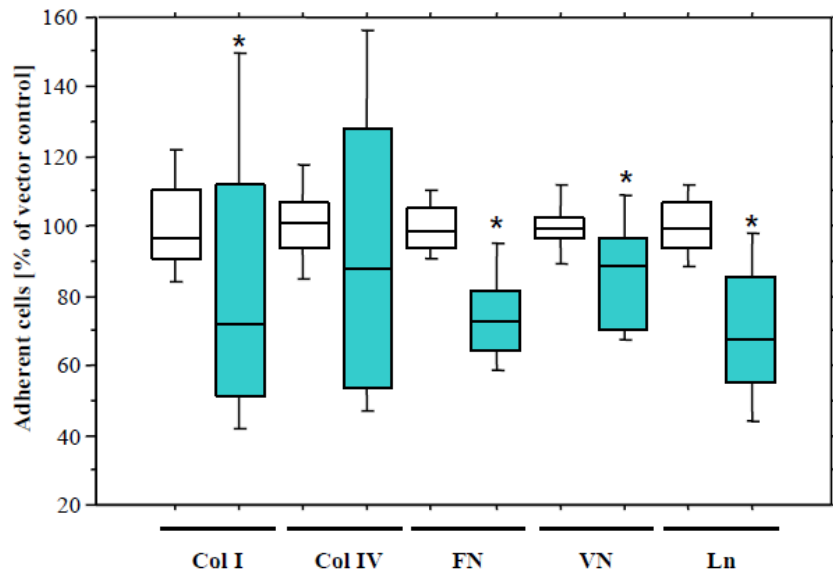


Fig. 22 Adhesion of MDA-MB-435 cells towards ECM proteins

Adhesion of MDA-MB-435 cells overexpressing uPAR-del4/5 towards collagen type I (Col I), fibronectin (FN), vitronectin (VN), and laminin (Ln). Vector control cells (white) and batch-transfected uPARdel4/5 overexpressing cells (green) were analyzed. At least 4 independent experiments were performed in triplicates each. The results are given in % relative to the cell number of adherent vector-transfected control cells. Whisker box plots indicate the 25th and 75th percentile, the vertical bars indicate the 10th and 90th percentile. The median is indicated by a bar within the box. Statistically significant differences ($p < 0.05$) are indicated by an asterisk.

6.1.4 Invasive capacity of breast cancer cells overexpressing uPAR-del4/5

The invasive capacity of cells overexpressing uPAR-del4/5 was determined using matrigelTM transwell assays. For this, 24 well transwell plates were coated with an artificial basement membrane called matrigelTM. The matrigelTM used in this assay is extracted from the Engelbreth-Holm-Swarm (EHS) mouse sarcoma. The basement membrane of this tumor mainly consists of laminin, collagen type IV, heparan sulfate, proteoglycans and entactin (see product description of the manufacturer). Cells were seeded in the upper part of the chamber in serum-free medium. The lower part of the chamber was filled with medium containing 10 % (v/v) FCS as a chemoattractant. Plates were incubated for 24 h, allowing the cells to degrade the basement membrane and migrate through the pores of the transwell into the lower side of the insert. After incubation, cells in the upper chamber were removed and the cells in the lower part were fixed, stained and counted. The number of invaded cells was normalized to the number of invaded

vector control cells. For this assay only the highly metastatic cell line MDA-MB-231 was used, as the other cell lines were not able to invade through the matrix. Batch-transfected uPAR-del4/5 overexpressing cells showed a significant reduction of their invasive capacity through matrigelTM. The effect was even stronger for cell clones with high (#2-6-12) and medium (#2-6-16) expression levels. Only the cell clone with a low expression of the splice variant showed no significant change (Fig. 23). The observed effects appear dependent on the level of uPAR-del4/5 expression as the number of invaded cells analysing high expressing cell clones was significantly lower compared to the number of invaded cells in the low expressing cell line (Fig. 23). In contrast to this, cells overexpressing wildtype uPAR showed a strong increase of invasive capacity (data not shown), as already described by others (Sato et al. 2010).

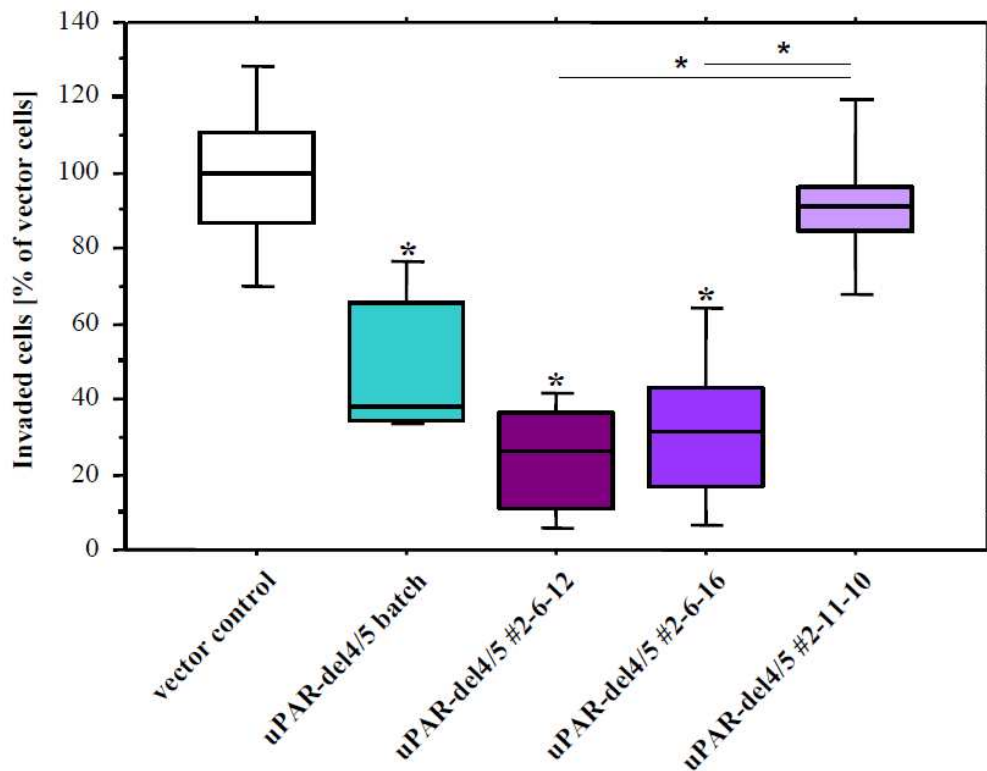


Fig. 23 Overexpression of uPAR-del4/5 affects the invasive capacity of MDA-MB-231 cells through matrigel™

Stably transfected MDA-MB-231 cells were seeded into the upper compartments of matrigel™-coated invasion chambers. After 24 h of incubation, invaded cells were fixed, stained, and counted. Invasive capacity of vector control cells (white), batch-transfected uPAR-del4/5 overexpressing cells (green), as well as cell clones with a high (dark purple), medium (blue) or low expression (violet) of uPAR-del4/5 were analyzed. At least three independent experiments were performed in triplicates each. The results are given in %, normalized to the number of invaded vector-transfected cells. Whisker box plots indicate the 25th and 75th percentile, the vertical bars indicate the 10th and 90th percentile. The median is indicated by a bar within the box. Statistically significant differences ($p < 0.05$) are indicated by an asterisk.

6.1.5 Effects of uPAR-del4/5 overexpressing MDA-MB-231 cells on lung colonisation in a xenograft mouse model

The xenograft mouse model is a highly accepted tool to study the regulation of human cells growth and metastasis in an *in vivo* environment (Clarke 1996).

In humans, breast cancer usually spreads *via* the lymphsystem and forms distant metastasis in the bone, brain, the adrenal gland the liver, and the lung. In contrast to this, mammary cancers in mouse nearly exclusively metastasize to the lungs *via*

the bloodstream. MDA-MB-231 cells are a commonly used human breast cancer xenograft model (Kim et al. 2004).

MDA-MB-231 cells transfected with the uPAR-del4/5 plasmid or the empty vector were tagged with the *lacZ*-gene via viral spin-infection. After XGal-staining *lacZ*-gene tagged cells appeared blue (Fig. 24). This allowed visualization of the transfected cells at the site of metastasis.

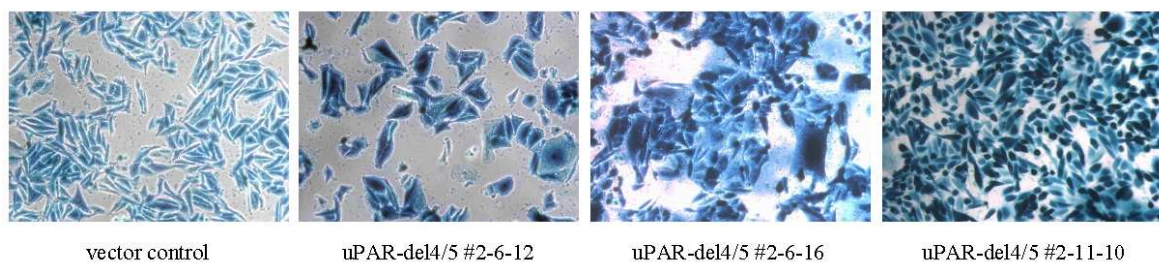


Fig. 24 XGal-stained *lacZ*-tagged MDA-MB-231 cells

MDA-MB-231 overexpressing uPAR-del4/5 or transfected with the empty vector were tagged with the *lacZ*-gene. Tagged cells express β -galactosidase which can be monitored by XGal-staining of the cells. β -galactosidase expressing cells convert the XGal substrate leading to an indigo blue staining.

Cells ($1 \cdot 10^6$) were injected into the tail vein of immune-compromised female nude mice CD1 nu/nu (Charles River; Sulzfeld). After 35 days, mice were sacrificed, lungs were prepared and XGal-stained. Blue colonies were counted on the surface of the lung. The entire xenograft experiment, including tagging the cells with the *lacZ*-gene was performed in collaboration with the laboratory of Prof. Dr. Achim Krüger (*Experimentelle Onkologie, Klinikum rechts der Isar*). The number of lung metastasis was significantly reduced in animals which were inoculated with cells overexpressing uPAR-del4/5 compared to mice injected with vector control cells (Fig. 25). The total number of metastases in animals injected with uPAR-del4/5 #2-11-10, low expression of uPAR-del/5, was extremely low. Only 5 out of 9 animals formed metastasis at all. Out of these 5 animals, 3 displayed only 1 colony along the whole lung. Therefore, the results of this group should be evaluated with caution.

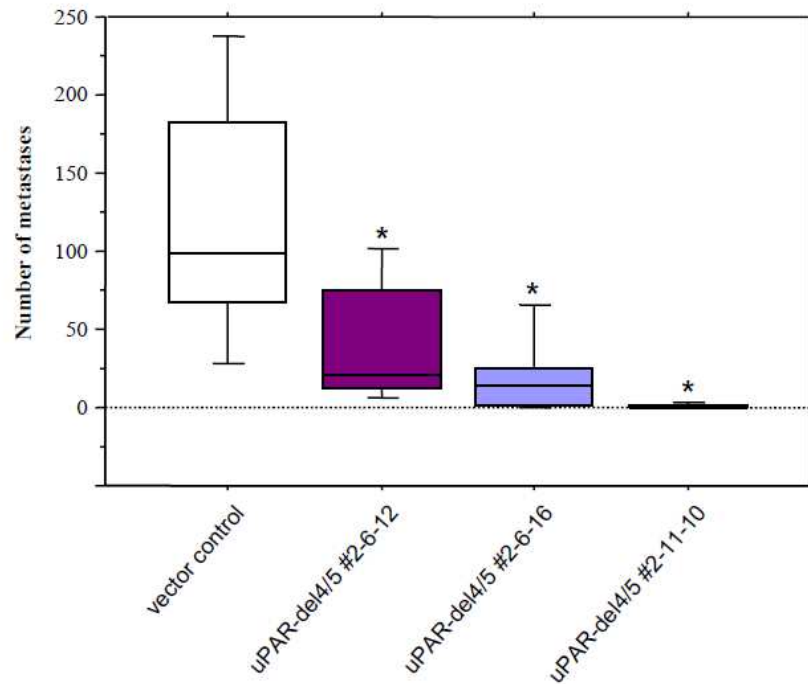


Fig. 25 Overexpression of uPAR-del4/5 affects lung colonization and metastatic growth of human breast cancer cells.

Stably transfected, *lacZ*-tagged, MDA-MB-231 cells were inoculated into nude mice *via* tail vein injection. Mice received either vector control cells (white columns, n=8) or uPAR-del4/5 overexpressing cell clones with a high (dark purple, n=9), medium (blue, n=7) or low expression (violet, n=9) of uPAR-del4/5. Animals were sacrificed at day 35 after injection, lungs were collected and stained with XGal. Metastases were counted in lungs of the mice. Whisker box plots indicate the 25th and 75th percentile, the vertical bars indicate the 10th and 90th percentile. Results are expressed as the median number of metastases. The median is indicated by a bar within the box. Statistically significant differences ($p < 0.05$) to the vector-control group are indicated by an asterisk.

6.2 Characterization of polyclonal antibodies directed against rab31

Rab31 mRNA levels in lymphnode-negative breast cancer tissue have been shown to be an independent prognostic factor for breast cancer. Therefore it would be very interesting, to also correlate protein levels of rab31 with the outcome of breast cancer patients. In the beginning of this study no antibodies directed to rab31 were commercially available. For this reason, polyclonal antibodies directed to rab31 were generated in collaboration with Pineda Antibody Service (Berlin). The medical dissertation of Sonja Schäfer (*Klinische Forschergruppe der Frauenklinik, Klinikum rechts der Isar*) describes the generation of antibodies directed against rab31 in detail.

Selected rabbit anti-rab31 antibodies were specifically purified for immunoglobulin IgG antibodies. For this, serum proteins were removed from immunized rabbit blood serum using protein A/G-chromatography. This procedure, performed by Pineda Antibody Service (Berlin) achieved a total IgG fraction with a purity of higher than 95 %.

6.2.1 Specificity of rab31 directed antibodies in immunocytochemical (ICC) staining

IgG-purified rabbit anti-rab31 antibodies as well as sera of immunized chicken were analyzed for specific staining using immunocytochemistry followed by CLSM analysis (Fig. 26). MDA-MB-435 cells overexpressing rab31 or mock-transfected cells were seeded on fibronectin-treated cell culture chamber slides and cultured for 24 h. Cells were fixed, permeabilized with 0.025 % (w/v) saponin and immunostained using either the purified rabbit anti-rab31 IgG antibodies or unpurified chicken anti-rab31 sera. Staining with the antibodies rabbit T1-IgG (RT1-IgG) and rabbit T2-IgG (RT2-IgG) resulted in a strong cytosolic staining in both cell lines. No differences in the staining pattern between vector control and rab31 overexpressing cells could be detected, indicating a nonspecific staining (Fig. 26 A and B). In contrast to this, the rabbit T3-IgG (RT3-IgG) antibody detects rab31 specifically in rab31 overexpressing cells. MDA-MB-435 vector control cells, which have no detectable endogenous mRNA expression of rab31 (Fig. 31)

remained unstained. Although, immunocytochemical stainings of MDA-MB-435 cells using the RT3-IgG antibody showed a specific detection of rab31, the staining intensity was not very bright (Fig. 26 C). RT4-IgG and all chicken anti-rab31 antibodies proved to be not suitable for immunocytochemical staining. Nevertheless, these antibodies showed rab31 specific reaction in other applications like Western blot.

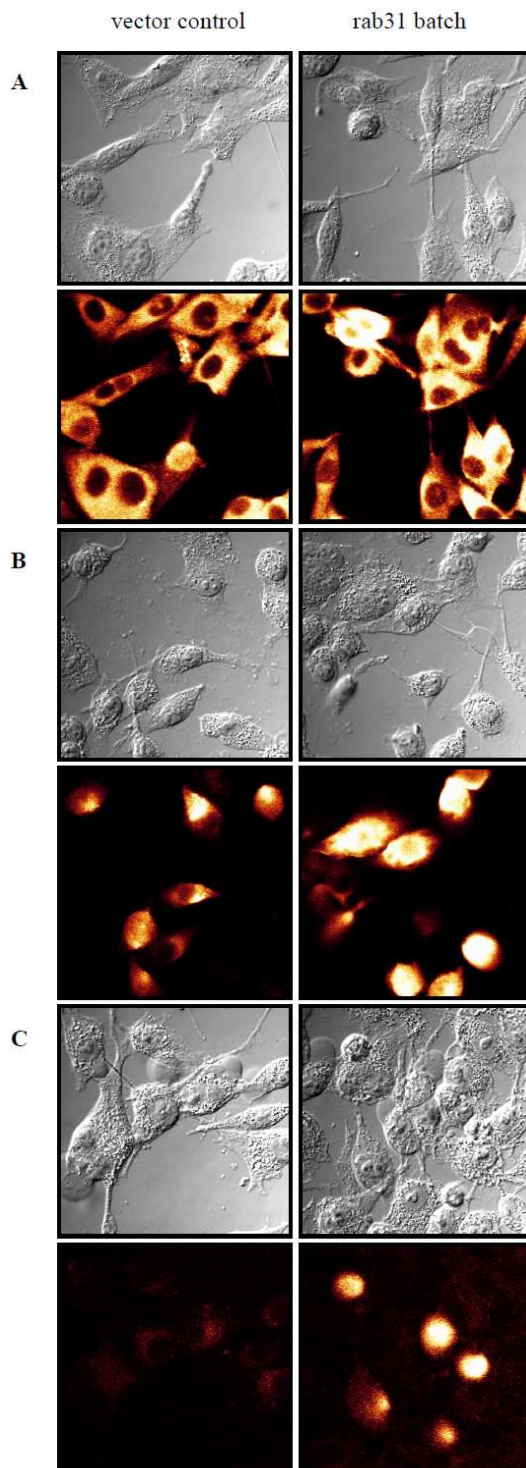


Fig. 26 Immunocytochemical staining of MDA-MB-435 cells using IgG-purified antibodies directed against rab31

MDA-MB-435 human breast cancer cells, stably transfected with rab31 or vector control were seeded on fibronectin-coated cell culture chamber slides and cultured for 24 h. Cells were fixed with 4 % (w/v) PFA solution, permeabilized with 0.025% (w/v) saponin and immunostained using pAbs directed against rab31.

A RT1-IgG,

B RT2-IgG and,

C RT3-IgG.

Signal was detected using a secondary Alexa488 conjugated goat anti-rabbit IgG.

6.2.2 Cross-reactivity of rab31 directed antibodies

Rab GTPases are highly conserved proteins. The Rab protein sharing highest amino acid identity with rab31 is rab22A. Rab31 belongs to the rab5 subfamily. Therefore, it was necessary to test whether the generated antibodies display any cross-reactivity with other Rab proteins. Recombinant rab5 and rab22A proteins were applied to SDS-PAGE followed by Western blot analysis. Staining with RT1-IgG antibody revealed no cross-reactivity signal for rab5 or rab22A (Fig. 27 A). Recombinant rab31 protein, N-terminally histidine tagged (rab31-His) was detected specifically using the antibodies RT1-IgG, RT3-IgG or RT4-IgG (Fig. 27 A, B and C). Antibodies RT3-IgG and RT4-IgG showed no cross-reactivity with rab5 but some with recombinant rab22A. However, equal amounts of rab31-His resulted in a much stronger signal (Fig. 27 B and C). Rab31 was specifically detected in total cell lysate from transfected breast cancer cells by the pAb RT1-IgG and RT3-IgG (Fig. 27 A and B). Rabbit RT4-IgG detected rab31 in total cell lysate but, there was also some unspecific reaction with proteins in the range from 20 -30 kDa (Fig. 27 C). Testing of the pAb RT2-IgG in Western blot analysis and one-sided ELISA revealed no sensitive detection of rab31-His (data not shown) compared to the sensitivity of the other generated pAbs. Therefore, pAb RT2-IgG was excluded from further analysis.

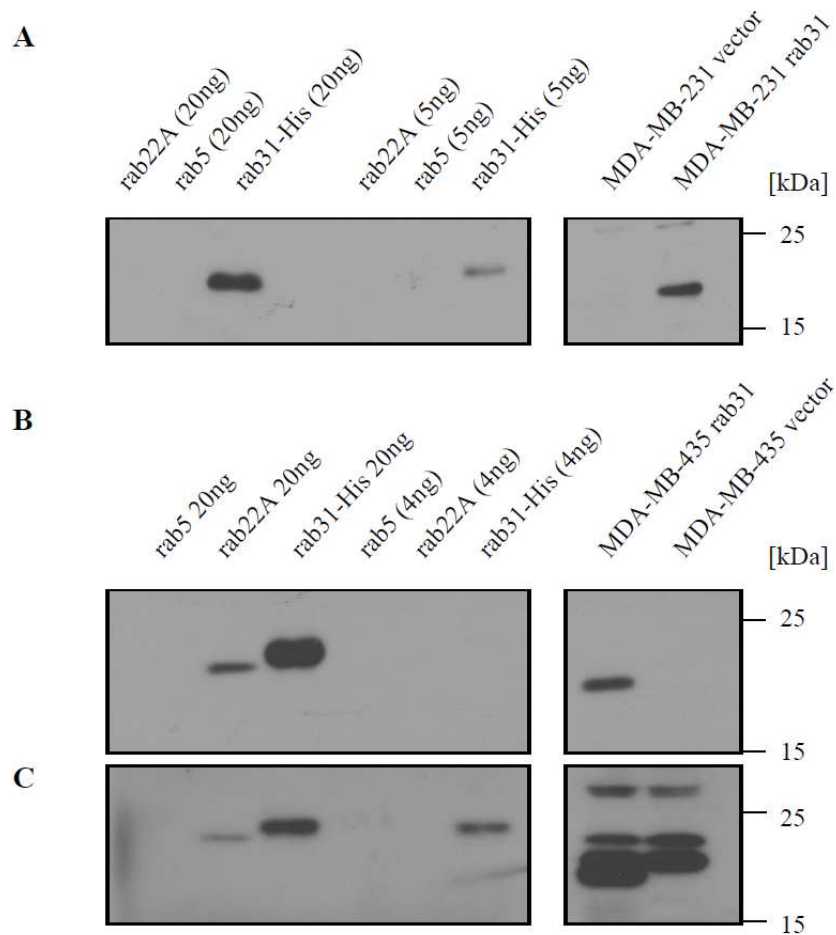


Fig. 27 Cross-reactivity of rabbit anti-rab31 antibodies

Breast cancer cells transfected with empty vector control or the rab31 expression plasmid were lysed and analyzed by Western blot. In addition, recombinant rab5, rab22A and rab31-His were applied to the gel. Membranes were stained using **A** the IgG-purified pAbs RT1-IgG, **B** RT3-IgG and **C** RT4-IgG directed to rab31 (1:2000 in 5 % (w/v) skimmed milk powder in TBST). Reactive proteins were visualized by chemiluminescence as described before.

Chicken T1 (ChT1) as well as Chicken T4 (ChT4) showed no cross-reaction with rab22A and rab5, but specifically detected rab31-His. In total cell lysate from rab31 overexpressing MDA-MB-231 cells, rab31 was detected by both pAbs. Though, both pAbs unspecifically reacted with other proteins in the cell lysate (Fig. 28 A and B).

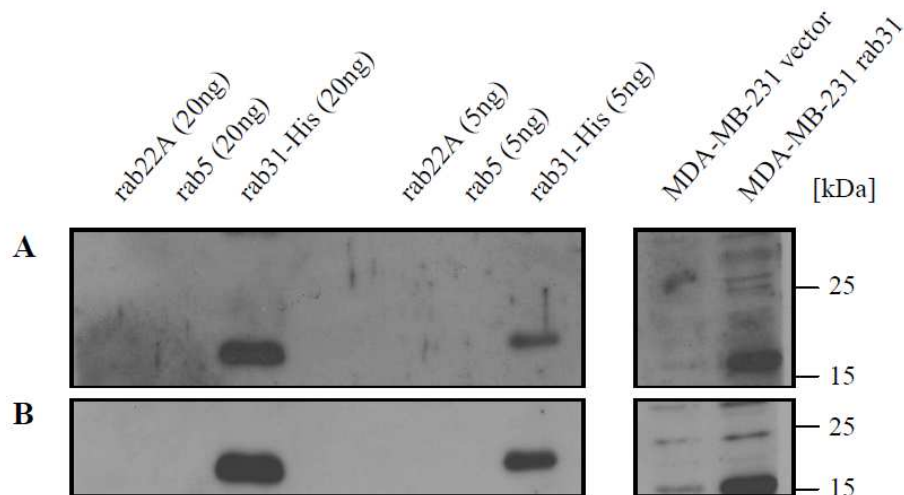


Fig. 28 Cross-reactivity of chicken anti-rab31 antibodies

MDA-MB-231 breast cancer cells transfected with empty vector control or the rab31 expression plasmid were lysed and analyzed by Western blot. In addition, recombinant rab5, rab22A and rab31-His were applied to the gel. Membranes were stained using the unpurified pAbs **A** ChT1 and **B** ChT4 directed to rab31 (1:2000 in 5 % (w/v) skimmed milk powder in TBST). Reactive proteins were visualized by chemiluminescence as described before.

6.2.3 Pre-selection of rab31 antibodies for the development of a rab31-ELISA format

For the determination of rab31 protein content in tumor samples a rab31-ELISA format is presently set up in collaboration with the *Institut für Pathologie, TU Dresden*. For pre-selection different rabbit / chicken antibody combinations were tested in ELISA, using determined amounts of rab31-His and glutathione S-transferase (GST) tagged rab31 (GST-rab31) as antigen. All possible combinations of catching and detection antibodies were tested. It has to be mentioned that the catching and detection antibody have to be derived from different species as long as the primary Abs are not directly conjugated to detecting enzymes like horse radish peroxidase (HRP). Table 4 represents the grading of the individual combination. ChT4 as catching pAb combined with RT1 as detection pAb (ChT4/RT1) as well the combination RT1/ChT4 showed the most unspecific result, because unspecific reaction with BSA was almost as strong as the specific binding to rab31-His and GST-rab31. A moderate binding specificity was monitored using chicken pAbs for catching and for the combinations

RT1/ChT1 and RT4/ChT4. Best results were achieved combining RT3/ChT1, RT3/ChT4 and RT4/ChT1 (Table 4).

Det. Cat.	RT1	RT3	RT4	ChT1	ChT4
RT1				→	↓
RT3				↑	↑
RT4				↑	→
ChT1	→	→	→		
ChT4	↓	→	→		

Table 4 Antibody combinations tested in ELISA

96 well microtiter plates were coated with catching antibody diluted in carbonate-buffer, after blocking with 2 % (w/v) BSA in TBS determined amounts of recombinant protein were applied to the wells followed by incubation with a second primary antibody (detection antibody) derived from another species. For read out, plates were incubated with a secondary horse radish peroxidase (HRP)-conjugated antibody, followed by addition of the TMB-substrate and addition of 0.5 M H₂SO₄. The chromogenic change was monitored at 450 nm. All possible antibody combinations were tested and rated with arrows based on specific antigen binding. ↓ poor combination; → moderate combination; ↑ good combination.

The three best pAb combinations were used to set up standard curves of recombinant protein, ranging from 1 ng/ml up to 80 ng/ml (Fig. 29). The combination RT3 as catching together with ChT1 as detection pAb showed a strong dose-dependent signal for GST-rab31 as antigen. The signal for the same amount of rab31-His was much weaker at each concentration. Still, the increased dose-dependent binding compared to BSA remained obvious (Fig. 29 A). The same was true for the combination RT3 (detection pAb) and ChT4 (detection pAb). This combination revealed smaller differences in binding efficiency comparing rab31-His and GST-rab31 (Fig. 29 B). The combination of RT4 (catching pAb) with ChT1 (detection pAb) gave the most specific reaction of all combinations with GST-rab31. Unspecific background binding remained low. Again, dramatic differences in binding GST-rab31 *versus* rab31-His were observed (Fig. 29 C).

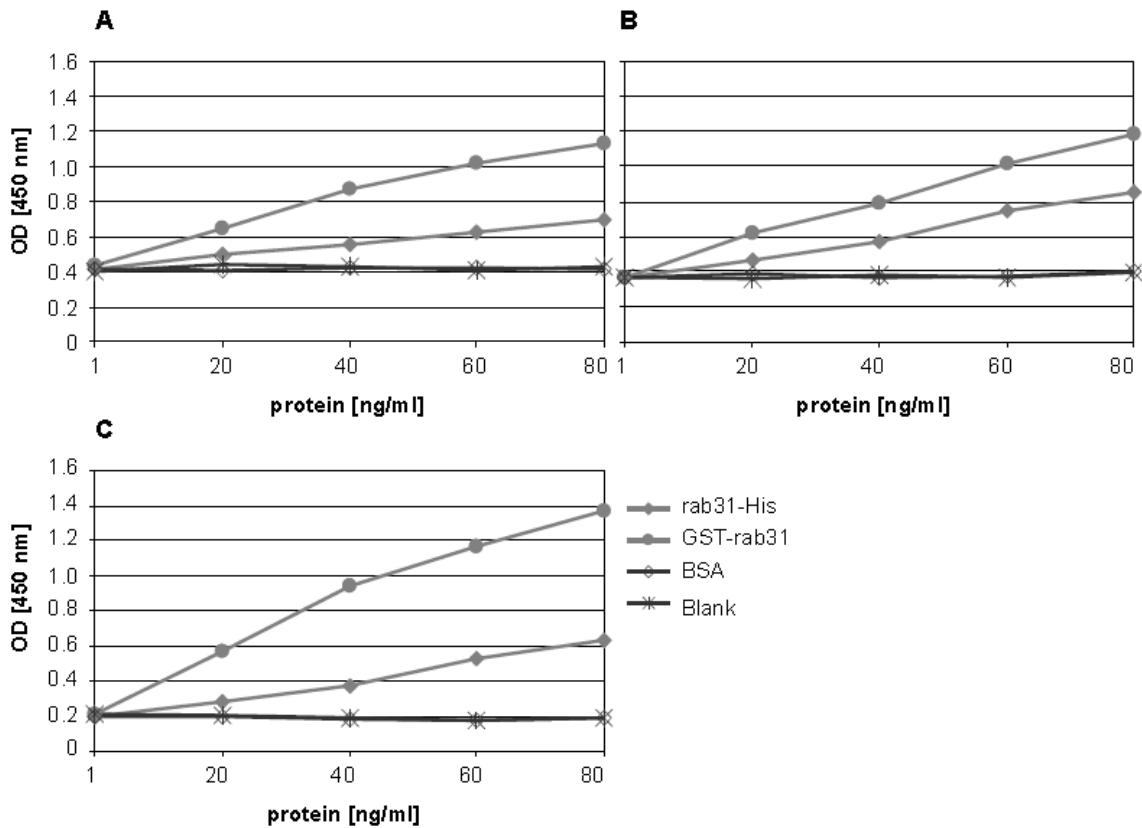


Fig. 29 ELISA standard curves using different combinations of rab31 pAbs

Dose-dependent antigen binding was tested, using different pAb combinations. **A** 96 well plates were coated with the catching pAb RT3 (1:1000 in carbonate-buffer). Recombinant protein was applied to the wells at determined concentration (1 ng/ml up to 80 ng/ml), followed by incubation with a detection pAb ChT1 (1:5000). **B** Plates were coated with the catching pAb RT3 (1:4000 in carbonate-buffer). Recombinant protein was applied to the wells at determined concentration (1 ng/ml up to 80 ng/ml). Followed by incubation with a detection pAb ChT4 (1:5000). **C** Plates were coated with the catching pAb RT4 (1:1000 in carbonate-buffer). Recombinant protein was applied to the wells at determined concentration (1 ng/ml up to 80 ng/ml), followed by incubation with a detection pAb ChT1 (1:5000).

6.2.4 Immunohistochemical staining of breast cancer tissue

The generated antibodies RT3-IgG and RT4-IgG were used to analyze rab31 expression in breast cancer tissue immunohistochemically. This experiment was done in collaboration with the *Institut für Pathologie, TU Dresden*. Figure 30 represents the typical staining pattern found in breast cancer tissue stained with RT3-IgG or RT4-IgG, respectively. We observed a cellular staining pattern, which was in accordance to published data of the human protein atlas (see www.proteinatlas.org), as well as to immunocytochemical studies (Ng et al. 2007). Thus, we detected a weak to moderate cytoplasmic as well as partial strong

perinuclear and/or nuclear staining of cancer cells, whereas stromal cells were less frequently stained in breast cancer (Fig. 30).

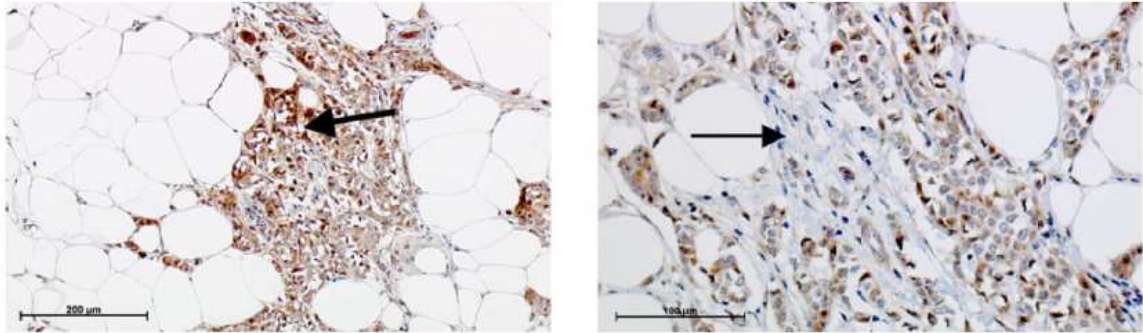


Fig. 30 Immunohistochemical staining of breast cancer tissue using a rab31 directed pAb
Immunohistochemical staining of paraffin-embedded, formalin-fixed breast cancer specimens with pAb RT4-IgG. Specific immunostaining is observed in the cytoplasm as well as in the nucleus of cancer cells (left panel), stromal cells are stained less frequently (right panel).

6.3 Characterization of breast cancer cell lines overexpressing rab31

6.3.1 Selection of breast cancer cell lines

Endogenous rab31 mRNA expression was quantified in different breast cancer cell lines using quantitative PCR. Based on the mRNA expression levels depicted in figure 31, MDA-MB-231 cells were chosen for further analysis, because this cell line has a moderate endogenous expression of rab31. Furthermore, CAMA-1 and MDA-MB-435 cells were selected for stable transfection, as they both have no detectable rab31 mRNA expression.

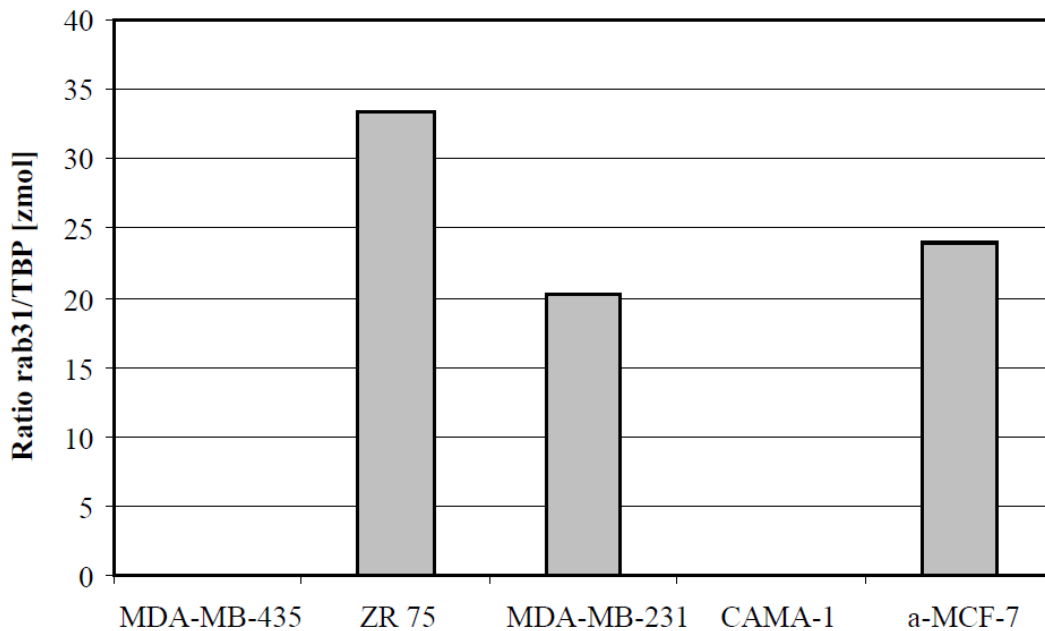


Fig. 31 Quantitative PCR analysis of different breast cancer cell lines

Rab31 mRNA expression of wildtype MDA-MB-435, ZR75, MDA-MB-231, CAMA-1 and a-MCF-7 breast cancer cells was determined using quantitative PCR as described before. RNA content was calculated relative to the measured amount of the TATA-box binding protein (TBP) for each cell line.

6.3.2 Stable transfection of breast cancer cell lines

Rab31 was identified as one out of seven differentially expressed genes in breast cancer tissue with high uPAR-del4/5 RNA levels. Analysis of 280 lymphnode-negative breast cancer samples for rab31 RNA expression revealed that this small GTPase represents a new independent prognostic factor for breast cancer (Kotzsch et al. 2008). The tumor-biological role of rab31 is completely unknown.

Therefore, we started to investigate the tumor-biological role of rab31 in different breast cancer cell lines *in vitro* and *in vivo*.

Three different breast cancer cell lines MDA-MB-231, MDA-MB-435 and CAMA-1 were stably transfected with the eukaryotic expression plasmid pRcRSV containing the rab31 cDNA sequence. As a control, the cell lines were transfected with the empty expression vector pRcRSV (vector control).

As already described for uPAR-del4/5 overexpressing cells, single cell clones were isolated in two rounds of subcloning in order to get cell lines with a homogeneous high, medium or low expression level.

Rab31 protein levels were determined by Western blot analysis. Immunostaining with pAb RT3-IgG revealed an endogenous expression of rab31 in vector control cells and medium expression levels in batch-transfected cells (Fig. 32 A). Cell clone #1-13-10 represented the highest expression of rab31 compared to the medium expression of clone #2-22-11 and the low expression of clone #1-9-9. As loading control, the membrane was stained for the endogenous housekeeping control protein GAPDH (Fig. 32 A). To avoid measurement of artefacts, due to looking at single cells, a number of cell clones with similar rab31 levels were isolated and analyzed (Fig. 32 B).

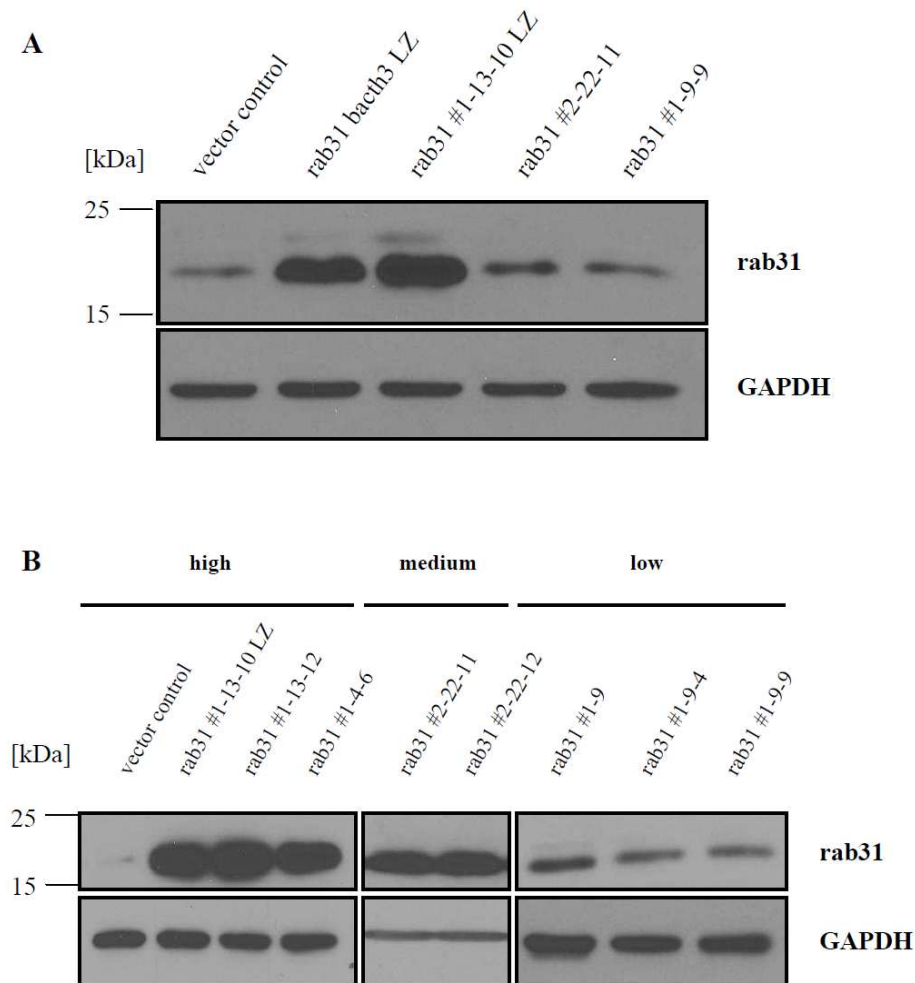


Fig. 32 Western blot analysis of MDA-MB-231 cells overexpressing rab31

MDA-MB-231 cells transfected with empty vector control or the rab31 expression plasmid were lysed and analyzed by Western blots. Membranes were stained using the pAb RT3-IgG (1:2000 in 5 % (w/v) skimmed milk powder in TBST). Reactive proteins were visualized by chemiluminescence as described before. For control of equal loading, membranes were stripped and subsequently stained using a mAb detecting the endogenous control GAPDH. **A** Cell lysates of cell clones expressing different levels of rab31. **B** Lysates of cell clones with similar expression levels.

Rab31 expression was further analyzed using immunocytochemical staining followed by CLSM analysis, as described earlier. The monoclonal antibody C-15 (Santa Cruz Biotechnology, Santa Cruz, California, USA) was used for immunocytochemical staining, as none of the in house-generated rab31 antibodies was suitable in ICC (Fig. 26). The immunocytochemical staining showed an overexpression of rab31 in stably transfected cells compared to vector control cells. Enhanced rab31 staining was detected in the cytosol, indicating the predominantly cytosolic localization of the protein (Fig. 33). Moreover, batch-

transfected cells showed a heterogeneous expression pattern of rab31. After two rounds of subcloning, cell lines with a homogeneous expression were isolated. Only batch-transfected cells, and the high expressing cell clone #1-13-10 are depicted here (Fig. 33).

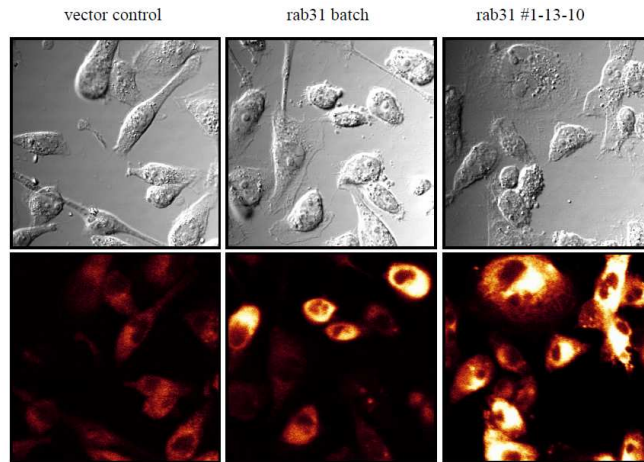


Fig. 33 Immunocytochemical staining of MDA-MB-231 cells overexpressing rab31

MDA-MB-231 human breast cancer cells, stably transfected with rab31 or vector control, were seeded on fibronectin-coated cell culture chamber slides and cultured for 24 h. Cells were fixed, permeabilized with 0.025 % (w/v) saponin and immunostained using a mAb (C-15) directed against rab31 (dilution 1:100). The signal was detected using a secondary Alexa488 conjugated goat anti-rabbit IgG.

In addition, rab31 overexpression was analyzed in the non-metastatic cell line CAMA-1. Cells were stably transfected with the plasmid containing the rab31 cDNA or the empty vector. Single cell clones were isolated as described before. Expression of rab31 was monitored using Western blot. CAMA-1 vector control cells had no detectable endogenous expression of rab31. This was also confirmed using quantitative PCR (Fig. 31). Batch-transfected cells and cell clones with high (#1-7-21), medium (#1-7-15) and very low (#1-8-5) expression were isolated (Fig. 34 A). As a control, cell clones with similar expression levels of rab31 were isolated and analyzed (Fig. 34 B).

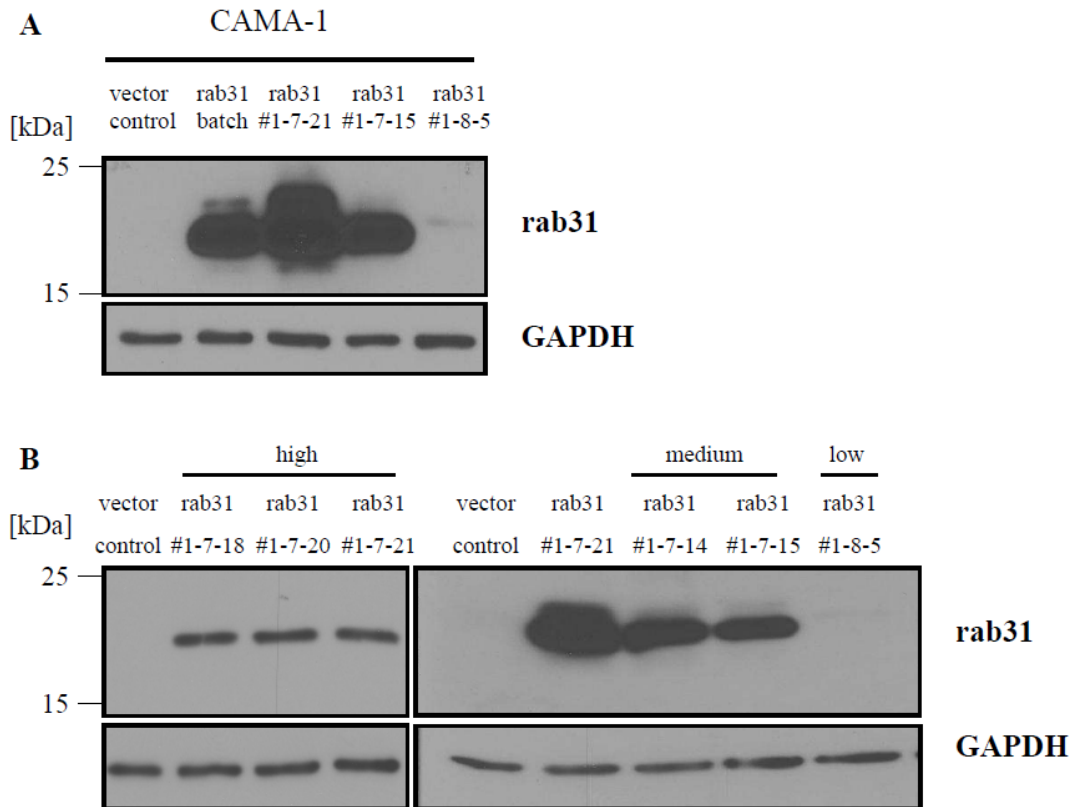


Fig. 34 Western blot CAMA-1 rab31 cell clones with similar expression levels

CAMA-1 cells transfected with empty vector control or the rab31 expression plasmid were lysed and analyzed by Western blot. Membranes were stained using the pAb RT3-IgG (1:2000 in 5 % (w/v) skimmed milk powder in TBST). Reactive proteins were visualized by chemiluminescence as described before. For control of equal loading, membranes were stripped and subsequently stained using a mAb detecting the endogenous housekeeping control protein GAPDH. **A** Cell lysates of cell clones expressing different levels of rab31. **B** Lysates of cell clones with similar expression levels.

The immunocytochemical staining depicted in figure 35, verifies the homogeneous expression in the subcloned stable transfected CAMA-1 cell line. Nearly every cell in the visual field shares equal levels of rab31, in all three different clones #1-7-18, #1-7-20 and #1-7-21 (Fig. 35).

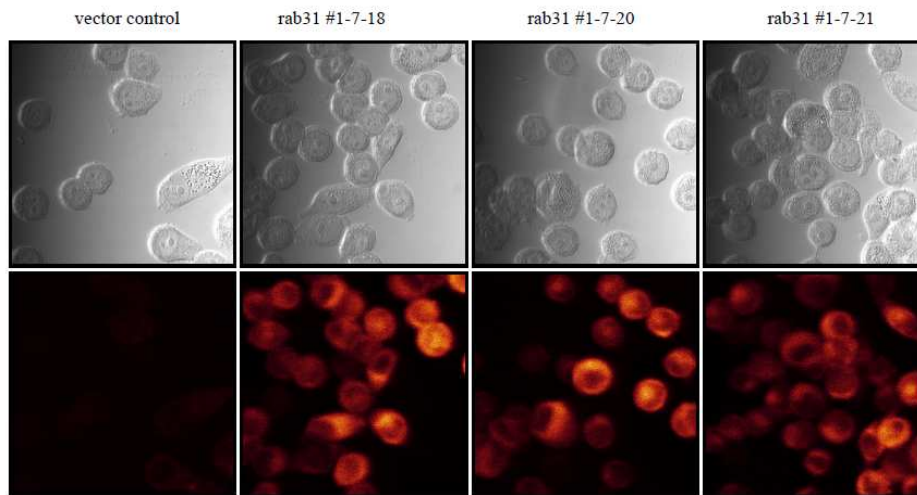


Fig. 35 Immunocytochemical staining of CAMA-1 cells overexpressing rab31

CAMA-1 human breast cancer cells, stably transfected with rab31 or vector control, were seeded on fibronectin-coated cell culture chamber slides and cultured for 24 h. Cells were fixed, permeabilized with 0.025 % (w/v) saponin, and immunostained using the mAb (C-15) directed against rab31 (dilution 1:100). The signal was detected using a secondary Alexa488 conjugated goat anti-rabbit IgG.

As a second breast cancer cell line without detectable rab31 expression, MDA-MB-435 cells were transfected with the rab31 cDNA containing plasmid or the empty vector. Western blot analysis, as well as quantitative PCR confirmed that MDA-MB-435 wildtype cells have no detectable expression of endogenous rab31. Batch-transfected cells showed a moderate overexpression of rab31 compared to mock transfected cells (Fig. 36).

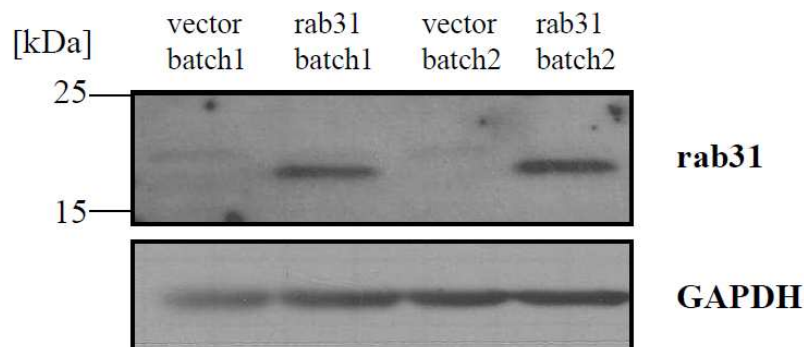


Fig. 36 Western blot analysis of MDA-MB-435 cells overexpressing rab31

MDA-MB-435 cells transfected with empty vector control or the rab31 expression plasmid, were lysed and analyzed by Western blot. Membranes were stained using the pAb RT3-IgG (1:2000 in 5% (w/v) skimmed milk powder in TBST). Reactive proteins were visualized by chemiluminescence as described before. For control of equal loading, membranes were stripped and subsequently stained using a mAb detecting the endogenous housekeeping control protein GAPDH.

Expression of rab31 in batch-transfected MDA-MB-435 cells was confirmed by immunocytochemical staining. MDA-MB-435 cells showed a homogeneous expression of rab31, therefore no single cell clones were isolated (Fig. 37).

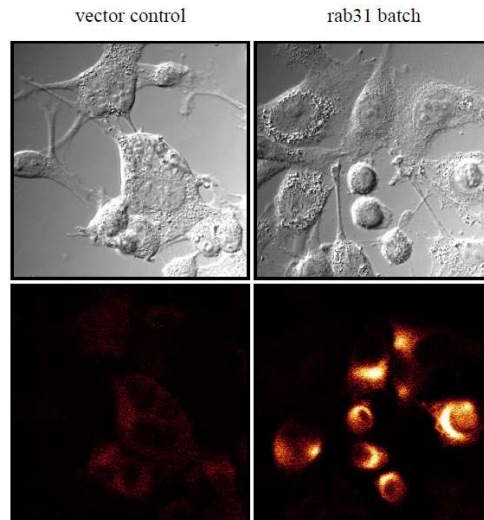


Fig. 37 Immunocytochemical staining of MDA-MB-435 cells overexpressing rab31

MDA-MB-435 human breast cancer cells, stably transfected with rab31 or vector control, were seeded on fibronectin-coated cell culture chamber slides and cultured for 24 h. Cells were fixed, permeabilized with 0.025 % saponin and immunostained using the mAb C-15 directed against rab31 (dilution 1:100). The signal was detected using a secondary Alexa488 conjugated goat anti-rabbit IgG.

6.3.3 Proliferation of breast cancer cell lines overexpressing rab31

The impact of rab31 overexpression on cell proliferation was analyzed using manual counting. Cells were seeded in 24 well plates, in triplicates for each time point. 24, 48, 72 and 96 h post-seeding, cells were detached from the well and counted in a Blaubrand[®] counting chamber under trypan blue exclusion.

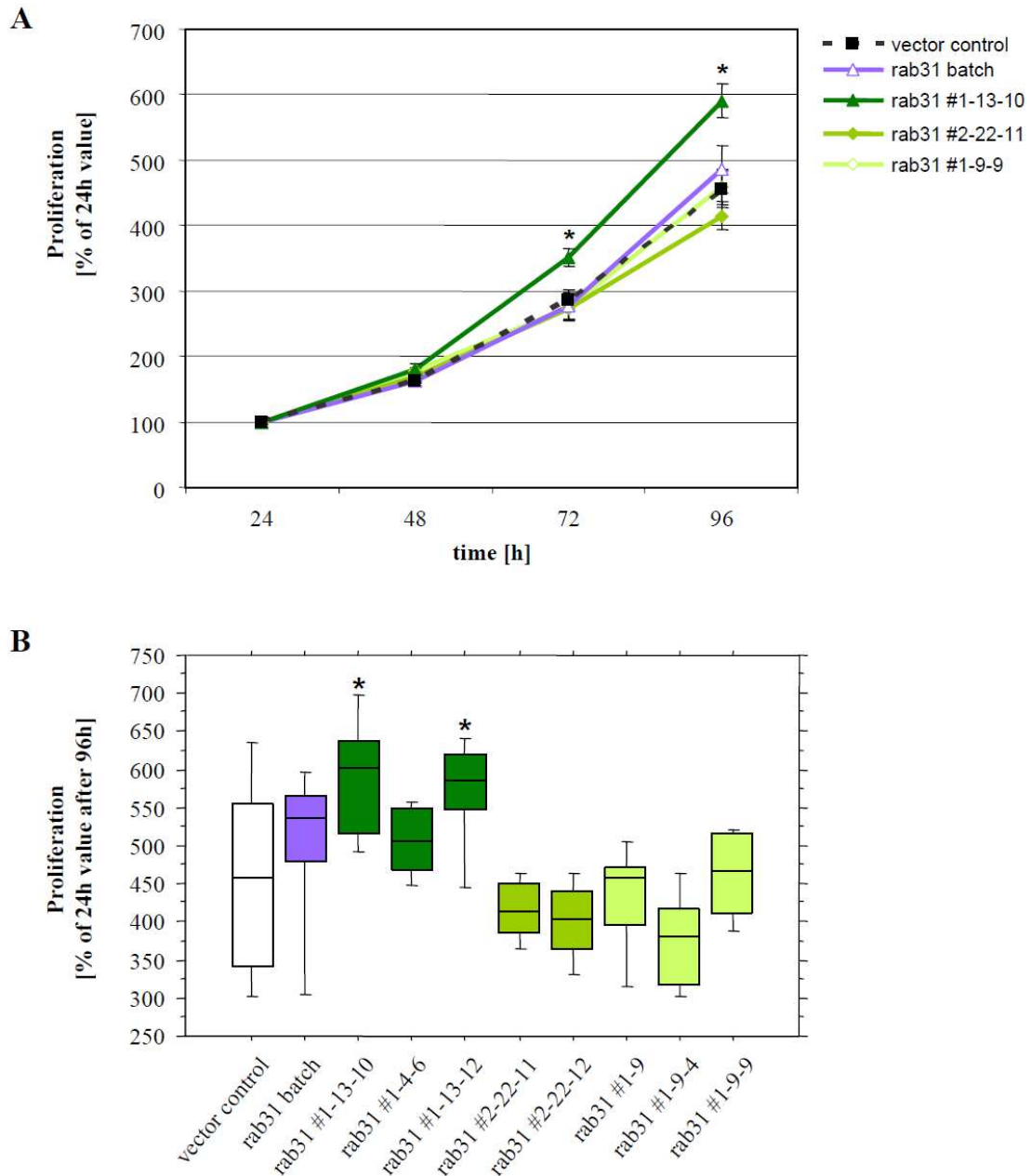


Fig. 38 Proliferation of MDA-MB-231 cells overexpressing rab31

Cells were seeded to 24 well plates, detached with 0.05 % EDTA-solution after 24, 48, 72 and 96 h and counted with a Blaubrand® counting chamber under trypan blue exclusion. **A** Analysis of vector control cells (grey), batch-transfected cells (blue) and cell clones with high (dark green), medium (green) and low expression (light green) of rab31. The graph shows the mean value of at least three independent experiments. **B** Cell clones with similar expression levels; vector control cells (white), high (dark green), medium (green) and low expression (light green) cell clones. Cell number at 24h was set to 100 %, and the increase in cell number after 96h was expressed relative to the 24 h value in %. At least three independent experiments were performed in triplicates each. Whisker box plots indicate the 25th and 75th percentile, the vertical bars indicate the 10th and 90th percentile. The median is indicated by a bar within the box. Statistically significant differences ($p < 0.05$) are indicated by an asterisk.

MDA-MB-231 cell clones overexpressing rab31 at high levels showed a significantly enhanced proliferation after 96 h. Cell clones with a medium and low expression showed no significant changes in proliferation after 96 h. The same was true for batch-transfected cells (Fig. 38 A). Analysis of cell clones with similar expression levels clarified that cell clones with similar levels of rab31 behave in a similar way with respect to cell growth. The high expressing cell clones #1-13-10 and #1-13-12 both represented an enhanced proliferation after 96 h of incubation. Only the third high expressing cell clone #1-4-6 showed no significant effect. But still a trend towards an enhanced cell growth was obvious for this cell clone (Fig. 38 B).

A similar effect on proliferation was monitored in CAMA-1 cells overexpressing rab31. In this cell line, which does not express endogenous rab31, small amounts of rab31 were sufficient to enhance the cell number after 96 h compared to vector control cells. Batch-transfected rab31 overexpressing cells as well as medium (#1-7-15) and high (#1-7-21) expressing cell clones were characterized by significantly enhanced proliferation after 96 h. Only cells expressing rab31 at low levels (#1-8-5) showed no significant effects in proliferation (Fig. 39 A). Analysis of cell clones with similar expression levels confirmed that cell clones with similar levels of rab31 proliferate in a similar way (Fig. 39 B).

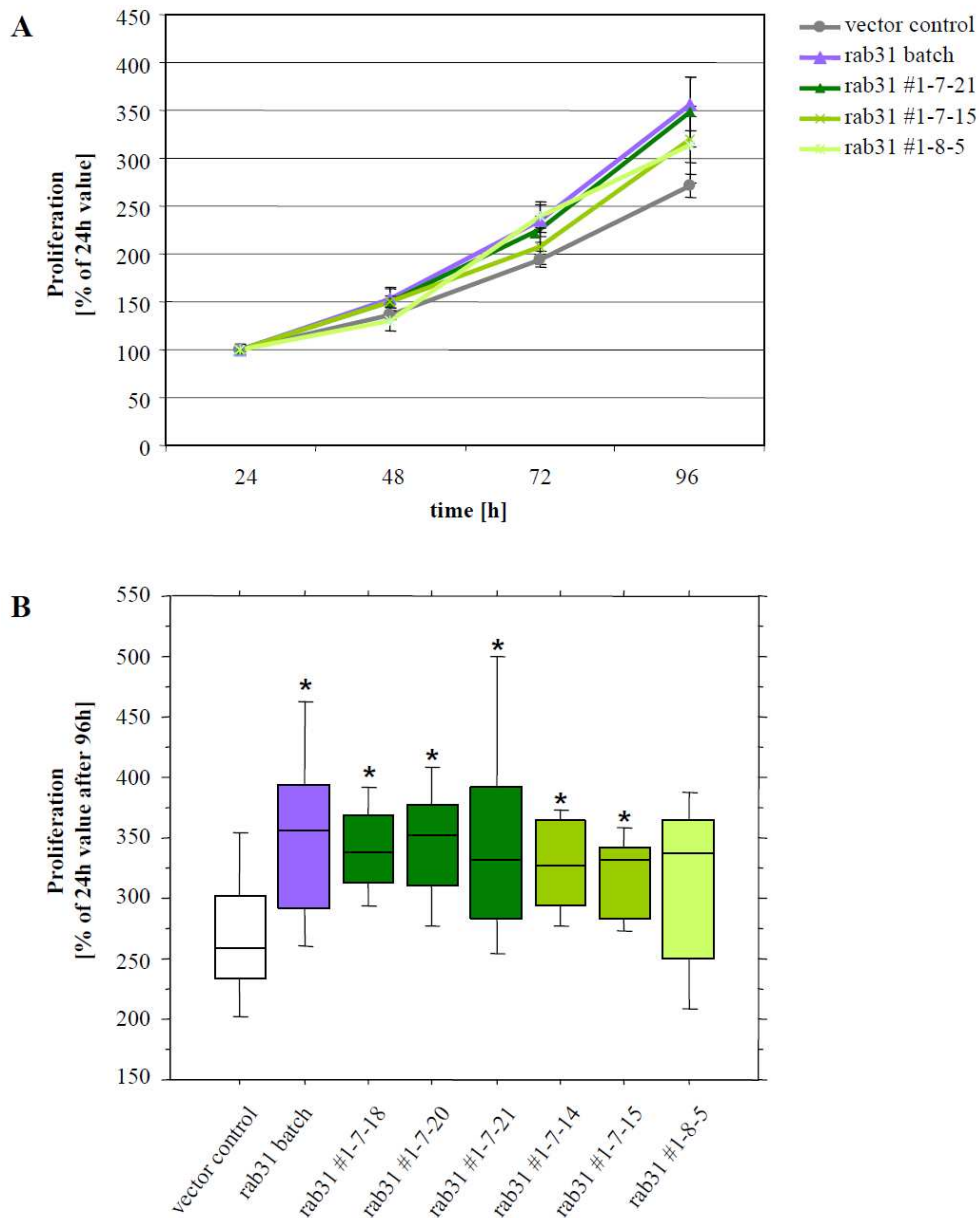


Fig. 39 Proliferation CAMA-1 rab31

Cells were seeded to 24 well plates, detached with 0.05 % EDTA-solution after 24, 48, 72 and 96 h and counted with a Blaubrand® counting chamber under trypan blue exclusion.

A Analysis of vector control cells (grey), batch-transfected cells (blue) and cell clones with high (dark green), medium (green) and low expression (light green) of rab31. The graph shows the mean value of at least three independent experiments. **B** Cell clones with similar expression levels; vector control cells (white), high (dark green), medium (green) and low expression (light green) cell clones. Cell number at 24 h was set to 100 %, and the increase in cell number after 96h was expressed relative to the 24 h value in %. At least three independent experiments were performed in triplicates each. Whisker box plots indicate the 25th and 75th percentile, the vertical bars indicate the 10th and 90th percentile. The median is indicated by a bar within the box. Statistically significant differences ($p < 0.05$) are indicated by an asterisk.

Analysis of a third breast cancer cell line, MDA-MB-435, illustrated again the proliferative effect of rab31 on breast cancer cells. MDA-MB-435 cells which have no endogenous expression of rab31 showed a significantly enhanced cell growth after 96 h compared to mock transfected control cells (Fig. 40).

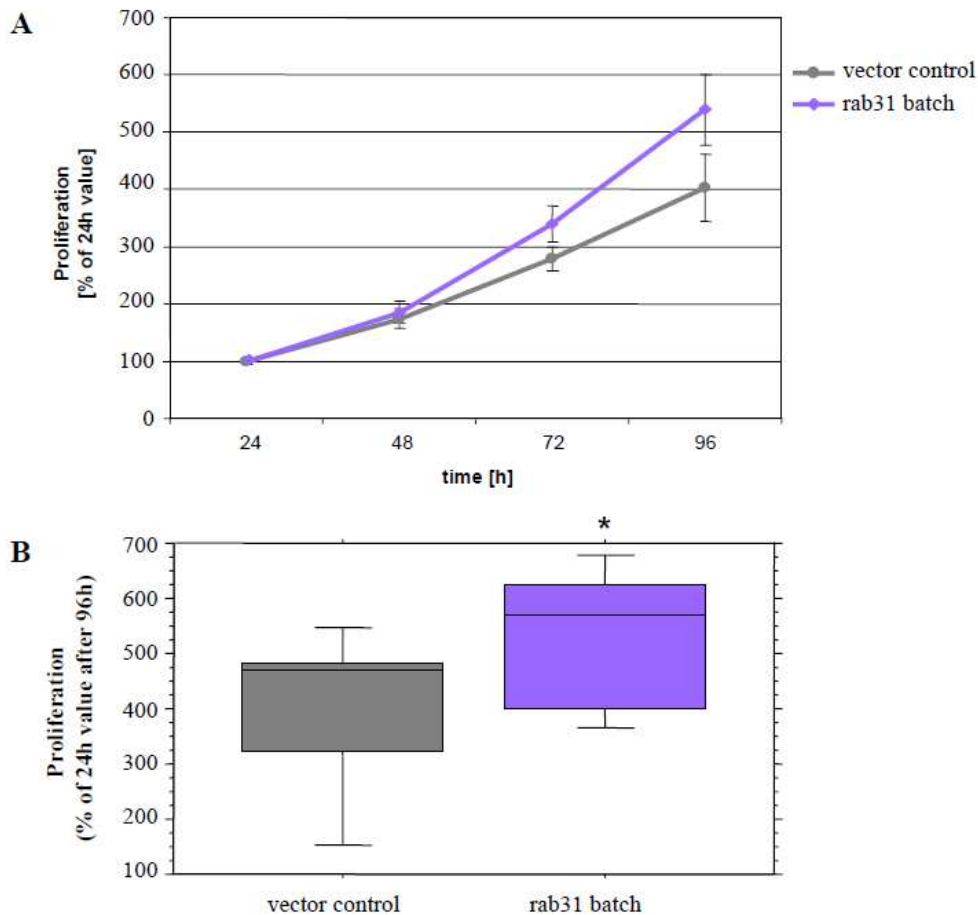


Fig. 40 Proliferation MDA-MB-435 rab31

MDA-MB-435 cells were seeded to 24 well plates, detached with 0.05 % EDTA-solution after 24, 48, 72 and 96 h and counted with a Blaubrand[®] counting chamber under trypan blue exclusion. The proliferation of vector control cells (grey) and batch-transfected rab31 overexpressing cells (blue) was analyzed. **A** The graph represents the mean value of at least three independent experiments at each time point. **B** Cell number at 24 h was set to 100 %, and the increase in cell number after 96 h was expressed relative to the 24 h value in %. At least three independent experiments were performed in triplicates each. Whisker box plots indicate the 25th and 75th percentile, the vertical bars indicate the 10th and 90th percentile. The median is indicated by a bar within the box. Statistically significant differences ($p < 0.05$) are indicated by an asterisk.

6.3.4 Adhesion to extracellular matrix proteins

Cellular adhesion of breast cancer cell lines overexpressing rab31 was conducted as described for uPAR-del4/5. Batch-transfected, rab31 overexpressing MDA-MB-231 cells showed a significantly reduced adhesion to collagen type IV. The high expressing cell clones (#1-13-10) showed the strongest decrease in adhesion compared to vector control cells. Cell clones with moderate (#2-22-11) expression of rab31 showed a moderate reduction of adhesive capacity. Low (1-9-9) expressing cells showed a small but significant reduced adhesion towards collagen type IV. Adhesion to collagen type IV decreased in a rab31 dose-dependent manner, because the adhesion of the high expressing cell clone was significantly lower compared to medium and low expressing cell clones. The difference between the medium expressing clone and cells with low expression was statistically not significant, but a trend was still obvious (Fig. 41 A). To avoid measurement of artefacts, multiple cell clones with similar expression levels were analyzed. Fig. 41 B demonstrates that cell clones with similar expression levels showed a similar adhesive capacity towards collagen type IV.

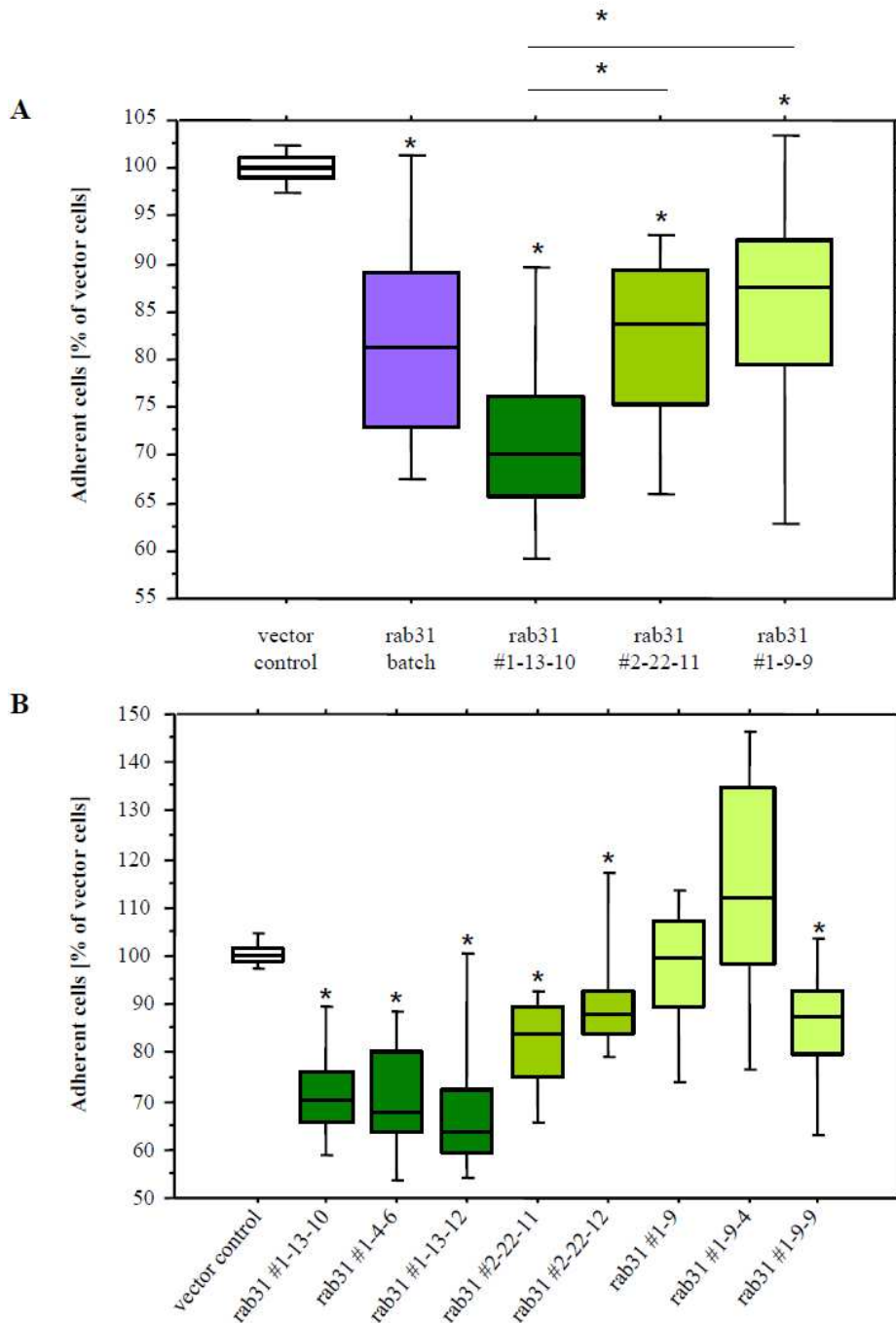


Fig. 41 Adhesion of MDA-MB-231 cells to collagen type IV

MDA-MB-231 cells were seeded on collagen type IV coated 96 well plates. After 2 h of cell cultivation, the number of adherent cells was monitored by the hexosaminidase activity assay. **A** Analysis of vector control cells (white), batch-transfected cells (blue) and cell clones with high (dark green), medium (green) and low expression (light green) of rab31. **B** Cell clones with similar expression levels; vector control cells (white), high (dark green), medium (green) and low expression (light green) cell clones. At least 4 independent experiments were performed in triplicates each. The results are given in % relative to the cell number of adherent vector-transfected control cells. Whisker box plots indicate the 25th and 75th percentile, the vertical bars indicate the 10th and 90th percentile. The median is indicated by a bar within the box. Statistically significant differences ($p < 0.05$) are indicated by an asterisk.

When adhesion was tested to other extracellular matrix components like fibronectin, vitronectin, laminin or collagen type I, similar results were observed as described for collagen type IV (table 5).

	rab31 batch	rab31 #1-13-10	rab31 #1-4-6	rab31 #1-13-12	rab31 #2-22-11	rab31 #2-22-12	rab31 #1-9	rab31 #1-9-4	rab31 #1-9-9
FN	84.7* +/- 3.2	71.6* +/- 3.0	74.9* +/- 3.5	68.1* +/- 6.3	93.4* +/- 7.1	99.5 +/- 12.2	100.8 +/- 6.0	119.4 +/- 8.8	95.8 +/- 4.7
VN	82.3* +/- 3.3	63.1* +/- 3.3	67.6* +/- 3.1	65.8* +/- 3.9	83.8* +/- 4.3	94.2* +/- 7.2	97.8 +/- 5.8	115.2 +/- 7.3	90.2* +/- 4.9
Ln	81.4* +/- 5.4	68.7* +/- 4.4	72.1* +/- 6.1	50.5* +/- 4.8	91.1 +/- 8.6	91.0 +/- 8.5	110.1 +/- 12.5	114.0 +/- 8.0	88.2* +/- 11.1
Col I	84.8* +/- 3.0	70.5* +/- 2.7	70.7* +/- 4.8	67.9* +/- 6.5	87.4* +/- 4.2	93.3* +/- 6.5	93.8* +/- 5.6	108.7 +/- 9.0	81.6* +/- 5.8
Col IV	82.3* +/- 4.0	72.0* +/-3.1	70.4* +/-4.2	69.6* +/-7.0	82.4* +/- 4.6	91.8* +/- 6.1	97.3 +/- 6.0	113.4 +/- 8.7	85.6* +/- 5.0

Table 5 Adhesion of MDA-MB-231 cells overexpressing rab31 to components of the extracellular matrix

Adhesion of MDA-MB-231 cell clones overexpressing rab31 towards fibronectin (FN), vitronectin (VN), laminin (Ln), collagen type I (Col I) and collagen type IV (Col IV). At least 4 independent experiments were performed in triplicates each. The results are given as the mean value in %, relative to the cell number of adherent vector-transfected control cells. Statistically significant differences ($p < 0.05$) are indicated by an asterisk.

When adhesion of a second breast cancer cell line CAMA-1 was analyzed, the differences in adhesion were even more pronounced than the effects measured in MDA-MB-213 cells. Again, batch-transfected rab31 overexpressing cells showed a moderate but significant reduction of adhesion towards collagen type IV. CAMA-1 cells with high expression (#1-7-21) of rab31 showed the strongest reduction in adhesion. Cell with a moderate overexpression (#1-7-15) showed a significantly reduced adhesion compared to vector control cells. Adhesion of moderate expressing cell clones was not significantly different from high expressing cell clones. Low expressing cell clones (#1-8-5) also showed a small but significant reduction of adhesion to collagen type IV compared to vector control cells. The

effect is, like already shown in MDA-MB-231 cells, rab31 dose-dependent because cell clones with a low expression showed a significantly higher adhesion to collagen type IV compared to cell clones with medium or low expression of rab31 (Fig. 42 A).

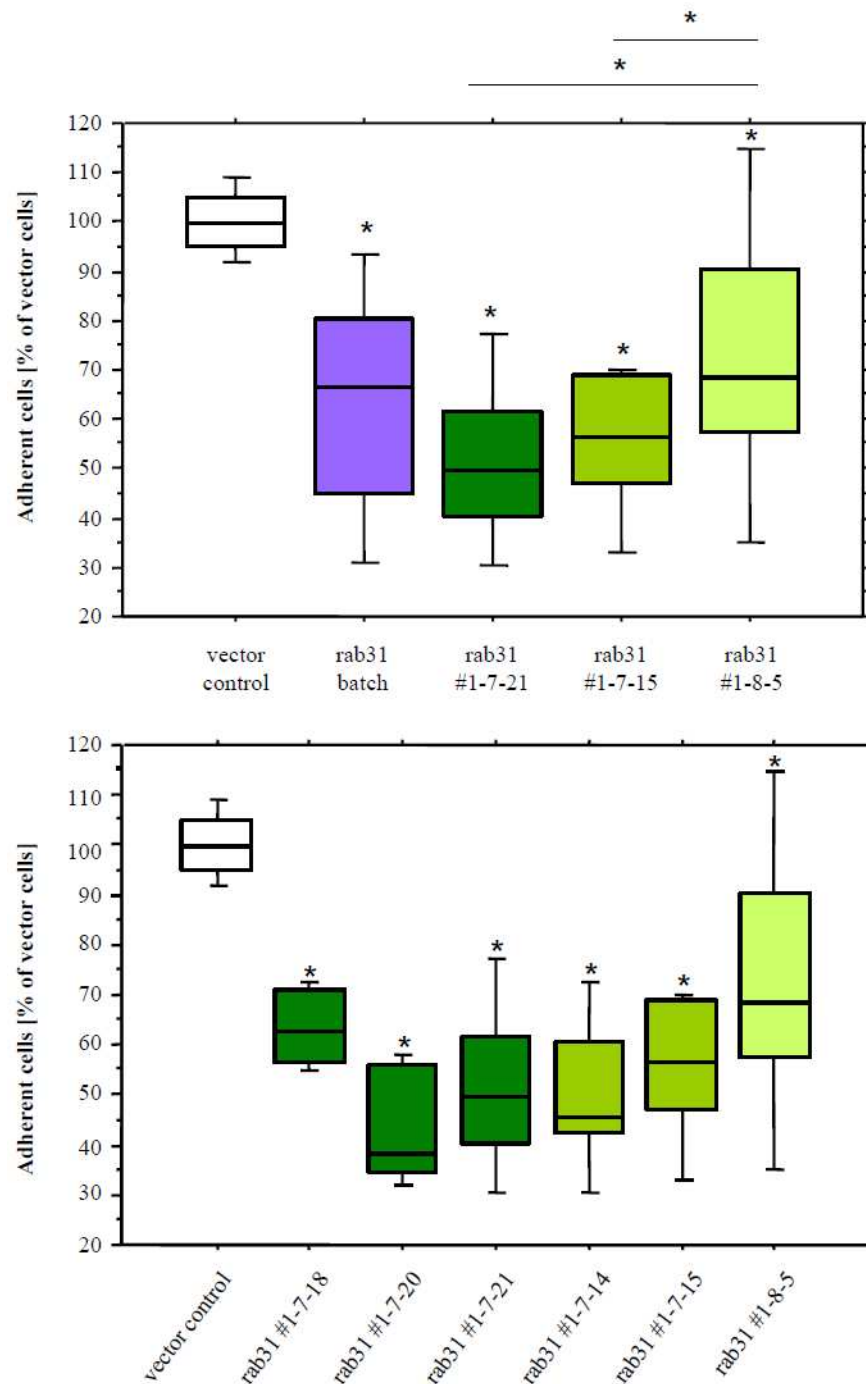


Fig. 42 Adhesion of CAMA-1 cells overexpressing rab31 to collagen type IV

CAMA-1 cells were seeded on collagen type IV coated 96 well plates. After 2 h of cell cultivation, the number of adherent cells was monitored by the hexosaminidase activity assay. **A** Analysis of vector control cells (white), batch-transfected cells (blue) and cell clones with high (dark green), medium (green) and low expression (light green) of rab31. **B** Cell clones with similar expression levels; vector control cells (white), high (dark green), medium (green) and low expression (light green) cell clones. At least 4 independent experiments were performed in triplicates each. The results are given in % relative to the cell number of adherent vector-transfected control cells. Whisker box plots indicate the 25th and 75th percentile, the vertical bars indicate the 10th and 90th percentile. The median is indicated by a bar within the box. Statistically significant differences ($p < 0.05$) are indicated by an asterisk.

Analysis of clones with similar expression levels revealed that medium and high expressing cell clones represent a similar adhesive phenotype (Fig. 42 B; table 6).

	rab31 batch	rab31 #1-7-18	rab31 #1-7-20	rab31 #1-7-21	rab31 #1-7-14	rab31 #1-7-15	rab31 #1-8-5
VN	93.5 +/- 6.8	60.5* +/- 5.2	59.5* +/- 5.1	71.3* +/- 3.9	74.4* +/- 5.1	78.4* +/- 5.8	84.1* +/- 4.2
Col I	71.0* +/- 5.1	57.9* +/- 8.8	47.0* +/- 8.9	48.6* +/- 4.5	51.7* +/- 6.6	60.1* +/- 5.1	70.4* +/- 7.8
Col IV	63.6* +/- 7.3	63.3* +/- 4.2	44.3* +/- 6.6	51.5* +/- 4.5	49.9* +/- 6.3	54.9* +/- 6.4	72.7* +/- 8.0

Table 6 Adhesion of CAMA-1 cells overexpressing rab31 to components of the extracellular matrix

CAMA-1 cell clones overexpressing rab31 show a significantly reduced adhesion towards vitronectin (VN), collagen type I (Col I) and collagen type IV (Col IV). At least 4 independent experiments were performed in triplicates each. The results are given as the mean value in %, relative to the cell number of adherent vector-transfected control cells. Statistically significant differences ($p < 0.05$) are indicated by an asterisk.

In the third breast cancer cell line MDA-MB-435, only batch-transfected cells were analyzed. The overexpression of rab31 led to a slight but significant decrease of adhesion towards the extracellular matrix proteins collagen type I, fibronectin, vitronectin and laminin. Interestingly, adhesion to collagen type IV was not significantly altered (Fig. 43).

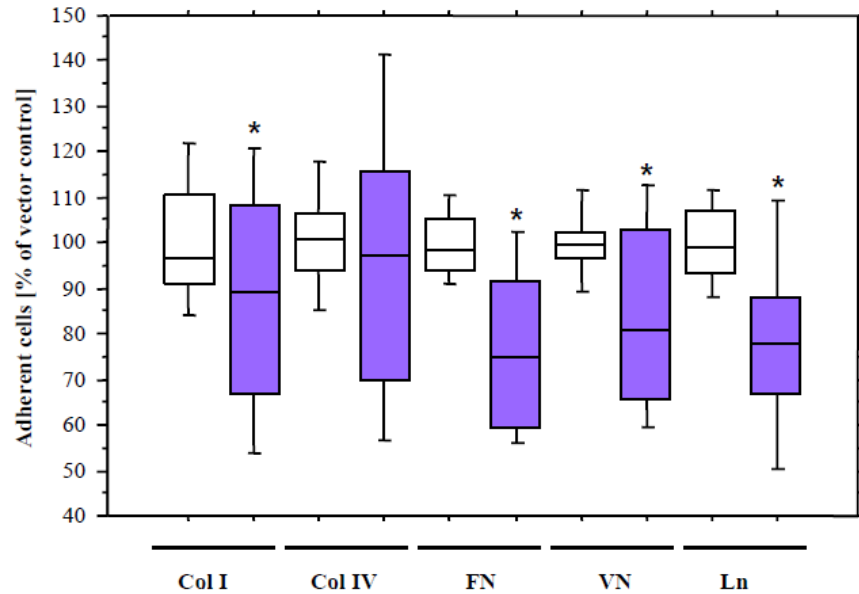


Fig. 43 Adhesion of MDA-MB-435 cells overexpressing rab31 on different ECMs

Adhesion of MDA-MB-435 cells overexpressing rab31 towards collagen type I (Col I), collagen type IV (Col IV), fibronectin (FN), vitronectin (VN), and laminin (Ln). At least 4 independent experiments were performed in triplicates each. The results are given in % relative to the cell number of adherent vector-transfected control cells. Whisker box plots indicate the 25th and 75th percentile, the vertical bars indicate the 10th and 90th percentile. The median is indicated by a bar within the box. Statistically significant differences ($p < 0.05$) are indicated by an asterisk.

6.3.5 Matrigel™ invasion assay

The invasive capacity of MDA-MB-231 cells overexpressing rab31 was determined using the matrigel™ invasion assay as described before for uPAR-del4/5 overexpressing cells.

Batch-transfected MDA-MB-231 cells showed a moderate but significant reduction of the invasive capacity through matrigel™. Only few cells with a homogeneous high (#1-13-10) and medium (#2-22-11) expression were able to degrade the matrix and migrate through the pores of the transwell insert. The invasive capacity of cells with high or medium expression was comparable. No significant differences in invasion compared to vector control cells, were observed for cells with a low (#1-9-9) expression of rab31. The invasive capacity of high and medium expressing cells was significantly reduced compared to cells with a low expression of rab31 (Fig. 44 A). Analyzing MDA-MB-231 cell clones with similar expression levels of rab31, all clones with high or medium expression showed a comparable reduction of invasive capacity through matrigel™ (Fig. 424 B). The same was true for two cell clones with a low expression, #1-9-4 and #1-9-9, since both showed no significant effect. Unexpectedly, cell clone #1-9 which was sharing a comparable expression level of rab31 like #1-9-4 and #1-9-9 showed a significantly reduced invasive capacity through matrigel™ (Fig. 44 B).

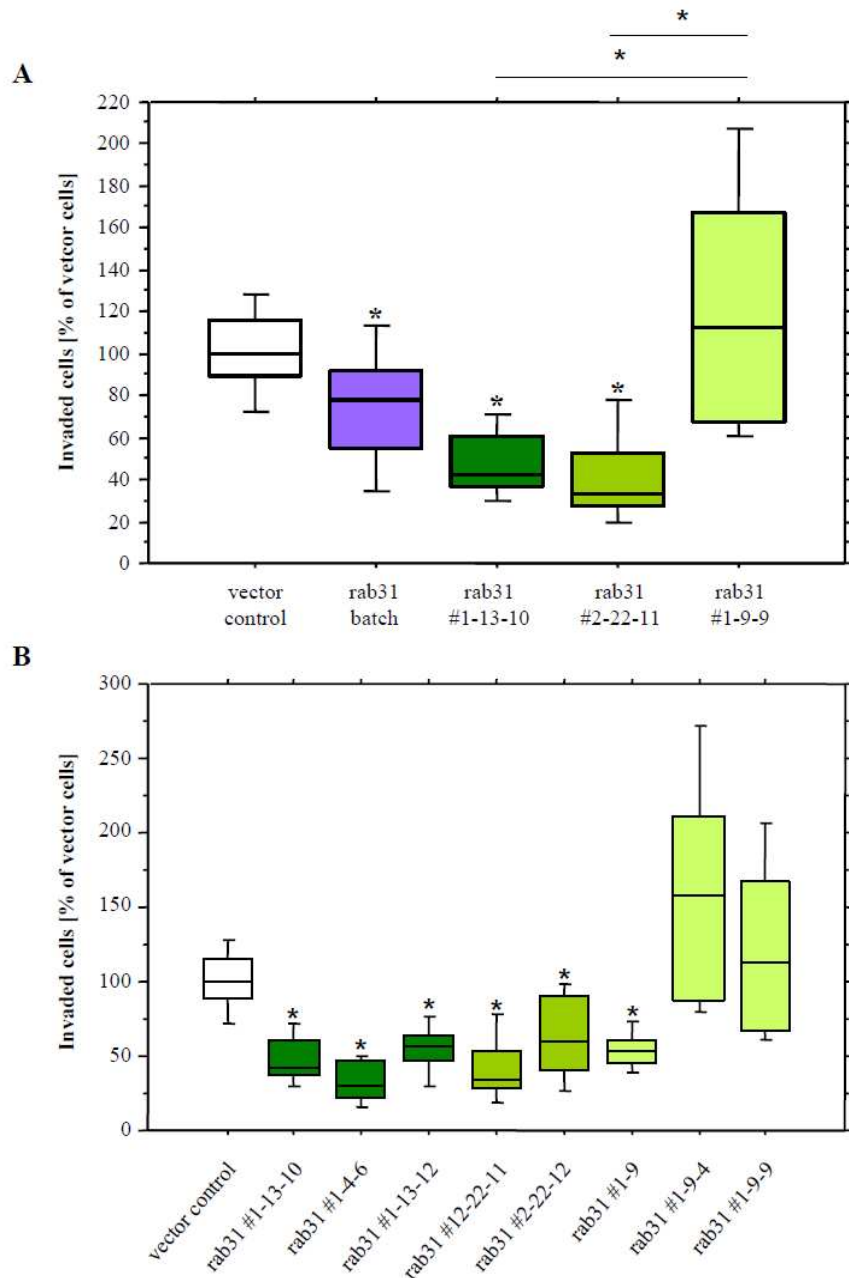


Fig. 44 Invasive capacity of MDA-MB-231 cells overexpressing rab31

Stably transfected MDA-MB-231 cells were seeded into the upper compartments of matrigel™-coated invasion chambers. After 24 h of incubation, invaded cells were fixed, stained, and counted. **A** Analysis of vector control cells (white), batch-transfected cells (blue) and cell clones with high (dark green), medium (green) and low expression (light green) of rab31. **B** Cell clones with similar expression levels; vector control cells (white), high (dark green), medium (green) and low expression (light green) cell clones. At least three independent experiments were performed in triplicates each. The results are given in %, normalized to the number of invaded vector-transfected cells. Whisker box plots indicate the 25th and 75th percentile, the vertical bars indicate the 10th and 90th percentile. The median is indicated by a bar within the box. Statistically significant differences ($p < 0.05$) are indicated by an asterisk.

6.3.6 Effects of rab31 overexpressing MDA-MB-231 cells on lung metastasis in a xenograft mouse model

MDA-MB-231 cells transfected with the rab31 plasmid or the empty vector were tagged with the *lacZ*-gene as described before for uPAR-del4/5 overexpressing cells. Figure 45 shows XGal-stained MDA-MB-231 cells overexpressing rab31, which were tagged with the *lacZ*-gene.

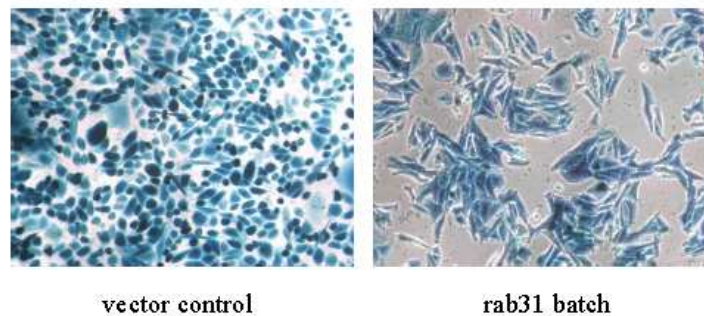


Fig. 45 XGal-staining of MDA-MB-231 cells

MDA-MB-231 overexpressing rab31 or transfected with the empty vector were tagged with the *lacZ*-gene. Tagged cells express β -galactosidase which can be monitored by XGal-staining of the cells. β -galactosidase expressing cells convert the XGal substrate leading to an indigo blue staining.

Cells were injected into the tail vein of immune-compromised female nude mice CD1 nu/nu. After 35 days mice were sacrificed, lungs were prepared and XGal stained. Blue colonies were counted on the surface of the lung. The entire xenograft experiment was performed in collaboration with the laboratory of Prof. Dr. Achim Krüger from the department *Experimentelle Onkologie, Klinikum rechts der Isar*. The number of lung metastasis was significantly reduced in animals which were inoculated with cells overexpressing rab31 compared to mice injected with vector control cells (Fig. 46).

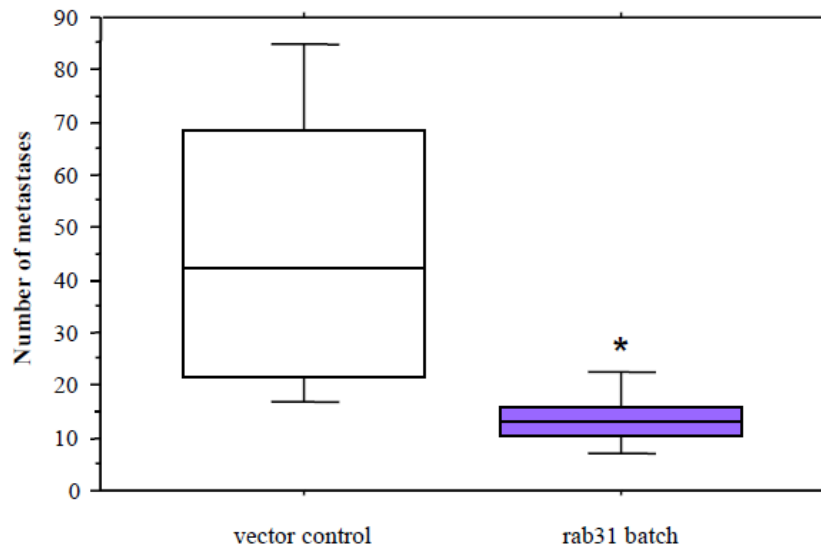


Fig. 46 Overexpression of rab31 affects lung colonization and metastatic growth of human breast cancer cells

Stably transfected, *lacZ*-tagged, MDA-MB-231 cells were inoculated into nude mice *via* tail vein injection. Mice received either vector control cells (white column, n=7) or batch-transfected rab31 cells (blue column, n=7). Animals were sacrificed at day 35 after injection. Lungs were collected and stained with XGal. Metastases were counted in lungs of the mice. Whisker box plots indicate the 25th and 75th percentile, the vertical bars indicate the 10th and 90th percentile. Results are expressed as the median number of metastases. The median value is indicated by a bar within the box. Statistically significant differences ($p < 0.05$) to the vector-control group are indicated by an asterisk.

6.4 Modulated matrixmetalloprotease (MMP) expression of MDA-MB-231 cells

The urokinase-system and matrixmetalloproteinases (MMPs) play a key role in degrading components of the ECM which is a crucial step in tumor metastasis (Yodkeeree et al. 2009). As shown before, the overexpression of uPAR-del4/5 in MDA-MB-231 cells results in a decreased invasive capacity through matrigelTM and a reduced amount of lung metastasis *in vitro*. Therefore, we started to investigate the expression and activity of the gelatine metalloprotease MMP9 in stable transfected MDA-MB-231 cells.

Stable transfected MDA-MB-231 cells were cultured in serumfree medium for 48 h. Cell culture plates were either pre-treated with collagen type IV or left untreated. Supernatant was collected and equal amounts were applied to a gelatine zymogram gel. The zymogram in figure 47 represents elevated expression of

proMMP9 in uPAR-del4/5 overexpressing cells compared to vector control cells. Rab31 overexpressing cells showed a reduced expression of proMMP9 compared to vector control cells. Expression and activity of MMP9 was not influenced by seeding the cells to collagen type IV pre-treated plates (Fig. 47).

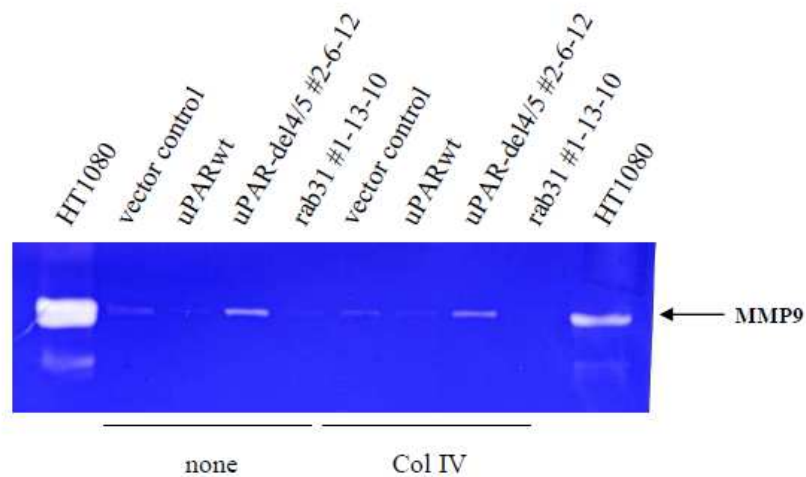


Fig. 47 Gelatine zymogram of cultured medium from MDA-MB-231 cells

MDA-MB-231 cells transfected with empty vector, uPARwt, uPAR-del4/5 or rab31 were seeded on collagen type IV treated or untreated plates. Conditioned serumfree medium was collected after 48h and analyzed in a zymogram as described before. Conditioned medium of PMA stimulated HT1080 cells was used as a positive control.

Simultaneously, supernatants were applied to standard acrylamide gels and analyzed by Western blot. By using a proMMP9 directed antibody (E9), we were able to confirm the results obtained in zymogram analysis (Fig. 48). ProMMP9 levels were elevated in uPAR-del4/5 overexpressing cell supernatant, when compared to vector control cells (Fig 48).

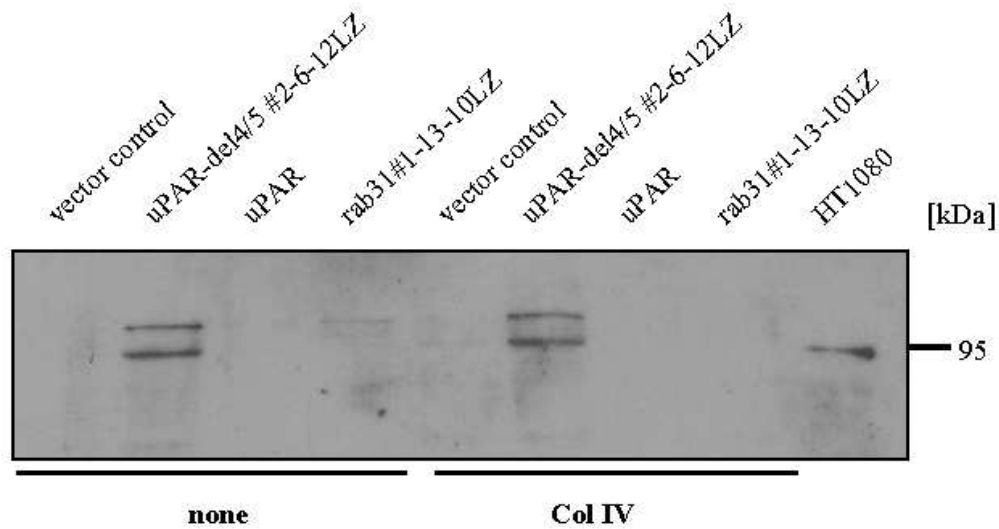


Fig. 48 Western blot analysis of MMP9 expression in cultured medium from MDA-MB-231 cells

MDA-MB-231 cells transfected with empty vector, uPARwt, uPAR-del4/5 or rab31 were seeded on collagen type IV treated or untreated plates. Conditioned medium, serumfree medium was collected after 48 h and analyzed in Western blot analysis as described before. Conditioned medium of PMA stimulated HT1080 cells was used as positive control. ProMMP9 was visualized using the antibody E9 (diluted 1:2000).

6.5 The extracellular signal-regulated kinase 1 and 2 (Erk1/2)

The uPA-uPAR complex activates many signaling pathways. One of these is the Ras-Raf-MEK-Erk pathway (Luo et al. 2011). The extracellular signal-regulated kinase 1 and 2 (Erk1/2) cascade transmits mostly mitogenic signals (Li et al. 2010). This signaling cascade responds to a variety of growth factors (EGF, NGF, PDGF, etc.), mitogens and environmental stimulations, leading to the activation and phosphorylation of Erk1/2. Hyper-phosphorylation of Erk1/2 has been found in many human malignant tumors including oral cancer, melanoma and breast cancer (Luo et al. 2011).

Stable transfected MDA-MB-231 cells overexpressing uPAR-del4/5 or rab31 showed no significant difference in the amounts of total Erk (p42/p44). Furthermore, levels of phosphorylated Erk (p-p42/p-p44) remain unchanged (Fig. 49). Seeding cells on fibronectin (data not shown) or collagen type IV pre-treated plates did not alter Erk1/2 phosphorylation. Overexpression of uPARwt led to an enhanced phosphorylation of Erk1/2 (Fig. 49). This result is in line with several

studies from other groups which show decreased phosphorylation of Erk1/2 when uPARwt is silenced (Li et al. 2010).

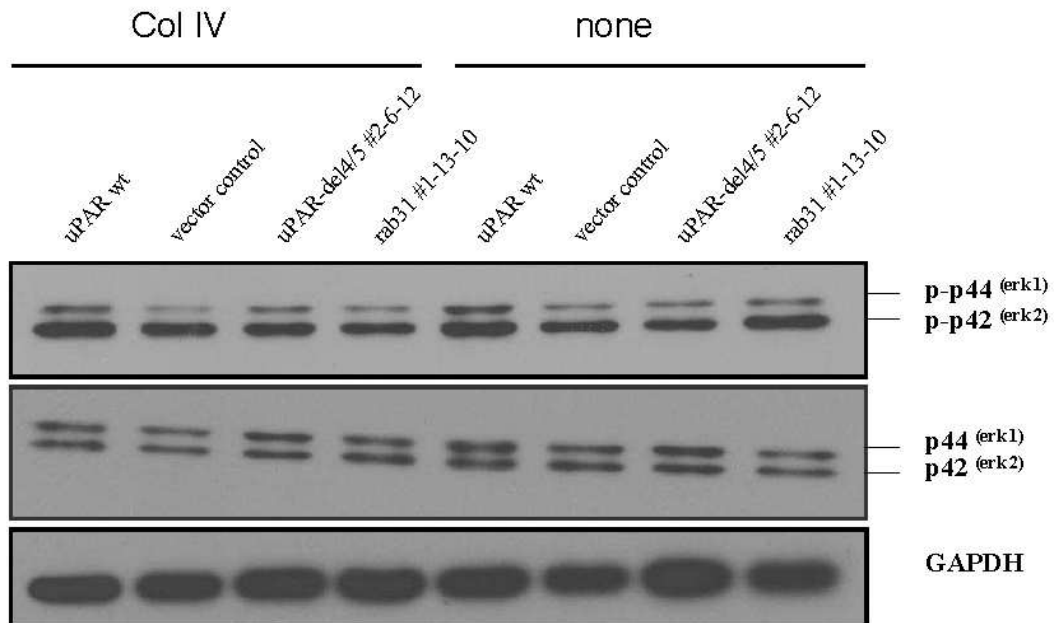


Fig. 49 Erk 1/2 phosphorylation of MDA-MB-231 breast cancer cells

Detection of total Erk1/2 expression and Erk1/2 phosphorylation by Western blot analysis. MDA-MB-231 cells transfected with uPAR-del4/5, uPARwt, rab31 or empty vector were cultured on collagen type IV treated or untreated plates for 24 h. Cell lysates were prepared for Western blot analysis as described. As endogenous control membrane were stained using a mAb directed to GAPDH. One representative image of a typical Western blot analysis is depicted.

6.6 EGFR signaling in rab31 overexpressing MDA-MB-231 cells

The epidermal growth factor receptor (EGFR) is a ubiquitously expressed cell surface receptor. As a receptor tyrosine kinase it has functions in the growth and development of differentiated cells. Many cancers are characterized by the overexpression of EGFR and subsequently misregulated EGFR signaling. In addition to the signaling events initiated by ligand binding, EGFR stimulation also triggers the internalization of the ligand-receptor complex *via* clathrin coated pits. EGFR internalization is an important regulative mechanism of receptor signaling (Ceresa et al. 2006).

Using affinity pull-down assays and co-immunoprecipitation analysis Ng et al. could show that rab31 associates with EGFR in a GTP-dependent manner. Furthermore, they could show that rab31 modulates EGFR trafficking in the epidermoid carcinoma cell line A431 (Ng et al. 2009). Therefore, we had a look on the tyrosine-phosphorylation pattern of rab31 overexpressing MDA-MB-231 cells. Cells were seeded on 6 well plates and were cultured in serumfree medium overnight. Cells were treated with 100 ng/ml EGF for 10 or 20 min at 37 °C, or left untreated. Reaction was stopped by putting the cells on ice and subsequent washes with cold PBS. Cells were lysed using a buffer containing phosphatase inhibitors. Equal amounts of total protein were applied to an 8 % acrylamide gel, followed by Western blot analysis. Staining with a phospho-tyrosine specific antibody (PY20) revealed a time dependent phosphorylation pattern. Untreated cells showed no tyrosine-phosphorylation of proteins with a molecular weight of approximately 170 kDa (molecular weight of EGFR). After 10 min stimulation with EGF, rab31 overexpressing cells represented a stronger EGFR-phosphorylation signal compared to vector control cells. After stimulation for 20 min, tyrosine-phosphorylation signal of rab31 overexpressing cells almost disappeared, whereas vector control cells showed maximum phosphorylation (Fig. 50). The total EGFR receptor was equally expressed in both cell lines and did not change expression upon EGF stimulation. As loading control membranes were stained with mAb against GAPDH.

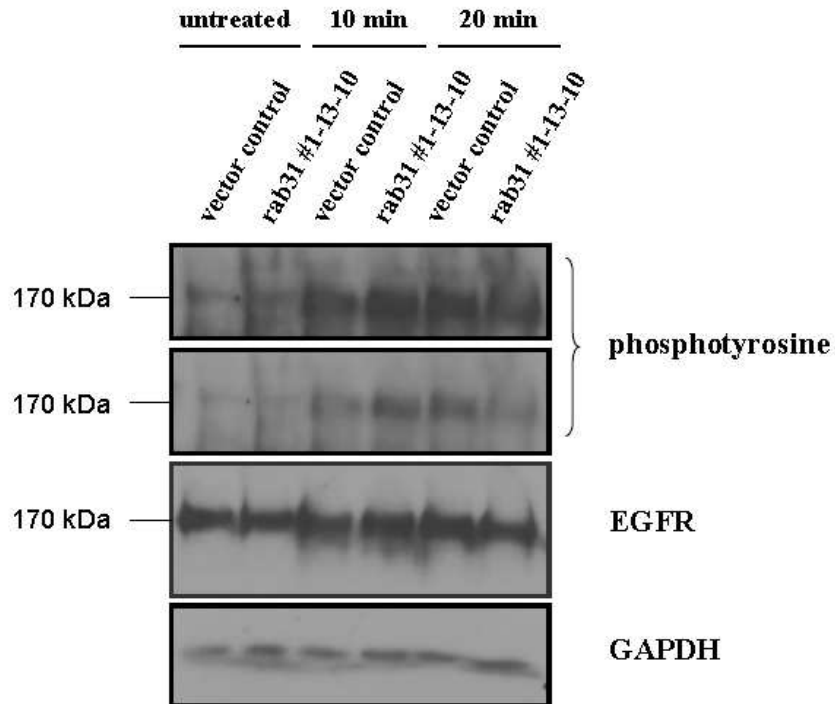


Fig. 50 Tyrosine-phosphorylation of EGF treated MDA-MB-231 cells overexpressing rab31

Detection of EGFR expression and tyrosine-phosphorylation by Western blot analysis. MDA-MB-231 cells transfected with rab31 or empty vector were treated with 100 ng/ml EGF 10 or 20 min at 37 °C or left untreated. Cell lysates were prepared for Western blot analysis as described. In order to normalize variations of protein concentrations and blotting efficiency, membranes were stripped and reprobbed with mAb directed to GAPDH. One representative image of a typical Western blot analysis is depicted.

7 Discussion

7.1 Characterization of breast cancer cell lines overexpressing uPAR-del4/5

Splicing is a highly regulated process of eukaryotes. Most primary transcripts (about 90 %) have to undergo splicing reactions, in which exons are joined together and non-coding intervening sequences, named introns are removed (Ward et al. 2010). Usage of alternative mRNA splicing can lead to several protein products encoded by one single gene. By this mechanism combinations of different exons and different intron/exon junctions are used to generate different splice products from the same primary transcript. Incorrectly spliced mRNAs which are not degraded by the so-called nonsense-mediated mRNA degradation can be translated to truncated, mutated, misfolded, and/or unstable proteins. Beside this, proteins are described missing complete protein domains, which may result in a loss or gain of function (Fackenthal et al. 2008).

The splicing pattern can be altered by polymorphisms or mutations which occur near splice sites or within splicing regulatory sequences. These changes can result in the expression of different mRNA variants which is a common feature of malignant disorders. It is not yet clear, whether alternative splicing results from a general deregulation of tumor cell functions, and by this way represents a by-product of cellular transformation, or if alternative splicing itself contributes to the malignant phenotype of cancer cells (Ward et al. 2010; Fackenthal et al. 2008).

uPAR-del4/5 is a splice variant of the urokinase receptor uPAR. The wildtype receptor is composed of three homolog domains D1, D2 and D3. In the splice variant exon 4 and exon 5 are cut off, leading to the deletion of the complete D2 of the wildtype receptor (Luther et al. 2003). The newly derived protein consisting of D1 and D3 fused together exhibits prognostic relevance in breast cancer patients (Luther et al. 2003; Kotzsch et al. 2008). Whether uPAR-del4/5 exhibits unique characteristics in the tumorbiology of breast cancer cells is analyzed in this study.

Three different breast cancer cell lines were stably transfected with a plasmid encoding the urokinase receptor splice variant or the empty vector as a control. Furthermore, cell clones with homogeneous high, medium or low expression of uPAR-del4/5 were analyzed for dose-dependent effects. Immunocytochemical

staining of transfected breast cancer cells revealed that the splice variant, analogously to the GPI-linked wildtype receptor, is predominantly located to the cell membrane.

Overexpression of uPAR-del4/5 in the human breast cancer cell lines MDA-MB-231 and CAMA-1 did not have effects on the proliferation of the cells. Only the proliferation of MDA-MB-435 cells overexpressing uPAR-del4/5 was significantly increased after 72 and 96 h. These cell line specific differences in proliferation may be explained by a differential expression profile of the breast cancer cell lines, with respect to expression of proteins important for proliferation. Integrins are only one example for the numerous proteins regulating cell proliferation. A recent study by Taherian et al. investigated integrin expression in MDA-MB-231 and MDA-MB-435 cells (Taherian et al. 2011). Interestingly, MDA-MB-435 cells consistently express higher levels of integrins. Especially, expression of the β_3 subunit and the heterodimer $\alpha_v\beta_3$ were highly elevated compared to MDA-MB-231 cells (Taherian et al. 2011). These data indicate a cell type specific effect of uPAR-del4/5 *in vitro* due to a cell line specific expression pattern of e.g. integrins.

Cellular adhesion was significantly impaired in all three investigated breast cancer cell lines, when uPAR-del4/5 expression was upregulated. In the non-invasive CAMA-1 cells, significant differences in adhesion were observed comparing high expressing and low expressing uPAR-del4/5 transfected cell clones. The invasive capacity of cells, as well as the number of lung metastasis in an experimental mouse lung colonization model could only be investigated using the highly invasive MDA-MB-231 cell line. The invasion through matrigelTM was significantly impaired when uPAR-del4/5 was overexpressed, observing the strongest reduction of invasive capacity in high expressing cell clones and monitoring only small differences when cell clones expressing low levels of the splice variant were analyzed.

Moreover, the number of lung metastasis was significantly reduced, when mice were injected with MDA-MB-231 cells overexpressing uPAR-del4/5. As only very few animals in the low expression group exhibit any metastasis at all, this result should be discussed with caution. However, the results observed for high and

medium expressing cell clones were in perfect line with the already published data of batch-transfected cells (Sato et al. 2010).

The extracellular matrix is a complex structural entity surrounding and supporting cells in all tissue and organs. It is composed of matrix molecules like the glycoprotein fibronectin, collagens, laminins, proteoglycans, and non-matrix proteins including growth factors (Berrier et al. 2007; Madsen et al. 2008). Cell-matrix adhesions are essential for cell migration, tissue organization, and differentiation. Abnormalities in matrix organisation and cell-ECM interactions contribute extensively to diseases like chronic atherosclerosis, and during tumor invasion and dissemination of metastasis. Integrins are cell surface adhesion receptors which mediate the cell-ECM communication across the plasma membrane by means of bidirectional signal transmission. The extracellular domains of integrin receptors bind ECM ligands and divalent cations. Furthermore, they can associate laterally with other cell surface receptors like e.g. uPAR (Madsen et al. 2008; Berrier et al. 2007).

The binding of uPA to its receptor does not only focus the proteolytic activity of the urokinase-system to the cell membrane but it also increases vitronectin binding by uPAR (Smith et al. 2010) and therefore enhances cellular adhesion to the matrix. In addition to this, binding of uPA to its receptor is a major determinant of physical and functional interactions of uPAR with a number of integrins (Blasi et al. 2002). Integrin-uPAR interaction was shown to be involved in tumor-associated functions, like for example tumor cell survival, adhesion, cell motility and angiogenesis (Alfano et al. 2005; Blasi et al. 2002).

It was described earlier, that uPAR binds uPA in its central cavity, this binding includes residues from all three domains (Smith et al. 2010). As already demonstrated by our group, uPAR-del4/5 does not interact with uPA applying a sensitive solid-phase ligand-binding assay and an uPA/uPAR-complex ELISA. In addition, we demonstrated that uPAR-del4/5 is not able to bind vitronectin (Sato et al. 2010).

The observed phenotype of uPAR-del4/5 overexpressing cells resembles the phenotype of uPARwt-silenced cells in some aspects. Several groups analyzed

MDA-MB-231 cells, which express relatively high levels of endogenous uPARwt and uPA in RNA interference studies. All of them describe a reduced invasive capacity through matrigelTM and a reduced number of metastasis in animal models when uPAR expression is silenced (Kunigal et al. 2007; Subramanian et al. 2006). This leads to the hypothesis that uPAR-del4/5 could act as a dominant-negative receptor, for example by competing with endogenous uPARwt for binding to certain integrins such as $\alpha_5\beta_1$ or $\alpha_v\beta_3$. Also the intact three domain structure of the receptor as well as uPA binding is implicated with uPAR-integrin interaction (Blasi et al. 2010) it remains to be determined whether uPAR-del4/5 exhibits a unique three-dimensional structure favouring integrin interaction.

The absence of a complete domain in the splice variant leads to structural changes in the protein which may enforce binding of uPAR-del4/5 to interacting proteins such as integrins. Assuming the splice variant as a dominant-negative receptor, available integrins would preferentially bind uPAR-del4/5 leaving no or few interaction partners for the wildtype receptor. This might on the one hand lead to effects similar to uPAR silencing due to interrupted integrin mediated cell adhesion, migration and cell signaling. On the other hand, uPAR-del4/5 binding to integrin might alter directly the broad spectrum of integrin induced cell signaling.

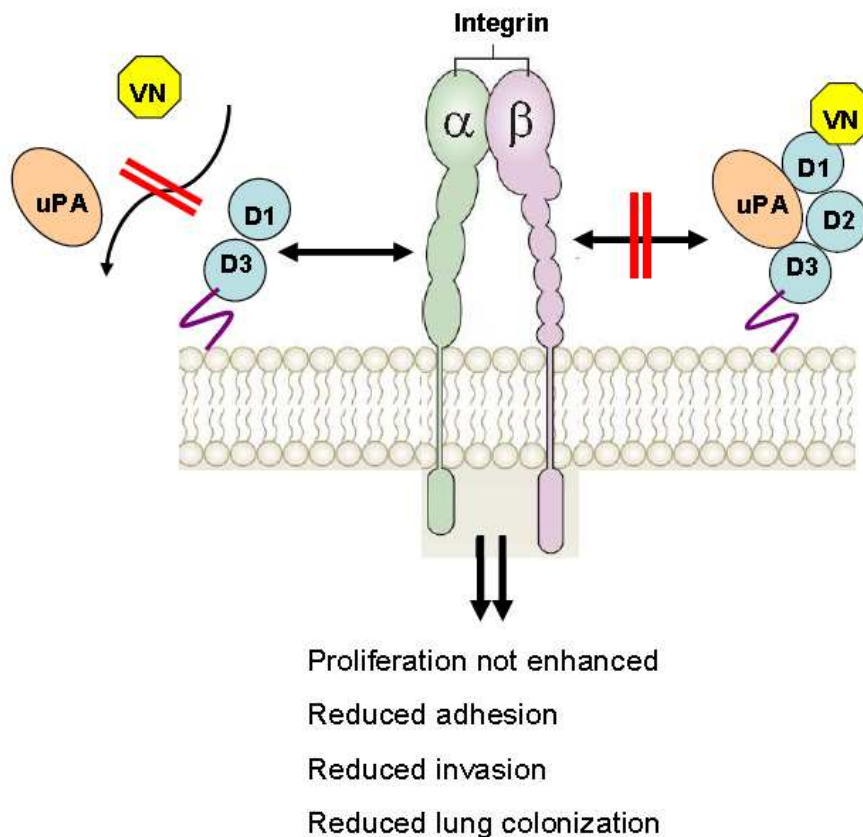


Figure 51. Scheme of possible uPAR-del4/5 integrin interaction

The splice variant, lacking D2 is not able to bind uPA and VN. Thinking of uPAR-del4/5 as a dominant-negative receptor, interaction of uPARwt with integrins, will be inhibited. As a consequence to this integrin signaling will be inhibited or altered.

MDA-MB-231 and CAMA-1 cells overexpressing uPAR-del4/5 show no significant changes in proliferation. This is in line with our investigations on Erk1/2 activation in MDA-MB-231 cells. Erk and p38 MAPK pathways are major players in cell proliferation, survival and G0-G1-S phase transition (Li et al. 2010). Like uPAR-del4/5 overexpressing cells, uPARwt silenced cells show no significant difference in the amounts of total Erk1/2 when compared to vector control cells. However, the levels of phosphorylated Erk1/2 were decreased significantly when uPARwt expression was silenced in MDA-MB-231 cells (Kunigal et al. 2007; Subramanian et al. 2006). In contrast to this, overexpression of uPAR-del4/5 did not have significant effects on Erk1/2 activation.

As already mentioned, expression of uPAR-del4/5 significantly affects cellular invasion *in vitro* as well as lung colonization *in vivo*. These processes depend on the expression and activity of matrix degrading enzymes like plasmin and MMPs

and the capacity of the cell to adhere to or detach from the matrix, which is mainly regulated by the expression/activation of adhesion molecules like integrins (Ungefroren et al. 2011). Matrix degradation is a key event triggering cancer invasion and metastasis. The interaction of uPA with its receptor uPAR plays an essential role in the proteolytic degradation of extracellular matrix and the basement membrane, which encapsels the primary tumor (Li et al. 2010). As uPAR-del4/5 is not able to bind uPA, the proteolytic activity is not focused to the cell membrane. This is one explanation for the less invasive phenotype of uPAR-del4/5 overexpressing cells.

As already mentioned, beside of uPA and plasmin, MMPs are key enzymes in cellular proteolysis. MMPs are a family of zinc-dependent endopeptidases. They are composed of three domains, the pro-peptide, the catalytic domain, and the hemopoxin-like C-terminal domain. In their enzymatically inactive pro-form a cysteine of the pro-domain interacts with the zinc ion in the catalytic site. Upon disruption of this interaction *via* a mechanism called cysteine-switch, access to the catalytic site is enabled and the enzyme becomes active. The cysteine-switch can be initiated by the proteolytic removal of the pro-domain by serine proteases like trypsin, plasmin and kallikreins, or other activated metalloproteases. In addition MMPs can be activated by chemical modification of the cysteine residue (Kohrmann et al. 2009; Kessenbrock et al. 2010). MMP function *in vivo* mainly depends on the local balance between the protease and physiological inhibitors, mainly tissue inhibitors of metalloproteinases (TIMPs). The pathophysiological relevance of increased expression of MMPs in tumor tissues depends on whether endogenous inhibitors or activating enzymes in the microenvironment are present (Kessenbrock et al. 2010).

It was described earlier by Rao et al. that uPAR-mediated signaling events result in the expression of cathepsin B and MMP9 during macrophage differentiation (Rao et al. 1995). Interestingly, the same effect regarding the MMP9 expression was observed in uPAR-del4/5 overexpressing breast cancer cells.

It is known for a long time that MMPs mediate ECM degradation, leading to cancer cell invasion and metastasis. However, MMPs exert more functions, in addition to simply degrading the ECM. Growth factors are released by the process of matrix

degradation. Growth factors, cytokines and chemokines can be activated by MMPs. Additionally, surface proteins like cytokine receptors, cell adhesion molecules and uPAR can be cleaved (Bauvois 2011). MMP9 plays a crucial role in cell signaling by controlling the bioavailability and bioactivity of molecules that target receptors which regulate cell growth, migration, inflammation and angiogenesis. With respect to cell signaling, MMPs under several circumstances do exhibit tumor-suppressing effects (Klein et al. 2011; Kessenbrock et al. 2010; Bauvois 2011). These tumor-suppressive effects might be an explanation for the observed effects in uPAR-del4/5 overexpressing MDA-MB-231 cells.

Based on the elevated proMMP9 expression monitored in conditioned medium of MDA-MB-231 cells overexpressing uPAR-del4/5 one would expect an enhanced proteolytic activity of the cells and subsequently a more invasive phenotype. Surprisingly, *in vitro* and *in vivo* the opposite effect was monitored. This phenomenon might be explained by either alterations in activating proMMP9, an overexpression of MMP9 inhibitors, or by additional non-proteolytic functions of MMP9.

Taken together the described effects of uPAR-del4/5 overexpression in breast cancer cell lines lead to the conclusion that the uPAR-del4/5 protein acts as a forceful tumor suppressor. This observation stays in contrast to the clinical data which show a poor prognosis of patients expressing high mRNA levels of uPAR-del4/5 (Kotzsch et al. 2008; Luther et al. 2003). The measured uPAR-del4/5 mRNA levels might reflect the malignant status of the diseases, not the functions arising from high protein levels of the protein. In addition, it may be important to correlate uPAR-del4/5 protein levels instead of mRNA with the survival of the patients.

One has to consider, that uPAR-del4/5 might not be the reason for the poor outcome of the patient, but rather a defence mechanism of the body as response to the disease. Another hypothesis concerning the unexpected *in vitro* results is based on the heterogeneity of tumors and the tumor microenvironment (Hanahan et al. 2011). The complex interactions of tumor cells with the ECM and tumor surrounding non-neoplastic cells, like endothelial cells, cancer-associated

fibroblasts, mesenchymal stem cells, a variety of immune cells and tumor associated macrophages, modulate tumor growth and the development of metastasis (Ungefroren et al. 2011). One can speculate whether the properties of different cell types, being present within a tumor, are necessary to turn the tumor-suppressive functions of uPAR-del4/5 into tumor /metastasis promoting functions. It has been already described that the bidirectional interaction of tumor cells with non-cancerous cells can either stimulate tumor cells to metastasize, or can keep them in a dormant state (Calorini et al. 2010). ECM proteins, growth factors, cytokines and chemokines are only examples of molecules secreted by the stromal cells which can stimulate cancer cells to a more aggressive phenotype (Calorini et al. 2010). Therefore, one can speculate that stromal cells secrete proteases which degrade the basement membrane enclosing the primary tumor. The less adhesive phenotype of the uPAR-del4/5 expressing cancer cells may enable the dissemination of the cells from the primary tumor, which opens the way to tumor metastasis.

7.2 Characterization of breast cancer cell lines overexpressing rab31

Rab proteins constitute the largest family of monomeric small GTPases. Numerous studies have established that Rab proteins are distributed to distinct intracellular compartments and regulate transport between organelles. Mutations in Rab GTPases as well as altered Rab expression or activity were shown to be involved in neurologic and neurodegenerative diseases, lipid storage disorders and cancer (Agola et al. 2011). A growing number of Rab proteins such as rab5, rab11, rab21, rab25, and rab27B were shown to be associated with tumor growth/behavior and prognosis of breast cancer patients (Subramani et al. 2010; Yang et al. 2011; Hendrix et al. 2010). However, still few data are available on rab31 expression in cancer in general and breast cancer or its impact on disease progression in particular (Heinonen et al. 2011; Chen et al. 1996; Yim et al. 2009; Kotzsch et al. 2011; Hwang et al. 2011). Abba et al. (2005) described that rab31 mRNA was overexpressed in ER α -positive breast cancer tissue. This result is in line with recently published observations that high rab31 mRNA expression is

associated with poor prognosis of lymphnode-negative breast cancer patients in the primary tumor (Kotzsch et al. 2008).

To analyze possible cellular effects of variable rab31 protein expression, we stably transfected breast cancer cell lines with the eukaryotic expression plasmid pRcRSV harboring the rab31 cDNA sequence. In general, data based on unphysiologically high protein overexpression should be interpreted with caution. However, applying Western blot analysis and, in particular, a newly developed sensitive ELISA for quantification of rab31 (data not shown, collaboration with the *Institut für Pathologie, TU Dresden*), we found that, in MDA–MB-231 cells as an example, rab31 protein was increased only up to about 5-fold in the high expressing clones (≈ 2 ng/mg total protein). In a study by Bao et al. (2002), the physiological rab31 content in platelets was estimated to be approximately 5 ng/mg total protein. Thus, it can be concluded that in the present study the rab31 levels were modulated within a physiologic range.

On one hand, overexpression of rab31 induced an enhanced proliferation of breast cancer cells. Interestingly, using cell lines with endogenous rab31 expression (MDA-MB-231), high levels of rab31 were necessary to monitor a significant elevation of proliferation, whereas already moderate levels of rab31 led to a significant effect on proliferation in cell lines with no detectable endogenous rab31 expression (CAMA-1 and MDA-MB-435). On the other hand, high levels of rab31 in breast cancer cells resulted in significantly reduced adhesion towards ECM proteins as well as invasive capacity. Likewise, the effects on adhesion and invasion were dose-dependent, because effects monitored in low expressing cell clones differed significantly from those observed in high expressing cell clones. Comparing cell lines with differential endogenous rab31 levels, again the strongest effects were detected in breast cancer cell lines without detectable endogenous rab31 expression (CAMA-1 and MDA-MB-435). In line with its reduced invasive capacity in matrigelTM invasion assays, we observed a significantly reduced amount of lung metastasis in a xenograft mouse model after injection of MDA-MB-231 cells overexpressing rab31 into the tail vein compared to mice injected with vector control cells. Since the development and growth of tumor metastases require that neoplastic cells must either have the potential to shift between

proliferative and invasive phenotypes or simply express both simultaneously (Gao et al. 2005), this results suggest that overexpression of rab31 may lead to a proliferative phenotype in breast cancer cells.

	rab31 expression	
	low	high
Proliferation	+	++
Adhesion	++	+
Invasion	++	+
Lung colonization	++	-

Figure 52. Characteristics of MDA-MB-231 cells expressing different levels of rab31

MDA-MB-231 cells expressing high levels of rab31 proliferate faster, compared to cells expressing low rab31 levels. Adhesion to ECM proteins, as well as the invasive capacity through matrigel™ decreased with increasing rab31 expression. Furthermore, the ability of breast cancer cells to colonize the lung *in vivo* was dramatically impaired when rab31 expression was elevated.

In the present work, breast cancer cells overexpressing rab31 revealed an enhanced proliferation of the cells. Rab25 is the best described Rab protein with elevated mRNA levels in ovarian and breast cancer (Cheng et al. 2005). The proposed mechanism, how rab25 regulates cell proliferation and survival might be plausible also for rab31. Rab25 regulates receptor internalization, formation of vesicles, intracellular trafficking and receptor recycling. In addition to this, elevated rab25 expression in ovarian cancer cells was shown to result in the activation of Akt and the downregulation of bax and bak levels. As a consequence to this, cells show increased proliferation and decreased apoptosis (Cheng et al. 2005). As already mentioned before, Ng et al. (2009) could show that rab31 interacts with the EGFR and modulates its internalization in the epidermoid carcinoma cell lines A431. Furthermore, rab31 was shown to be involved in the transport of vesicles from the TGN to endosomes (Rodriguez-Gabin et al. 2001). The functional similarity of rab31 and rab25 with respect to receptor internalization, as well as the similarities in localization lead us to the conclusion, that high levels of rab31 may

also influence signaling pathways which are regulated by rab25. This could explain the pro-proliferative characteristics of high rab31 protein levels.

Recently it was shown that rab31 translation is regulated by the mRNA binding protein HuR (Heinonen et al. 2011). HuR is aberrantly expressed at early stages of breast carcinogenesis and associated with reduced survival in breast cancer (Heinonen et al. 2007; Heinonen et al. 2005). Through its post-transcriptional influence on specific target mRNAs, HuR can alter the cellular response to proliferative, apoptotic, differentiation and other stimuli (Srikantan et al. 2012). By enhancing the stability of rab31 transcripts and regulation of their translation, HuR may cause higher rab31 levels in tumor cells. In fact, when HuR expression was silenced in epithelial 184B5Me breast cancer cells, a significant reduction of rab31 mRNA expression was observed (Heinonen et al. 2011). As expected and consistent with published results for other cancer types, HuR overexpression in MDA-MB-231 breast cancer cells resulted in increasing cellular growth rates and alterations in cell cycle kinetics *in vitro* (Gubin et al. 2010). Surprisingly, however, HuR overexpression significantly interfered with tumor growth *in vivo*, whereas vector control and wild type MDA-MB-231 cells grew similarly and resulted in much larger tumors than those formed by HuR overexpressing cells. This is very similar to our observations, surprisingly, indicating a strongly reduced metastatic capacity of these cancer cells in a xenograft mouse model despite the fact that high rab31 mRNA levels in tumor tissue are associated with a poor prognosis in breast cancer patients (Kotzsch et al. 2008) and overexpression of rab31 *in vitro* leads to increased proliferation.

Rab31 is a member of the rab5 subfamily, which includes rab5, rab21, rab22A, and rab31 (Delprato et al. 2004; Carney et al. 2006). All in all, there is little information about downstream effectors of these Rab proteins. Some members of this subfamily have been shown to regulate internalization and recycling pathways of integrins (rab21, rab5) as well as growth factor receptors like EGFR (rab5, rab22A), thereby controlling/driving processes such as cell adhesion, proliferation migration involved in tumor invasion and metastasis (Pellinen et al. 2006; Woller et al. 2011; Chen et al. 2009). Rab5 and rab22A are sharing high amino acid

similarity with rab31 (Chen et al. 1996). Within the N-terminal 167 residues, rab31 shares 85 identical plus 60 homologous amino acids (= 86.8 % homology) with rab5, and even 133 identical plus 20 homologous amino acids (= 91.6 % homology) with rab22A. Rab5 has a broad range of functions in intracellular trafficking and receptor internalization. For instance, rab5 is one of a set of Rab proteins controlling integrin recycling. In detail, rab5 regulates endocytosis and recycling of beta-integrins. Knockdown of rab5 prevents integrin signaling from activating rac to promote cell migration and the apoptotic signaling pathway (Subramani et al. 2010). GEFs, such as members of the RIN family, play a key role in the regulation of rab5 functions. RIN proteins, however, do not exclusively activate rab5. Recently it was described that e.g. RIN3 showed enhanced nucleotide exchange reaction to rab31 compared to rab5 (Kajiho et al. 2011). Therefore, rab31 overexpression may lead to a reduced rab5 activity causing altered integrin internalization, subsequent cell migration and finally reduced invasive capacity. Additionally, rab31 may also have functions in growth factor receptor internalization in breast cancer cell lines. As previously described by Ng et al. (2009), rab31 interacts with EGFR and modulates its internalization in the epidermoid carcinoma cell line A431. EGFR-ligand complexes continue signaling from intracellular signaling endosomes (Miaczynska et al. 2010; Chia et al. 2009). EGFR signaling from endosomes differs quantitatively and qualitatively from that at the plasma membrane. Depending on its localization within the cell, the EGFR associates with different signaling adaptors. Therefore, alterations in EGFR internalization and trafficking can affect the pattern as well as the duration of signal transduction (Chia et al. 2009). Interestingly, the same study indicated that EGFR signaling is not limited to the essential EGFR internalization/transport Rabs like rab4, rab5, rab7 and rab11. Rather, any Rab protein whose overexpression can alter endocytic trafficking could potentially influence EGFR signaling in a cell or tissue specific manner (Chia et al. 2009).

Analysis of the EGFR-phosphorylation status in MDA-MB-231 cells overexpressing rab31 revealed a time-dependent alteration of phosphorylation. Upon EGF stimulation for 10 min, rab31 overexpressing cells showed an enhanced tyrosine-phosphorylation status compared to vector control.

Prolongation of EGF-stimulation to 20 min revealed maximum phosphorylation of vector control cells and a tyrosine-phosphorylation of rab31 overexpressing cells compromising the unstimulated phenotype. Total EGFR expression was not altered by rab31 overexpression.

These results might reflect an altered response to EGFR internalization signals of rab31 overexpressing cells. It is already described, that EGFR signaling *via* Ras increases the activity of the GEF RIN1. This leads to the association of rab5 with signal-transducing adaptor molecule 2 (STAM2) and subsequent increased internalization and degradation of EGFR (Agola et al. 2011). Although no direct interaction of RIN1 with rab31 was detected in a cell free assay, expression of RIN1 in HEK293T cells enhanced the amount of GTP-bound rab31 (Kajiho et al. 2011). Additionally, high GEF activity of RIN2 and RIN3 is described for rab31 (Kajiho et al. 2011). As already mentioned, rab5 specific RIN proteins were demonstrated to interact also with rab31. Therefore, it must be considered that other rab5 specific proteins such as STAMs, also not exclusively bind one single Rab protein. Interaction of rab31 with RIN proteins and STAMs could explain the observed alterations in EGFR activation, internalization and recycling.

Like uPAR-del4/5, rab31 *in vitro* exerts more a tumor suppressive phenotype rather than a metastasis promoting one. Rab31 mRNA expression analysis of tumors from breast cancer patients revealed a correlation of high rab31 levels with a poor prognosis of the patients (Kotzsch et al. 2008). This contrary phenotype might be explained –similar to uPAR-del4/5- by the interplay of tumor cells with tumor surrounding non-tumor cells and the tumor-microenvironment. Matrix degrading proteases secreted by the tumor-stroma could degrade the basal membrane and the ECM surrounding the primary tumor. The reduced adhesion of rab31 overexpressing cells facilitates the cells to disseminate from the primary tumor, representing the first steps of tumor metastasis. In addition, one may speculate that rab31 expression is upregulated as a response to the expression of other metastasis promoting factors.

7.3 Link between uPAR-del4/5 and rab31

Breast cancer patients expressing both uPAR-del4/5 and rab31 mRNA at high levels show a significantly worse DMFS and overall survival (OS) compared to patients expressing both proteins at low levels. Rab31 and uPAR-del4/5 mRNA values have independent but additive pure prognostic relevance in lymphnode-negative breast cancer patients (Kotzsch et al. 2008). As described in this study, the overexpression of uPAR-del4/5 and rab31 exerts similar effects on the tumorbiologically relevant processes like adhesion and invasion. Even in a xenograft mouse lung colonization model similar results were obtained. The clinical data and the results shown in this study indicate that uPAR-del4/5 and rab31 act in independent but possibly associated tumor relevant signaling pathways.

Up to now, we have no data indicating how these two proteins act together. It can be speculated that rab31 might be somehow linked to uPAR-del4/5 *via* the supposed uPAR-del4/5-integrin interaction. Rab5 is involved in internalization and recycling of beta integrins (Subramani et al. 2010). Therefore one can speculate that rab31 also exerts functions in integrin internalization. This could lead to altered integrin signaling and rac activation causing changes in cell migration and apoptosis. Another link might be related to the internalization of other uPAR interaction partners like EGFR and G-protein-coupled receptors, or by internalization of uPAR itself.

Recently it could be shown that rab31 is involved in the transport of MPRs, especially of the cation-dependent mannose 6-phosphate receptor, from the TGN to endosomes (Rodriguez-Gabin et al. 2009; Kajihio et al. 2011).

In eukaryotic cells, MPRs are key components of the lysosomal enzyme targeting system that bind newly synthesized Man-6-P-containing acid hydrolases and function as efficient cargo transporters from the TGN to endosomal/lysosomal compartments (Chavez et al. 2007; Bohnsack et al. 2009). The two distinct MPRs, the 46 kDa cation-dependent mannose 6-phosphate (Man-6-P) receptor (CD-MPR) and the 300 kDa cation-independent Man-6-P receptor (CI-MPR), are the sole members of the P-type lectin family (Kim et al. 2009). Although CD-MPR and CI-MPR bind the same array of proteins, the respective affinity of each MPR for

different phosphorylated glycoproteins varies. This provides a biochemical mechanism, which, in part, may explain the interaction of the two MPRs with overlapping yet distinct subsets of ligands *in vivo* (Sleat et al. 1997). The CI-MPR has been described to bind proteins bearing the Man-6-P recognition marker as well as the peptide hormone IGF-II and to be implicated in numerous cellular processes, including cell growth, apoptosis, and cell migration (Dahms et al. 1994; Dahms et al. 2002). In addition, CI-MPR has been shown to interact also with a number of proteins that do not contain Man-6-P such as uPAR (Nykjaer et al. 1998; Kreiling et al. 2003; Olson et al. 2004). The uPAR binding epitope on CI-MPR is different from those binding Man-6-P and IGF-II. Binding of uPAR to MPRs seems to be specific for CI-MPR and independent of uPA. CI-MPR was proposed to be involved in the turnover of uPAR and to regulate the cell surface concentration of uPAR by directing uPAR to lysosomes as well as internalizing uPAR when it interacts with uPA (Nykjaer et al. 1998). The detection of uPAR in endosomes agrees well with the primary function of MPRs, which is the transport of ligands from the TGN or cell surface to the endosome. Interestingly, both pro-uPA/uPA and uPAR were upregulated in CI-MPR knockdown cells (Schiller et al. 2009).

Since uPAR as well as rab31 mRNA are known to be regulated by the RNA binding protein HuR *in vitro* and *in vivo* (Tran et al. 2003; Heinonen et al. 2011), the observed higher uPAR-del4/5 as well as rab31 expression in metastazing breast cancer may be due to higher HuR expression in these tumors and points to a possible link between rab31 and the uPA/uPAR system in cancer cells. All three factors, HuR, uPAR-del4/5 and rab31 have been demonstrated to modulate cellular processes such as proliferation, adhesion and/or invasion. Strikingly, although high expression levels of these three factors are clearly associated with a poor prognosis of breast cancer patients, in experimental animal xenograft tumor models –using the same breast cancer cell line MDA-MB-231- overexpression in each case unexpectedly leads to a seemingly reduced tumorigenicity. Since tumor progression is known to be a multi-step process including transition of the malignant phenotype of tumor cells between a more proliferative versus invasive phenotype as well as interactions between tumor cells and tumor-associated

stromal cells. The results obtained with the xenograft animal models, therefore, may not directly mirror the malignant potential of rab31-, uPAR-del4/5- or HuR-overexpressing tumors in human breast cancer. With regard to the plasticity of tumor cells in dependence on rab31 or uPAR-del4/5 expression, our results, however, indicate that rab31 and uPAR-del4/5 expression is involved in modulation of tumor-relevant biological processes.

7.4 Conclusion

The urokinase receptor splice variant uPAR-del4/5 and rab31 are prognostic factors in breast cancer patients (Kotzsch et al. 2008). Both proteins show a tumor suppressive phenotype in *in vitro* invasion assays and in xenograft mouse experiments. Patients expressing both proteins at high levels on the mRNA level have a worsened outcome compared to patients expressing only one of these proteins at high levels. Nevertheless, multivariate analysis revealed uPAR-del4/5 and rab31 as independent prognostic factors (Kotzsch et al. 2008). This data indicate that uPAR-del4/5 and rab31 are proteins relevant for tumorbiological processes. Presumably, the proteins play key roles in independent but associated tumor relevant signaling pathways. It remains to be investigated how these proteins alter adhesion and invasion of the breast cancer cells, and how they interact with other cells within the tumor or with tumor surrounding cells.

8 References

- Abba MC, Hu Y, Sun H, Drake JA, Gaddis S, Baggerly K, Sahin A and Aldaz CM (2005). "Gene expression signature of estrogen receptor alpha status in breast cancer." BMC Genomics **6**: 37.
- Agarwal R, Jurisica I, Mills GB and Cheng KW (2009). "The emerging role of the RAB25 small GTPase in cancer." Traffic **10**(11): 1561-8.
- Agola J, Jim P, Ward H, Basuray S and Wandinger-Ness A (2011). "Rab GTPases as regulators of endocytosis, targets of disease and therapeutic opportunities." Clin Genet.
- Alfano D, Franco P, Vocca I, Gambi N, Pisa V, Mancini A, Caputi M, Carriero MV, Iaccarino I and Stoppelli MP (2005). "The urokinase plasminogen activator and its receptor: role in cell growth and apoptosis." Thromb Haemost **93**(2): 205-11.
- Andreasen PA, Egelund R and Petersen HH (2000). "The plasminogen activation system in tumor growth, invasion, and metastasis." Cell Mol Life Sci **57**(1): 25-40.
- Andreasen PA, Kjoller L, Christensen L and Duffy MJ (1997). "The urokinase-type plasminogen activator system in cancer metastasis: a review." Int J Cancer **72**(1): 1-22.
- Armstrong J (2000). "How do Rab proteins function in membrane traffic?" Int J Biochem Cell Biol **32**(3): 303-7.
- Bao X, Faris AE, Jang EK and Haslam RJ (2002). "Molecular cloning, bacterial expression and properties of Rab31 and Rab32." Eur J Biochem **269**(1): 259-71.
- Barr FA (2009). "Rab GTPase function in Golgi trafficking." Semin Cell Dev Biol **20**(7): 780-3.
- Bass R and Ellis V (2009). "Regulation of urokinase receptor function and pericellular proteolysis by the integrin alpha(5)beta(1)." Thromb Haemost **101**(5): 954-62.
- Bauvois B (2011). "New facets of matrix metalloproteinases MMP-2 and MMP-9 as cell surface transducers: Outside-in signaling and relationship to tumor progression." Biochim Biophys Acta **1825**(1): 29-36.

- Beaufort N, Leduc D, Rousselle JC, Magdolen V, Luther T, Namane A, Chignard M and Pidard D (2004). "Proteolytic regulation of the urokinase receptor/CD87 on monocytic cells by neutrophil elastase and cathepsin G." J Immunol **172**(1): 540-9.
- Behrendt N, Ploug M, Patthy L, Houen G, Blasi F and Dano K (1991). "The ligand-binding domain of the cell surface receptor for urokinase-type plasminogen activator." J Biol Chem **266**(12): 7842-7.
- Berrier AL and Yamada KM (2007). "Cell-matrix adhesion." J Cell Physiol **213**(3): 565-73.
- Blasi F and Carmeliet P (2002). "uPAR: a versatile signalling orchestrator." Nat Rev Mol Cell Biol **3**(12): 932-43.
- Blasi F and Sidenius N (2010). "The urokinase receptor: focused cell surface proteolysis, cell adhesion and signaling." FEBS Lett **584**(9): 1923-30.
- Bohnsack RN, Song X, Olson LJ, Kudo M, Gotschall RR, Canfield WM, Cummings RD, Smith DF and Dahms NM (2009). "Cation-independent mannose 6-phosphate receptor: a composite of distinct phosphomannosyl binding sites." J Biol Chem **284**(50): 35215-26.
- Cailleau R, Olive M and Cruciger QV (1978). "Long-term human breast carcinoma cell lines of metastatic origin: preliminary characterization." In Vitro **14**(11): 911-5.
- Cailleau R, Young R, Olive M and Reeves WJ, Jr. (1974). "Breast tumor cell lines from pleural effusions." J Natl Cancer Inst **53**(3): 661-74.
- Calorini L and Bianchini F (2010). "Environmental control of invasiveness and metastatic dissemination of tumor cells: the role of tumor cell-host cell interactions." Cell Commun Signal **8**: 24.
- Carney DS, Davies BA and Horazdovsky BF (2006). "Vps9 domain-containing proteins: activators of Rab5 GTPases from yeast to neurons." Trends Cell Biol **16**(1): 27-35.
- Casey JR, Petranka JG, Kottra J, Fleenor DE and Rosse WF (1994). "The structure of the urokinase-type plasminogen activator receptor gene." Blood **84**(4): 1151-6.
- Ceresa BP and Bahr SJ (2006). "rab7 activity affects epidermal growth factor:epidermal growth factor receptor degradation by regulating endocytic trafficking from the late endosome." J Biol Chem **281**(2): 1099-106.

- Chambers AF (2009). "MDA-MB-435 and M14 cell lines: identical but not M14 melanoma?" Cancer Res **69**(13): 5292-3.
- Chaurasia P, Aguirre-Ghiso JA, Liang OD, Gardsvoll H, Ploug M and Ossowski L (2006). "A region in urokinase plasminogen receptor domain III controlling a functional association with alpha5beta1 integrin and tumor growth." J Biol Chem **281**(21): 14852-63.
- Chavez CA, Bohnsack RN, Kudo M, Gotschall RR, Canfield WM and Dahms NM (2007). "Domain 5 of the cation-independent mannose 6-phosphate receptor preferentially binds phosphodiesterases (mannose 6-phosphate N-acetylglucosamine ester)." Biochemistry **46**(44): 12604-17.
- Chen D, Guo J, Miki T, Tachibana M and Gahl WA (1996). "Molecular cloning of two novel rab genes from human melanocytes." Gene **174**(1): 129-34.
- Chen PI, Kong C, Su X and Stahl PD (2009). "Rab5 isoforms differentially regulate the trafficking and degradation of epidermal growth factor receptors." J Biol Chem **284**(44): 30328-38.
- Cheng KW, Lahad JP, Gray JW and Mills GB (2005). "Emerging role of RAB GTPases in cancer and human disease." Cancer Res **65**(7): 2516-9.
- Chia WJ and Tang BL (2009). "Emerging roles for Rab family GTPases in human cancer." Biochim Biophys Acta **1795**(2): 110-6.
- Clarke R (1996). "Human breast cancer cell line xenografts as models of breast cancer. The immunobiologies of recipient mice and the characteristics of several tumorigenic cell lines." Breast Cancer Res Treat **39**(1): 69-86.
- Cortese K, Sahores M, Madsen CD, Tacchetti C and Blasi F (2008). "Clathrin and LRP-1-independent constitutive endocytosis and recycling of uPAR." PLoS One **3**(11): e3730.
- Czekay RP, Kuemmel TA, Orlando RA and Farquhar MG (2001). "Direct binding of occupied urokinase receptor (uPAR) to LDL receptor-related protein is required for endocytosis of uPAR and regulation of cell surface urokinase activity." Mol Biol Cell **12**(5): 1467-79.
- Dahms NM and Hancock MK (2002). "P-type lectins." Biochim Biophys Acta **1572**(2-3): 317-40.
- Dahms NM, Wick DA and Brzycki-Wessell MA (1994). "The bovine mannose 6-phosphate/insulin-like growth factor II receptor. Localization of the insulin-

- like growth factor II binding site to domains 5-11." J Biol Chem **269**(5): 3802-9.
- de Bock CE and Wang Y (2004). "Clinical significance of urokinase-type plasminogen activator receptor (uPAR) expression in cancer." Med Res Rev **24**(1): 13-39.
- Delprato A, Merithew E and Lambright DG (2004). "Structure, exchange determinants, and family-wide rab specificity of the tandem helical bundle and Vps9 domains of Rabex-5." Cell **118**(5): 607-17.
- Duffy MJ and Duggan C (2004). "The urokinase plasminogen activator system: a rich source of tumour markers for the individualised management of patients with cancer." Clin Biochem **37**(7): 541-8.
- Fackenthal JD and Godley LA (2008). "Aberrant RNA splicing and its functional consequences in cancer cells." Dis Model Mech **1**(1): 37-42.
- Fogh J, Wright WC and Loveless JD (1977). "Absence of HeLa cell contamination in 169 cell lines derived from human tumors." J Natl Cancer Inst **58**(2): 209-14.
- Gao CF, Xie Q, Su YL, Koeman J, Khoo SK, Gustafson M, Knudsen BS, Hay R, Shinomiya N and Vande Woude GF (2005). "Proliferation and invasion: plasticity in tumor cells." Proc Natl Acad Sci U S A **102**(30): 10528-33.
- Goud B and Gleeson PA (2010). "TGN golgins, Rabs and cytoskeleton: regulating the Golgi trafficking highways." Trends Cell Biol **20**(6): 329-36.
- Gubin MM, Calaluze R, Davis JW, Magee JD, Strouse CS, Shaw DP, Ma L, Brown A, Hoffman T, Rold TL and Atasoy U (2010). "Overexpression of the RNA binding protein HuR impairs tumor growth in triple negative breast cancer associated with deficient angiogenesis." Cell Cycle **9**(16): 3337-46.
- Hanahan D and Weinberg RA (2000). "The hallmarks of cancer." Cell **100**(1): 57-70.
- Hanahan D and Weinberg RA (2011). "Hallmarks of cancer: the next generation." Cell **144**(5): 646-74.
- Heinonen M, Bono P, Narko K, Chang SH, Lundin J, Joensuu H, Furneaux H, Hla T, Haglund C and Ristimaki A (2005). "Cytoplasmic HuR expression is a prognostic factor in invasive ductal breast carcinoma." Cancer Res **65**(6): 2157-61.

- Heinonen M, Fagerholm R, Aaltonen K, Kilpivaara O, Aittomaki K, Blomqvist C, Heikkila P, Haglund C, Nevanlinna H and Ristimaki A (2007). "Prognostic role of HuR in hereditary breast cancer." Clin Cancer Res **13**(23): 6959-63.
- Heinonen M, Hemmes A, Salmenkivi K, Abdelmohsen K, Vilen ST, Laakso M, Leidenius M, Salo T, Hautaniemi S, Gorospe M, Heikkila P, Haglund C and Ristimaki A (2011). "Role of RNA binding protein HuR in ductal carcinoma in situ of the breast." J Pathol **224**(4): 529-39.
- Hendrix A, Braems G, Bracke M, Seabra M, Gahl W, De Wever O and Westbroek W (2010). "The secretory small GTPase Rab27B as a marker for breast cancer progression." Oncotarget **1**(4): 304-8.
- Hoyer-Hansen G, Ronne E, Solberg H, Behrendt N, Ploug M, Lund LR, Ellis V and Dano K (1992). "Urokinase plasminogen activator cleaves its cell surface receptor releasing the ligand-binding domain." J Biol Chem **267**(25): 18224-9.
- Hwang KA, Park SH, Yi BR and Choi KC (2011). "Gene alterations of ovarian cancer cells expressing estrogen receptors by estrogen and bisphenol a using microarray analysis." Lab Anim Res **27**(2): 99-107.
- Itzen A and Goody RS (2011). "GTPases involved in vesicular trafficking: structures and mechanisms." Semin Cell Dev Biol **22**(1): 48-56.
- Kajiho H, Sakurai K, Minoda T, Yoshikawa M, Nakagawa S, Fukushima S, Kontani K and Katada T (2011). "Characterization of RIN3 as a guanine nucleotide exchange factor for the Rab5 subfamily GTPase Rab31." J Biol Chem **286**(27): 24364-73.
- Kessenbrock K, Plaks V and Werb Z (2010). "Matrix metalloproteinases: regulators of the tumor microenvironment." Cell **141**(1): 52-67.
- Kim JB, O'Hare MJ and Stein R (2004). "Models of breast cancer: is merging human and animal models the future?" Breast Cancer Res **6**(1): 22-30.
- Kim JJ, Olson LJ and Dahms NM (2009). "Carbohydrate recognition by the mannose-6-phosphate receptors." Curr Opin Struct Biol **19**(5): 534-42.
- Klein T and Bischoff R (2011). "Physiology and pathophysiology of matrix metalloproteinases." Amino Acids **41**(2): 271-90.
- Kohrmann A, Kammerer U, Kapp M, Dietl J and Anacker J (2009). "Expression of matrix metalloproteinases (MMPs) in primary human breast cancer and

- breast cancer cell lines: New findings and review of the literature." BMC Cancer **9**: 188.
- Kotzsch M, Dorn J, Doetzer K, Schmalfeldt B, Krol J, Baretton G, Kiechle M, Schmitt M and Magdolen V (2011). "mRNA expression levels of the biological factors uPAR, uPAR-del4/5 and rab31, displaying prognostic value in breast cancer, are not clinically relevant in advanced ovarian cancer." Biol Chem **392**(11): 1047-51.
- Kotzsch M, Sieuwerts AM, Grosser M, Meye A, Fuessel S, Meijer-van Gelder ME, Smid M, Schmitt M, Baretton G, Luther T, Magdolen V and Foekens JA (2008). "Urokinase receptor splice variant uPAR-del4/5-associated gene expression in breast cancer: identification of rab31 as an independent prognostic factor." Breast Cancer Res Treat **111**(2): 229-40.
- Kreiling JL, Byrd JC, Deisz RJ, Mizukami IF, Todd RF, 3rd and MacDonald RG (2003). "Binding of urokinase-type plasminogen activator receptor (uPAR) to the mannose 6-phosphate/insulin-like growth factor II receptor: contrasting interactions of full-length and soluble forms of uPAR." J Biol Chem **278**(23): 20628-37.
- Kruger A, Schirmacher V and Khokha R (1998). "The bacterial lacZ gene: an important tool for metastasis research and evaluation of new cancer therapies." Cancer Metastasis Rev **17**(3): 285-94.
- Kunigal S, Lakka SS, Gondi CS, Estes N and Rao JS (2007). "RNAi-mediated downregulation of urokinase plasminogen activator receptor and matrix metalloprotease-9 in human breast cancer cells results in decreased tumor invasion, angiogenesis and growth." Int J Cancer **121**(10): 2307-16.
- Li C, Cao S, Liu Z, Ye X, Chen L and Meng S (2010). "RNAi-mediated downregulation of uPAR synergizes with targeting of HER2 through the ERK pathway in breast cancer cells." Int J Cancer **127**(7): 1507-16.
- Llinas P, Le Du MH, Gardsvoll H, Dano K, Ploug M, Gilquin B, Stura EA and Menez A (2005). "Crystal structure of the human urokinase plasminogen activator receptor bound to an antagonist peptide." Embo J **24**(9): 1655-63.
- Lodhi IJ, Chiang SH, Chang L, Vollenweider D, Watson RT, Inoue M, Pessin JE and Saltiel AR (2007). "Gapex-5, a Rab31 guanine nucleotide exchange factor that regulates Glut4 trafficking in adipocytes." Cell Metab **5**(1): 59-72.

- Luo J, Sun X, Gao F, Zhao X, Zhong B, Wang H and Sun Z (2011). "Effects of ulinastatin and docetaxel on breast cancer invasion and expression of uPA, uPAR and ERK." J Exp Clin Cancer Res **30**: 71.
- Luther T, Flossel C, Albrecht S, Kotsch M and Muller M (1996). "Tissue factor expression in normal and abnormal mammary gland." Nat Med **2**(5): 491-2.
- Luther T, Kotsch M, Meye A, Langerholc T, Fussel S, Olbricht N, Albrecht S, Ockert D, Muehlenweg B, Friedrich K, Grosser M, Schmitt M, Baretton G and Magdolen V (2003). "Identification of a novel urokinase receptor splice variant and its prognostic relevance in breast cancer." Thromb Haemost **89**(4): 705-17.
- Luther T, Magdolen V, Albrecht S, Kasper M, Riemer C, Kessler H, Graeff H, Muller M and Schmitt M (1997). "Epitope-mapped monoclonal antibodies as tools for functional and morphological analyses of the human urokinase receptor in tumor tissue." Am J Pathol **150**(4): 1231-44.
- Lutz V, Reuning U, Kruger A, Luther T, von Steinburg SP, Graeff H, Schmitt M, Wilhelm OG and Magdolen V (2001). "High level synthesis of recombinant soluble urokinase receptor (CD87) by ovarian cancer cells reduces intraperitoneal tumor growth and spread in nude mice." Biol Chem **382**(5): 789-98.
- Madsen CD and Sidenius N (2008). "The interaction between urokinase receptor and vitronectin in cell adhesion and signalling." Eur J Cell Biol **87**(8-9): 617-29.
- McMahon B and Kwaan HC (2008). "The plasminogen activator system and cancer." Pathophysiol Haemost Thromb **36**(3-4): 184-94.
- Mengele K, Napieralski R, Magdolen V, Reuning U, Gkazepis A, Sweep F, Brunner N, Foekens J, Harbeck N and Schmitt M (2010). "Characteristics of the level-of-evidence-1 disease forecast cancer biomarkers uPA and its inhibitor PAI-1." Expert Rev Mol Diagn **10**(7): 947-62.
- Mercatante DR, Sazani P and Kole R (2001). "Modification of alternative splicing by antisense oligonucleotides as a potential chemotherapy for cancer and other diseases." Curr Cancer Drug Targets **1**(3): 211-30.
- Miaczynska M and Bar-Sagi D (2010). "Signaling endosomes: seeing is believing." Curr Opin Cell Biol **22**(4): 535-40.

- Montuori N, Visconte V, Rossi G and Ragno P (2005). "Soluble and cleaved forms of the urokinase-receptor: degradation products or active molecules?" Thromb Haemost **93**(2): 192-8.
- Ng EL, Ng JJ, Liang F and Tang BL (2009). "Rab22B is expressed in the CNS astroglia lineage and plays a role in epidermal growth factor receptor trafficking in A431 cells." J Cell Physiol **221**(3): 716-28.
- Ng EL, Wang Y and Tang BL (2007). "Rab22B's role in trans-Golgi network membrane dynamics." Biochem Biophys Res Commun **361**(3): 751-7.
- Nykjaer A, Christensen EI, Vorum H, Hager H, Petersen CM, Roigaard H, Min HY, Vilhardt F, Moller LB, Kornfeld S and Gliemann J (1998). "Mannose 6-phosphate/insulin-like growth factor-II receptor targets the urokinase receptor to lysosomes via a novel binding interaction." J Cell Biol **141**(3): 815-28.
- Olson LJ, Yammani RD, Dahms NM and Kim JJ (2004). "Structure of uPAR, plasminogen, and sugar-binding sites of the 300 kDa mannose 6-phosphate receptor." Embo J **23**(10): 2019-28.
- Pellinen T and Ivaska J (2006). "Integrin traffic." J Cell Sci **119**(Pt 18): 3723-31.
- Ploug M and Ellis V (1994). "Structure-function relationships in the receptor for urokinase-type plasminogen activator. Comparison to other members of the Ly-6 family and snake venom alpha-neurotoxins." FEBS Lett **349**(2): 163-8.
- Ploug M, Ronne E, Behrendt N, Jensen AL, Blasi F and Dano K (1991). "Cellular receptor for urokinase plasminogen activator. Carboxyl-terminal processing and membrane anchoring by glycosyl-phosphatidylinositol." J Biol Chem **266**(3): 1926-33.
- Pyke C, Eriksen J, Solberg H, Nielsen BS, Kristensen P, Lund LR and Dano K (1993). "An alternatively spliced variant of mRNA for the human receptor for urokinase plasminogen activator." FEBS Lett **326**(1-3): 69-74.
- Ragno P (2006). "The urokinase receptor: a ligand or a receptor? Story of a sociable molecule." Cell Mol Life Sci **63**(9): 1028-37.
- Rao NK, Shi GP and Chapman HA (1995). "Urokinase receptor is a multifunctional protein: influence of receptor occupancy on macrophage gene expression." J Clin Invest **96**(1): 465-74.

- Reuning U, Magdolen V, Hapke S and Schmitt M (2003). "Molecular and functional interdependence of the urokinase-type plasminogen activator system with integrins." Biol Chem **384**(8): 1119-31.
- Rodriguez-Gabin AG, Cammer M, Almazan G, Charron M and Larocca JN (2001). "Role of rRAB22b, an oligodendrocyte protein, in regulation of transport of vesicles from trans Golgi to endocytic compartments." J Neurosci Res **66**(6): 1149-60.
- Rodriguez-Gabin AG, Ortiz E, Demoliner K, Si Q, Almazan G and Larocca JN (2010). "Interaction of Rab31 and OCRL-1 in oligodendrocytes: its role in transport of mannose 6-phosphate receptors." J Neurosci Res **88**(3): 589-604.
- Rodriguez-Gabin AG, Yin X, Si Q and Larocca JN (2009). "Transport of mannose-6-phosphate receptors from the trans-Golgi network to endosomes requires Rab31." Exp Cell Res **315**(13): 2215-30.
- Sato S, Kopitz C, Grismayer B, Beaufort N, Reuning U, Schmitt M, Luther T, Kotzsch M, Kruger A and Magdolen V (2010). "Overexpression of the urokinase receptor mRNA splice variant uPAR-del4/5 affects tumor-associated processes of breast cancer cells in vitro and in vivo." Breast Cancer Res Treat **127**(3): 649-57.
- Schiller HB, Szekeres A, Binder BR, Stockinger H and Leksa V (2009). "Mannose 6-phosphate/insulin-like growth factor 2 receptor limits cell invasion by controlling alphaVbeta3 integrin expression and proteolytic processing of urokinase-type plasminogen activator receptor." Mol Biol Cell **20**(3): 745-56.
- Schmitt M, Harbeck N, Thomssen C, Wilhelm O, Magdolen V, Reuning U, Ulm K, Hofler H, Janicke F and Graeff H (1997). "Clinical impact of the plasminogen activation system in tumor invasion and metastasis: prognostic relevance and target for therapy." Thromb Haemost **78**(1): 285-96.
- Schmitt M, Mengele K, Napieralski R, Magdolen V, Reuning U, Gkazepis A, Sweep F, Brunner N, Foekens J and Harbeck N (2010). "Clinical utility of level-of-evidence-1 disease forecast cancer biomarkers uPA and its inhibitor PAI-1." Expert Rev Mol Diagn **10**(8): 1051-67.

- Sidenius N and Blasi F (2003). "The urokinase plasminogen activator system in cancer: recent advances and implication for prognosis and therapy." Cancer Metastasis Rev **22**(2-3): 205-22.
- Sleat DE and Lobel P (1997). "Ligand binding specificities of the two mannose 6-phosphate receptors." J Biol Chem **272**(2): 731-8.
- Smith HW and Marshall CJ (2010). "Regulation of cell signalling by uPAR." Nat Rev Mol Cell Biol **11**(1): 23-36.
- Srikantan S and Gorospe M (2012). "HuR function in disease." Front Biosci **17**: 189-205.
- Stenmark H and Olkkonen VM (2001). "The Rab GTPase family." Genome Biol **2**(5): REVIEWS3007.
- Subramani D and Alahari SK (2010). "Integrin-mediated function of Rab GTPases in cancer progression." Mol Cancer **9**: 312.
- Subramanian R, Gondi CS, Lakka SS, Jutla A and Rao JS (2006). "siRNA-mediated simultaneous downregulation of uPA and its receptor inhibits angiogenesis and invasiveness triggering apoptosis in breast cancer cells." Int J Oncol **28**(4): 831-9.
- Taherian A, Li X, Liu Y and Haas TA (2011). "Differences in integrin expression and signaling within human breast cancer cells." BMC Cancer **11**: 293.
- Tang CH and Wei Y (2008). "The urokinase receptor and integrins in cancer progression." Cell Mol Life Sci **65**(12): 1916-32.
- Tran H, Maurer F and Nagamine Y (2003). "Stabilization of urokinase and urokinase receptor mRNAs by HuR is linked to its cytoplasmic accumulation induced by activated mitogen-activated protein kinase-activated protein kinase 2." Mol Cell Biol **23**(20): 7177-88.
- Troeberg L and Nagase H (2004). "Zymography of metalloproteinases." Curr Protoc Protein Sci **Chapter 21**: Unit 21 15.
- Ungefroren H, Sebens S, Seidl D, Lehnert H and Hass R (2011). "Interaction of tumor cells with the microenvironment." Cell Commun Signal **9**: 18.
- Wang JS, Wang FB, Zhang QG, Shen ZZ and Shao ZM (2008). "Enhanced expression of Rab27A gene by breast cancer cells promoting invasiveness and the metastasis potential by secretion of insulin-like growth factor-II." Mol Cancer Res **6**(3): 372-82.

- Ward AJ and Cooper TA (2010). "The pathobiology of splicing." J Pathol **220**(2): 152-63.
- Woller B, Luiskandl S, Popovic M, Prieler BE, Ikonge G, Mutzl M, Rehmann H and Herbst R (2011). "Rin-like, a novel regulator of endocytosis, acts as guanine nucleotide exchange factor for Rab5a and Rab22." Biochim Biophys Acta **1813**(6): 1198-210.
- Yang PS, Yin PH, Tseng LM, Yang CH, Hsu CY, Lee MY, Horng CF and Chi CW (2011). "Rab5A is associated with axillary lymph node metastasis in breast cancer patients." Cancer Sci.
- Yim EK, Tong SY, Ho EM, Bae JH, Um SJ and Park JS (2009). "Anticancer effects on TACC3 by treatment of paclitaxel in HPV-18 positive cervical carcinoma cells." Oncol Rep **21**(2): 549-57.
- Yodkeeree S, Ampasavate C, Sung B, Aggarwal BB and Limtrakul P (2009). "Demethoxycurcumin suppresses migration and invasion of MDA-MB-231 human breast cancer cell line." Eur J Pharmacol **627**(1-3): 8-15.

9 Appendix

Breast Cancer Res Treat
DOI 10.1007/s10549-010-1042-5

PRECLINICAL STUDY

Overexpression of the urokinase receptor mRNA splice variant uPAR-del4/5 affects tumor-associated processes of breast cancer cells in vitro and in vivo

Sumito Sato · Charlotte Kopitz · Bettina Grismayer · Nathalie Beaufort · Ute Reuning · Manfred Schmitt · Thomas Luther · Matthias Kotsch · Achim Krüger · Viktor Magdolen

Received: 4 June 2010 / Accepted: 2 July 2010
© Springer Science+Business Media, LLC. 2010

Abstract uPAR, the three-domain membrane receptor of the serine protease urokinase, plays a crucial role in tumor growth and metastasis. Several mRNA splice variants of this receptor have been reported. One of these, uPAR-del4/5, lacking exons 4 and 5, and thus encoding a uPAR form lacking domain DII, is specifically overexpressed in breast cancer and represents a statistically independent prognostic factor for distant metastasis-free survival in breast cancer patients. The aim of the present study was to examine the molecular and cellular properties of the encoded uPAR-del4/5 protein. To investigate the impact of the uPAR-del4/5 overexpression on in vitro and in vivo aspects of tumor progression (e.g., proliferation, adhesion, invasion, metastatic seeding, and/or metastatic growth), we combined the analysis of transfected cancer cell lines with a murine xenograft tumor model. Increased expression of

uPAR-del4/5 in human cancer cells led to reduced adhesion to several extracellular matrix proteins and decreased invasion through Matrigel™, while cell proliferation was not affected in vitro. Moreover, invasion of uPAR-del4/5 overexpressing cells was not altered by addition of urokinase, while that of uPAR-wild-type overexpressing cells was drastically increased. Accordingly, we observed that, in contrast to uPAR-wild-type, uPAR-del4/5 does not interact with urokinase. On the other hand, when overexpressed in human breast cancer cells, uPAR-del4/5 distinctly impaired metastatic dissemination and growth in vivo. We demonstrate that the uPAR-del4/5 mRNA splice variant mediates tumor-relevant biological processes in vitro and in vivo. Our results thus illustrate how tumor-specific alternative splicing can distinctly impact the biology of the tumor.

Keywords Breast cancer · Splice variant · Adhesion · Invasion · Tumor xenograft · uPAR

S. Sato · B. Grismayer · N. Beaufort · U. Reuning · M. Schmitt · V. Magdolen (✉)
Clinical Research Unit, Department of Obstetrics and Gynecology, Technical University Munich, Ismaninger Str. 22, 81675 Munich, Germany
e-mail: viktor.magdolen@lrz.tum.de

S. Sato
Department of Surgery, Yokohama Asahi Central and General Hospital, 4-20-1 Wakabadai Asahi-ku, Yokohama, Kanagawa 241-0801, Japan

C. Kopitz · A. Krüger
Institute of Experimental Oncology and Therapy Research, Technical University Munich, Ismaninger Str. 22, 81675 Munich, Germany

T. Luther · M. Kotsch
Institute of Pathology, Dresden University of Technology, Fetscherstr. 74, 01307 Dresden, Germany

Introduction

The serine protease urokinase-type plasminogen activator (uPA), its serpin-type inhibitor PAI-1, and its cell surface receptor uPAR (CD87), drastically influence tumor cell proliferation, migration, invasion, and metastasis [1–3]. Accordingly, these factors represent important biomarkers in a number of malignancies, including breast cancer [4–6].

uPAR is an ubiquitous 45–60 kDa glycoprotein, which is composed of three homologous domains (DI, DII, and DIII, from the amino- to the carboxy terminus). It is anchored to the plasma membrane by a glycosyl phosphatidyl inositol (GPI) moiety [7]. uPAR exhibits features

Published online: 16 July 2010

 Springer

related to proteolysis as well as cell adhesion: on one hand, upon binding of its canonical ligand uPA, uPAR focuses the extracellular proteolytic network including plasmin and matrix metalloproteinases to the cell surface [2, 7, 8], on the other, it interacts with the adhesive extracellular matrix (ECM) protein vitronectin as well as with various integrins, thereby regulating cell adhesion and signaling [2, 8, 9]. For these reasons, uPAR is a major regulator of ECM remodeling and cell adhesion/migration [2, 8].

Recently, crystal structures of complexes between soluble uPAR (lacking the GPI anchor) and an antagonist peptide (interacting with the uPA binding site of uPAR) or the N-terminal fragment of uPA (ATF; harboring the uPAR-binding site) have been determined [10, 11]. These studies revealed that the three domains in uPAR are packed closely and form a cone-shaped central cavity which is wide open and displays a significant depth. The major contact areas between uPAR and these ligands are formed by DI and DII residues, respectively. Binding of uPA to uPAR dramatically increases the affinity of uPAR to vitronectin [12]. The crystal structure of the ternary complex of soluble uPAR, ATF and the uPAR-binding domain of vitronectin, SMB, showed that there is no direct contact between SMB and ATF, whereas the uPAR-binding site of uPA occupies the central cavity of the receptor, SMB binds to the outer side of DI and the DI–DII linker region [13]. Thus, uPA/uPAR-interaction may stabilize an active conformation of uPAR, leading to its high affinity binding to vitronectin.

Wild-type uPAR (uPAR-WT) is encoded by seven exons. Several mRNA splice variants of uPAR have been identified and their expression analyzed in human cells and tissues [14–16]. One of these splice variants, uPAR-del4/5, lacking exons 4 and 5, and thus encoding a uPAR form lacking domain DII, was found to be specifically overexpressed in breast and ovarian cancer cells [15]. Besides, high uPAR-del4/5 mRNA expression levels were found to be significantly associated with short disease-free survival of breast cancer patients [15, 17, 18]. Moreover, uPAR-del4/5 mRNA is a highly sensitive, statistically independent prognostic factor for distant metastasis-free survival in untreated node-negative breast cancer patients [18].

In order to investigate the tumor biological effects of uPAR-del4/5 splice variant expression, we stably transfected MDA-MB-231 breast cancer cells with expression plasmids encoding either this variant or wild-type uPAR. By proliferation, adhesion, and invasion assays, we first analyzed the phenotype of the cell transfectants *in vitro*, and then monitored the impact of uPAR-del4/5 overexpression on experimental metastasis in a xenograft tumor model in mice.

Materials and methods

Cell culture and cell transfection

The human breast adenocarcinoma cell line MDA-MB-231 (American Type Culture Collection [ATCC], Manassas, VA) was cultured in DMEM (Gibco BRL, Eggenstein, Germany) supplemented with 10% (v/v) fetal calf serum (FCS), 10 mM HEPES, 0.55 mM L-arginine and 0.272 mM L-asparagine (Sigma-Aldrich, Saint-Louis, MO). In some experiments, MDA-MB-435, CAMA-1, MCF-7 breast cancer cells (ATCC), and OV-MZ-6 ovarian cancer cells [19], respectively, were also used. Cells were routinely checked to be free of mycoplasma.

Cloning of pRcRSV-derived expression plasmids encoding uPAR (-variants) has been reported elsewhere [15]. Cells were transfected using Lipofectin® (Invitrogen, Karlsruhe, Germany). Cell transfectants were selected by addition of 1 mg/ml G418 to the cell culture medium (Gibco BRL). In an independent transfection experiment, clones of MDA-MB-231-uPAR-del4/5 cells were isolated by limited dilution.

ELISA

Cells were washed with phosphate-buffered saline (PBS), pH 7.4, then lysed for 60 min at 4°C in Tris-buffered saline (TBS), pH 7.4, containing 1% (v/v) Triton X-100 and a protease inhibitor cocktail (“complete + EDTA”; Roche Diagnostics, Mannheim, Germany). Cell lysates were centrifuged at 13,000×g for 15 min at 4°C. Protein content was determined using the Micro BCA™ protein assay reagent kit (Pierce, Stonehouse, UK). uPAR antigen was determined applying the IMUBIND uPAR ELISA kit #893 (American Diagnostica Inc., Stamford, CT). uPAR antigen levels in cell lysates are expressed as nanogram per milligram of total protein.

Western blot

Proteins, separated by electrophoresis on 12% (w/v) polyacrylamide gels (SDS-PAGE), were transferred to polyvinylidene fluoride membranes (Millipore Corporation, Bedford, MA) in a semi-dry transfer device (Biometra, Göttingen, Germany). Membranes were incubated for 60 min in PBS, pH 7.4, containing 0.1% (v/v) Tween-20 (PBS-T) and 5% (w/v) dried skimmed milk, followed by an overnight incubation with the primary monoclonal antibodies (mAb) IIF10 or IID7, both directed to uPAR, diluted in PBS-T supplemented with 1% (w/v) dried skimmed milk. The epitope-mapped mAb IIF10 is directed against DI, mAb IID7 against DII of uPAR [20]. After washes in PBS-T, binding of the antibodies was visualized

by incubation of the membranes with a horseradish peroxidase-conjugated secondary goat Ab against mouse Ig (Jackson ImmunoResearch Lab, West Grove, PA), followed by chemoluminescence reaction using ECL (Amersham Biosciences, Little Chalfont, UK).

Immunofluorescence

Cells were seeded in human fibronectin-coated (10 µg/ml, Becton-Dickinson, Heidelberg, Germany) 8-chamber glass slides (Permanox-type Lab-Tek slides; Nunc, Roskilde, Denmark) and cultured overnight. Cells were fixed in 4% (w/v) paraformaldehyde in PBS, pH 7.4, for 30 min at room temperature (RT). After several washes in PBS, cells were incubated for 1 h at RT in PBS containing 2% (w/v) bovine serum albumin (BSA), and then probed with mAb IIIIF10 diluted in PBS, 1% (w/v) BSA, for 1 h at RT. Cells were washed and incubated for 45 min at RT in the dark with the secondary Alexa488-labeled goat-anti-mouse IgG (Sigma-Aldrich) diluted in the same buffer. After final washes with PBS, cells were mounted in PBS and fluorescence signal intensity evaluated by confocal laser scanning microscopy (CLSM).

Solid-phase uPA binding assay

The solid-phase uPA-ligand-binding assay was performed in a similar manner as described previously [21]. Briefly, wells of microtiter plates (Maxisorb; Nunc) were coated overnight at 4°C with 100 µl of rec-uPAR₁₋₂₇₇ (1 µg/ml). After blocking, 100 µl of sample containing the amino-terminal fragment (ATF) of uPA (250 ng/ml) and 50 µl of cell culture supernatants were added to the wells for 1 h at RT. Cell culture supernatants were derived from vector-control Chinese hamster ovary (CHO) cells or from transfected CHO cells overexpressing soluble forms of uPAR-WT or uPAR-del4/5 [15]. After four washes, plates were incubated with biotinylated murine mAb #377 directed to the kringle domain of human uPA (American Diagnostica Inc.) for 1 h at RT. After washes in PBS, avidin-coupled peroxidase was added for 1 h at RT. Finally, wells were washed and binding of avidin-peroxidase detected by addition of 3,3',5,5'-tetramethylbenzidine (TMB; 1 mg/ml) and 0.003% (v/v) H₂O₂ in 0.1 M sodium acetate buffer, pH 6.0. After termination of the reaction with 0.5 M H₂SO₄, absorbance was measured at 450 nm.

Cell-based in vitro assays

Cell proliferation assays

Transfected cells were seeded in a 24-well plate at a density of 15,000 cells per well, and incubated for 48–96 h

at 37°C. After washes in PBS, cells were detached using PBS, 0.05% (w/v) EDTA, and living cells counted in a hemocytometer upon trypan blue exclusion under a light microscope.

Cell adhesion assays

96-well plates were coated overnight at 4°C with vitronectin (1 µg/well), fibronectin (1 µg/well), and collagen type I or IV (1 µg/well), all diluted in PBS. Cells were resuspended in culture medium containing 0.5% (w/v) BSA, seeded at a density of 40,000 cells/well, and allowed to adhere for 2 h at 37°C. Non-adherent cells were removed by washing with PBS and number of adherent cells quantified by a hexosaminidase activity assay. For this, cells were incubated with *p*-nitrophenyl-*N*-acetyl-β-D-glucosaminide (Sigma-Aldrich) diluted to 15 mM in a 100 mM sodium citrate buffer, pH 5.0, 0.5% (v/v) Triton X-100, for 90 min at 37°C. The reaction was terminated by the addition of stop buffer (0.2 M NaOH, 5 mM EDTA) and the optical density recorded at 405 nm.

Cell invasion assays

Invasion assays were performed using Transwell inserts (8 µm pore size; Becton-Dickinson). Basement membrane complex growth factor reduced MatrigelTM (11.3 mg/ml) was diluted 1:24 in cold PBS and applied to the upper side of the insert. After drying for 24 h in a laminar hood, inserts were rehydrated with FCS-free DMEM, 0.1% (w/v) BSA. Cells were resuspended in culture medium and seeded in the upper chamber of the device at a density of 50,000 cells/chamber. In some experiments, 2 µg of proteolytically active high-molecular-weight uPA (ProSpec-Tany TechnoGene, Rehovot, Israel) were added to the upper chamber. The lower chambers were filled with 750 µl DMEM supplemented with 10% (v/v) FCS as a chemoattractant. After 24 to 48 h of incubation at 37°C, MatrigelTM and non-invaded cells, located on the upper side of the insert, were removed with tissue paper, whereas invaded cells on the lower side of the insert were fixed, stained using Diff-Quick (Dade Behring AG, Switzerland), and counted under a light microscope.

Experimental animal model

MDA-MB-231 cells are tumorigenic and invasive cells, which upon intravenous injection in mice colonize to the lungs [22]. Transfected MDA-MB-231 cells were genetically tagged with the *lacZ* gene, allowing X-Gal staining, as reported previously [23]. Pathogen-free female athymic

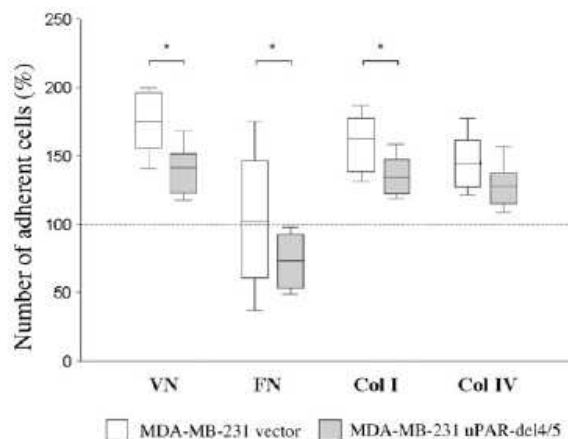


Fig. 2 uPAR-del4/5 overexpression reduces the adhesive capacity of human breast cancer cells in vitro. MDA-MB-231 cells were passed to cell culture plates which were pre-treated with the extracellular matrix proteins vitronectin (VN), fibronectin (FN), and type I (Col I) or type IV (Col IV) collagen. After 2 h of cell cultivation, the number of adherent cells was monitored by the hexosaminidase activity assay. Four independent experiments were performed in triplicates each. The results are given in %, normalized to the number of adherent vector-transfected cells onto uncoated wells. Whisker box plots indicate the 25th and 75th percentile, the vertical bars indicate the 10th and 90th percentile. The mean value is indicated by a bar within the box. Statistically significant differences ($P < 0.05$) are indicated by an asterisk

quantitative RT-PCR (data not shown). The uPAR antigen content, measured by a commercially available ELISA, was distinctly increased in uPAR-WT and uPAR-del4/5 overexpressing cells as compared to the vector-control cells (MDA-MB-231 vector-control cells: 6.5 ng/mg total protein; uPAR-WT cells: 51.7 ng/mg; uPAR-del4/5 cells: 12.0 ng/mg). It is of note that using this ELISA, we are not able to discriminate between endogenous and overexpressed protein and not between different forms of uPAR. Immunofluorescence further confirmed uPAR overexpression (Fig. 1b). The staining pattern was found to be rather heterogeneous within the transfected cell populations, as expected for batch-transfected cells. Moreover, both

uPAR-WT and uPAR-del4/5 displayed an enhanced membrane-staining pattern (Fig. 1b), strongly suggesting correct integration of the respective uPAR species into the cell membranes.

In vitro phenotype of uPAR-del4/5 overexpressing breast cancer cells

As compared to vector-transfected cells, neither uPAR-WT nor uPAR-del4/5 overexpressing MDA-MB-231 cells displayed significant differences with respect to cell morphology and cell proliferation (data not shown). In contrast, MDA-MB-231-uPAR-del4/5 cells showed a moderate (i.e., 14 to 20%) but significant ($P < 0.05$) reduction of their capacity to adhere to certain adhesive ECM proteins, such as vitronectin, fibronectin, and type I collagen (Fig. 2, Table 1). Interestingly, this reduced adhesive capacity of uPAR-del4/5 overexpressing cells was not restricted to the MDA-MB-231 cell line, since transfection of other human breast (i.e., MDA-MB-435, CAMA-1, and MCF-7) or ovarian (i.e., OV-MZ-6) cancer cell lines, reduced cell adhesion to various ECM components in the same fashion (Table 1). It is of note that uPAR-WT is an acknowledged pro-adhesive factor, for instance by engagement with its ligand vitronectin, in a number of cell types, including human breast and ovarian cancer cells [26, 27].

Next, uPAR-WT- and uPAR-del4/5 overexpressing cells were investigated and compared to vector-control cells in a MatrigelTM invasion assay. As expected, overexpression of uPAR-WT was associated with a distinct, about 3-fold enhanced cell invasive capacity, which was further about 2-fold enhanced in the presence of exogenously added uPA (Fig. 3a, lower panel). Strikingly, MDA-MB-231-uPAR-del4/5 cells displayed a strongly impaired invasion (i.e., about 40% reduction), which was not affected by the presence of uPA (Fig. 3a, upper panel). In fact, this latter observation was in agreement with solid-phase ligand-binding assays indicating efficient uPA binding to recombinant uPAR-WT, but not to uPAR-del4/5 protein (Fig. 4).

Table 1 uPAR-del4/5 overexpression reduces the adhesive capacity of human breast and ovarian cancer cells in vitro

	VN (% of the number of adherent vector-transfected cells)	FN	Col I	Col IV
MDA-MB-231	86.5 ± 5.5*	80.0 ± 23.1*	83.7 ± 11.7*	89.9 ± 17.7
MDA-MB-435	87.6 ± 17.3*	74.5 ± 16.7*	66.7 ± 25.4*	82.5 ± 36.3
CAMA-1	71.7 ± 17.9*	57.9 ± 28.3*	29.8 ± 14.8*	39.4 ± 21.8*
MCF-7	93.9 ± 4.0*	92.8 ± 5.3*	92.5 ± 2.8*	98.7 ± 6.6
OV-MZ-6	89.7 ± 6.4*	85.8 ± 11.2*	92.5 ± 6.9*	95.9 ± 13.7

Cell adhesion assays were performed as described in the legend to Fig. 2. Results were normalized to the number of adherent vector-transfected cells to uncoated wells and are expressed as the mean ± SE. At least four independent experiments were performed in triplicates. The asterisk indicates a statistically significant difference between uPAR-del4/5 overexpressing cells and vector-control cells ($P < 0.05$)

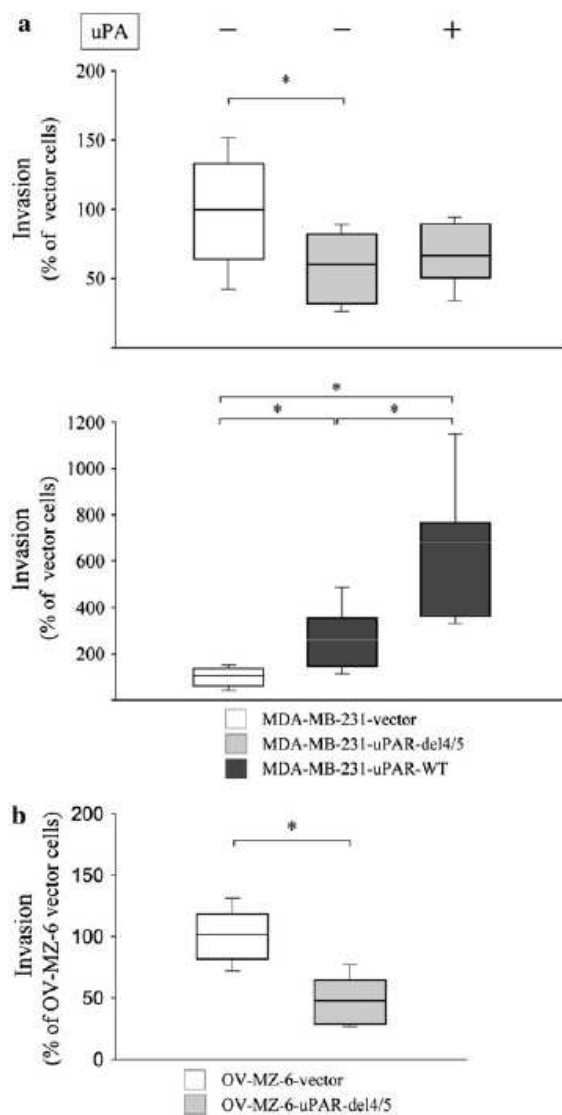


Fig. 3 uPAR-del4/5 overexpression reduces the invasive capacity of human breast and ovarian cancer cells in vitro. **a** Stably transfected MDA-MB-231 breast cancer cells were seeded into the upper compartments of MatrigelTM-coated invasion chambers in the absence or presence of 2 μ g of proteolytically active uPA. After 48 h of incubation, invaded cells were fixed, stained, and counted. Four independent experiments were performed in duplicates each. The results are given in %, normalized to the number of invaded vector-transfected cells, in the absence of uPA. **b** Stably transfected human ovarian cancer OV-MZ-6 cells were analyzed (in the absence of uPA) for their invasive capacity in a similar manner as described above for the MDA-MB-231 cells. Four independent experiments were performed in duplicates each. The results are given in %, normalized to the number of invaded vector-transfected cells. Whisker box plots indicate the 25th and 75th percentile, the vertical bars indicate the 10th and 90th percentile. The mean value is indicated by a bar within the box. Statistically significant differences ($P < 0.05$) are indicated by an asterisk

Again, reduced invasion upon uPAR-del4/5 transfection was confirmed in another cancer cell model, namely in human ovarian OV-MZ-6 cancer cells (Fig. 3b).

In vivo phenotype of uPAR-del4/5 overexpressing breast cancer cells

Lung is a major site for metastatic spread of cancer cells during breast cancer progression [28, 29]. In order to explore the impact of uPAR-del4/5 overexpression in vivo, we intravenously injected mice with MDA-MB-231-vector, -uPAR-WT, or -uPAR-del4/5 cells and analyzed incidence, number, and size of nodules of experimental lung metastases. Most mice of the vector and uPAR-WT groups (10/11 and 7/9, respectively; Fig. 5a) had numerous lung metastases (on the average 57 and 37, respectively; Fig. 5b). Moreover, 16.6 to 28.0% of the nodules were classified as macrometastases (size over 0.18 mm; Fig. 5c). Remarkably, in the group of mice which had received MDA-MB-231-uPAR-del4/5 cells, 5 out of 10 mice had no detectable lung metastasis (Fig. 5a). Similarly, the number of metastases in colonized lungs (on the average from 57 to 4; Fig. 5b) as well as the percentage of macrometastases (on the average from 16.6 to 0.8%, Fig. 5c) was considerably reduced in the uPAR-del4/5 group, as compared to the vector-control group. Similar results were observed upon injection of an independently generated MDA-MB-231-uPAR-del4/5 clone (Fig. 5), displaying a comparable antigen level, measured by ELISA (batch-transfected uPAR-del4/5 cells: 12.0 ng/mg; uPAR-del4/5 clone: 10.2 ng/mg). These observations suggest that overexpression of uPAR-del4/5 in vivo not only reduced adhesion, but also impaired growth of breast cancer cell-derived lung metastases in vivo.

Discussion

Aberrant mRNA splicing is a common feature of malignant disorders. Whether this process results from a general dysregulation of tumor cell functions, and thus represents a by-product of cellular transformation, or whether increased aberrant splicing contributes to the malignant phenotype of cancer cells, is a not yet conclusively answered question [30, 31]. Still, a growing number of evidence demonstrates that tumor-associated mRNA splicing may lead to cancer cell-specific production of new proteins displaying unique functions, which are crucially affecting cancer development. Mis-spliced mRNAs, which escape the so-called nonsense-mediated mRNA degradation, normally lead to synthesis of truncated, mutated, misfolded, and/or unstable proteins. However, by alternative splicing, it is also

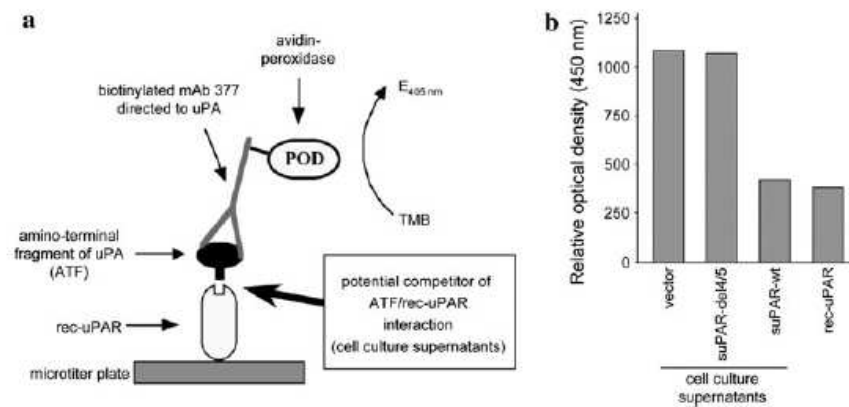


Fig. 4 uPAR-WT, but not uPAR-del4/5 interacts with uPA. **a** Schematic representation of the solid-phase uPA-ligand-binding assay ([21]; for details see also “Materials and methods” section). **b** Cell culture supernatants from stably transfected Chinese hamster ovary (CHO) cell lines [15] were added to ATF in the ligand-binding assay. Bars represent the amount of ATF bound to immobilized rec-uPAR. Whereas conditioned medium of vector-transfected control

cells as well as of cells overexpressing a soluble form of uPAR-del4/5 did not compete for binding of ATF to rec-uPAR, a significant reduction of rec-uPAR/ATF interaction was observed in the presence of conditioned medium from cells overexpressing uPAR-WT. Purified, soluble rec-uPAR, interfering with interaction of ATF to immobilized rec-uPAR, was used as a positive control in the assay

possible that certain protein domains are deleted from the encoded protein, which may result in loss or gain of function [31]. In a recent study on splice variants of the human *Adhesion* family of G protein-coupled receptors, more than half of the identified splice variants appeared to code for functional proteins, lacking one or more extracellular domains, which take part in protein–protein interactions, without affecting the seven transmembrane region. Thus, alternative splicing apparently can influence interaction of these receptors with other proteins [32].

The recently identified, tumor-associated variant of uPAR, uPAR-del4/5, displays the specific deletion of the complete DII of three-domain uPAR [15]. In fact, uPAR-del4/5 protein, consisting of domains DI + DIII fused together, exhibits unique characteristics significantly affecting the behavior of malignant cells: upon analyses of the impact of uPAR-del4/5 overexpression in human MDA-MB-231 breast cancer cells, we observed a significantly impaired cell adhesion and invasion in vitro, along with a distinctly decreased colonization of lungs (in terms of metastatic nodule occurrence, number, and size) in an experimental metastasis mouse model system.

Binding of uPA to its cell surface receptor uPAR involves all three domains of uPAR [2, 10]. As demonstrated by a sensitive solid-phase ligand-binding assay (Fig. 4) and by an uPA/uPAR-complex ELISA (data not shown), uPAR-del4/5 does not interact with uPA. Consequently, we observed that addition of uPA to uPAR-del4/5 overexpressing cells—in contrast to uPAR-WT overexpressing cells—had no effect on cell invasion through MatrigelTM (Fig. 3).

uPA/uPAR-interaction does not only focus proteolytic activity to the tumor cell surface, but is also a prerequisite

for the binding of another uPAR ligand, the ECM protein vitronectin [12]. Furthermore, interaction of uPA with uPAR is a major determinant of physical and functional interactions of uPAR with a number of integrins [2, 9] and is also involved in other tumor-associated functions, e.g. regarding tumor cell survival and angiogenesis [2, 33]. Obviously, uPAR-del4/5 is not capable of modulating these uPA-dependent, tumor-associated functions of uPAR-WT by competing for uPA binding. Still, overexpression of uPAR-del4/5 resulted in a moderate, significantly decreased cell adhesion to an array of adhesive ECM proteins (Fig. 2, Table 1). uPAR-del4/5 also strongly affected cellular invasion in vitro (Fig. 3), a process that depends on both extracellular proteolysis and cell adhesion/detachment capacities. In addition, overexpression of the uPAR-del4/5 splice variant led to a major reduction of experimental metastasis in vivo, compared to both vector control and uPAR-WT overexpressing cells (Fig. 5). It is tempting to speculate that such a phenotype might reflect the capacity of uPAR-del4/5 to behave as a dominant-negative receptor, e.g. via competition with endogenous uPAR-WT for binding to certain integrins such as $\alpha_5\beta_1$ or $\alpha_v\beta_3$ and/or via an additional uPAR-WT independent process.

uPAR-del4/5 mRNA is a statistically independent prognostic factor for distant metastasis-free survival in breast cancer patients. High levels of uPAR-del4/5 mRNA are associated with a poor prognosis of patients [15, 17, 18]. However, the results of the present article, especially regarding the reduced invasive capacity of uPAR-del4/5 overexpressing cells in vitro (Fig. 3) and the reduction in lung colonization of these cells in the in vivo experimental metastasis animal model (Fig. 5) rather advert to the

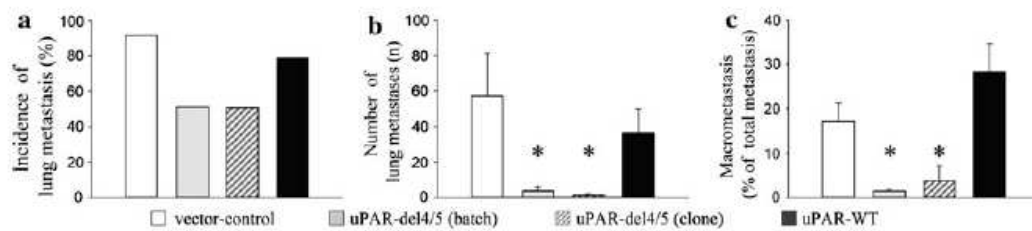


Fig. 5 Overexpression of uPAR-del4/5 affects lung colonization and metastatic growth of human breast cancer cells. Stably transfected, *lacZ*-tagged, MDA-MB-231 cells were inoculated into nude mice via tail vein injection. Mice received either vector-control cells (white columns), uPAR-del4/5 cells (gray columns) or uPAR-WT cells (black columns). In addition, an independently generated MDA-MB-231-uPAR-del4/5 transfected cell clone, displaying a comparable uPAR antigen level as the batch-transfected uPAR-del4/5 cell line (hatched gray columns), was analyzed. Animals were sacrificed at day

35 after injection, lungs were collected and stained with X-Gal. **a** The number of mice presenting lung metastasis is expressed as percentage of total mouse number. **b** Metastases were counted in lungs of the mice. Results are expressed as the mean number of metastases + SE counted in lungs colonized by cancer cells. **c** Metastases with a diameter ≥ 0.18 mm were considered as macrometastases. Histograms illustrate the mean percentage + SE of macro- versus total metastases in mice lungs. Statistically significant differences ($P < 0.05$) to the vector-control group are indicated by an asterisk

conclusion that the uPAR-del4/5 protein acts as a forceful tumor suppressor. On the one hand, high expression of uPAR-del4/5 mRNA might reflect the malignant status of the cancer disease, rather than the functions arising thereof at the protein level. On the other hand, as documented for the adverse effects of different PAI-1 concentrations on tumor angiogenesis [34], uPAR-del4/5 protein, depending on the height of its expression level, may display both agonistic and antagonistic properties. Therefore, further agonistic studies using clones expressing uPAR-del4/5 protein to a different extent (low vs. high expression) and/or variations of uPAR-del4/5: uPAR-WT protein ratios may help to explore this latter possibility.

The metastatic process requires a complex sequence of events [35]. Invasive tumor cells, originating from an in situ cancer surrounded by an intact basement membrane, degrade ECM proteins, induce reversible changes in cell-cell and cell-ECM adherence, and migrate through the ECM. The metastasizing cells then enter circulation, extravasate and disseminate to eventually colonize at a distant site, finally leading to micrometastases and angiogenic metastases. The experimental animal metastasis model used in the present study focuses on the later events of the metastatic process, i.e. metastatic seeding and growth. Here, uPAR-del4/5 overexpression did not only reduce occurrence and number of metastatic nodules, but also the percentage of macrometastases (Fig. 5), which indeed indicates an impact of the uPAR splice variant on extravasation of circulating tumor cells and/or tissue colonization, as well as on metastatic tumor growth.

In conclusion, although several uPAR mRNA splice variants have been described, some being clearly associated to disease [14–16], no experimental analysis of their cellular properties was reported so far. The present study, combining in vitro and in vivo experimental approaches, clearly demonstrates tumor biologically relevant effects

mediated by uPAR-del4/5 in human breast cancer and also ovarian cancer cells. Thus, production of uPAR-del4/5 might represent a striking example for tumor-associated alternative splicing leading to modified protein species strongly modulating tumor biological processes.

Acknowledgments This study was supported in part by grants provided by the Deutsche Krebshilfe e.V., Germany (Grant No. 106 162) to MK and VM, and by the Framework Programme 7 project HEALTH-2007-201279, Microenvimet to AK. We are grateful to Sabine Creutzburg, Katja Richter, and Antje Zobjack for excellent technical assistance.

Conflicts of interest statement None.

References

- Blasi F, Sidenius N (2010) The urokinase receptor: focused cell surface proteolysis, cell adhesion and signaling. *FEBS Lett* 584:1923–1930
- Blasi F, Carmeliet P (2002) uPAR: a versatile signalling orchestrator. *Nat Rev Mol Cell Biol* 3:932–943
- Reuning U, Magdolen V, Wilhelm O, Fischer K, Lutz V, Graeff H, Schmitt M (1998) Multifunctional potential of the plasminogen activation system in tumor invasion and metastasis. *Int J Oncol* 13:893–906
- Harbeck N, Kates RE, Gauger K, Willems A, Kiechle M, Magdolen V, Schmitt M (2004) Urokinase-type plasminogen activator (uPA) and its inhibitor PAI-1: novel tumor-derived factors with a high prognostic and predictive impact in breast cancer. *Thromb Haemost* 91:450–456
- Høyer-Hansen G, Lund IK (2007) Urokinase receptor variants in tissue and body fluids. *Adv Clin Chem* 44:65–102
- Harris L, Fritsche H, Mennel R, Norton L, Ravdin P, Taube S, Somerfield MR, Hayes DF, Bast RC (2007) American Society of Clinical Oncology 2007 update of recommendations for the use of tumor markers in breast cancer. *J Clin Oncol* 25:5287–5312
- Ploug M (2003) Structure-function relationships in the interaction between the urokinase-type plasminogen activator and its receptor. *Curr Pharm Des* 9:1499–1528

8. Smith HW, Marshall CJ (2010) Regulation of cell signalling by uPAR. *Nat Rev Mol Cell Biol* 11:23–36
9. Reuning U, Magdolen V, Hapke S, Schmitt M (2003) Molecular and functional interdependence of the urokinase-type plasminogen activator system with integrins. *Biol Chem* 384:1119–1131
10. Llinas P, Le Du MH, Gårdsvoll H, Danø K, Ploug M, Gilquin B, Stura EA, Ménez A (2005) Crystal structure of the human urokinase plasminogen activator bound to an antagonist peptide. *EMBO J* 24:1655–1663
11. Huai Q, Mazar AP, Kuo A, Parry GC, Shaw DE, Callahan J, Li Y, Yuan C, Bian C, Chen L, Furie B, Furie BC, Cines DB, Huang M (2006) Structure of human urokinase plasminogen activator in complex with its receptor. *Science* 311:656–659
12. Gårdsvoll H, Ploug M (2007) Mapping of the vitronectin-binding site on the urokinase receptor: involvement of a coherent receptor interface consisting of residues from both domain I and the flanking interdomain linker region. *J Biol Chem* 282:13561–13572
13. Huai Q, Zhou A, Lin L, Mazar AP, Parry GC, Callahan J, Shaw DE, Furie B, Furie BC, Huang M (2008) Crystal structures of two human vitronectin, urokinase and urokinase receptor complexes. *Nat Struct Mol Biol* 15:422–423
14. Stewart CE, Sayers I (2009) Characterisation of urokinase plasminogen activator receptor variants in human airway and peripheral cells. *BMC Mol Biol* 10:75
15. Luther T, Kotsch M, Meye A, Langerholc T, Fussel S, Olbricht N, Albrecht S, Ockert D, Muehlenweg B, Friedrich K, Grosser M, Schmitt M, Baretton G, Magdolen V (2003) Identification of a novel urokinase receptor splice variant and its prognostic relevance in breast cancer. *Thromb Haemost* 89:705–717
16. Pyke C, Eriksen J, Solberg H, Nielsen BS, Kristensen P, Lund LR, Danø K (1993) An alternatively spliced variant of mRNA for the human receptor for urokinase plasminogen activator. *FEBS Lett* 326:69–74
17. Kotsch M, Farthmann J, Meye A, Fuessel S, Baretton G, Tjan-Heijnen VC, Schmitt M, Luther T, Sweep FC, Magdolen V, Span PN (2005) Prognostic relevance of uPAR-del4/5 and TIMP-3 mRNA expression levels in breast cancer. *Eur J Cancer* 41:2760–2768
18. Kotsch M, Sieuwerts AM, Grosser M, Meye A, Fuessel S, Meijer-van Gelder ME, Smid M, Schmitt M, Baretton G, Luther T, Magdolen V, Foekens JA (2008) Urokinase receptor splice variant uPAR-del4/5-associated gene expression in breast cancer: identification of rab31 as an independent prognostic factor. *Breast Cancer Res Treat* 111:229–240
19. Möbus V, Gerharz CD, Press U, Moll R, Beck T, Mellin W, Pollow K, Knapstein PG, Kreienberg R (1992) Morphological, immunohistochemical and biochemical characterization of 6 newly established human ovarian carcinoma cell lines. *Int J Cancer* 52:76–84
20. Luther T, Magdolen V, Albrecht S, Kasper M, Riemer C, Kessler H, Graeff H, Müller M, Schmitt M (1997) Epitope-mapped monoclonal antibodies as tools for functional and morphological analyses of the human urokinase receptor in tumor tissue. *Am J Pathol* 150:1231–1244
21. Goretzki L, Bognacki J, Koppitz M, Rettenberger P, Magdolen V, Creutzburg S, Hammelburger J, Weidle UH, Wilhelm O, Kessler H, Graeff H, Schmitt M (1997) Quantitative assessment of interaction of urokinase-type plasminogen activator and its receptor (CD87) by use of a solid-phase uPA-ligand binding assay. *Fibrinol Proteol* 11:11–19
22. Krüger A, Soeltl R, Sopov I, Kopitz C, Arlt M, Magdolen V, Harbeck N, Gänsbacher B, Schmitt M (2001) Hydroxamate-type matrix metalloproteinase inhibitor batimastat promotes liver metastasis. *Cancer Res* 61:1272–1275
23. Kopitz C, Anton M, Gänsbacher B, Krüger A (2005) Reduction of experimental human fibrosarcoma lung metastasis in mice by adenovirus-mediated cystatin C overexpression in the host. *Cancer Res* 65:8608–8612
24. Krüger A, Schirmacher V, Khokha R (1998) The bacterial lacZ gene: an important tool for metastasis research and evaluation of new cancer therapies. *Cancer Metastasis Rev* 17:285–294
25. Beaufort N, Leduc D, Eguchi H, Mengele K, Hellmann D, Masegi T, Kamimura T, Yasuoka S, Fend F, Chignard M, Pidard D (2007) The human airway trypsin-like protease modulates the urokinase receptor (uPAR, CD87) structure and functions. *Am J Physiol Lung Cell Mol Physiol* 292:1263–1272
26. Wei Y, Lukashev M, Simon DI, Bodary SC, Rosenberg S, Doyle MV, Chapman HA (1996) Regulation of integrin function by the urokinase receptor. *Science* 273:1551–1555
27. Xue W, Mizukami I, Todd RF, Petty HR (1997) Urokinase-type plasminogen activator receptors associate with beta1 and beta3 integrins of fibrosarcoma cells: dependence on extracellular matrix components. *Cancer Res* 57:1682–1689
28. Krüger A, Soeltl R, Lutz V, Wilhelm OG, Magdolen V, Rojo EE, Hantzopoulos PA, Graeff H, Gänsbacher B, Schmitt M (2000) Reduction of breast carcinoma tumor growth and lung colonization by overexpression of the soluble urokinase-type plasminogen activator receptor (CD87). *Cancer Gene Ther* 7:292–299
29. Setyono-Han B, Sturzebecher J, Schmalix WA, Muehlenweg B, Sieuwerts AM, Timmermans M, Magdolen V, Schmitt M, Klijn JG, Foekens JA (2005) Suppression of rat breast cancer metastasis and reduction of primary tumour growth by the small synthetic urokinase inhibitor WX-UK1. *Thromb Haemost* 93:779–786
30. Ward AJ, Cooper TA (2010) The pathobiology of splicing. *J Pathol* 220:152–163
31. Fackenthal JD, Godley LA (2008) Aberrant RNA splicing and its functional consequences in cancer cells. *Dis Model Mech* 1:37–42
32. Bjarnadóttir TK, Geirardsdóttir K, Ingemansson M, Mirza MA, Fredriksson R, Schiöth HB (2007) Identification of novel splice variants of *Adhesion G* protein-coupled receptors. *Gene* 387:38–48
33. Alfano D, Franco P, Vocca I, Gambi N, Pisa V, Mancini A, Caputi M, Carriero MV, Iaccarino I, Stoppelli MP (2005) The urokinase plasminogen activator and its receptor: role in cell growth and apoptosis. *Thromb Haemost* 93:205–211
34. Durand MK, Bodker JS, Christensen A, Dupont DM, Hansen M, Jensen JK, Kjelgaard S, Mathiasen L, Pedersen KE, Skeldal S, Wind T, Andreasen PA (2004) Plasminogen activator inhibitor-1 and tumour growth, invasion, and metastasis. *Thromb Haemost* 91:438–449
35. Steeg PS (2003) Metastasis suppressors alter the signal transduction of cancer cells. *Nat Rev Cancer* 3:55–63

Danksagung

Ich möchte mich sehr herzlich bedanken bei:

Prof. Dr. Viktor Magdolen, für die intensive Betreuung meiner Arbeit, seine fachliche Kompetenz, die guten Tipps und die Unterstützung und die Korrektur meiner Dissertationsschrift. Außerdem vielen Dank für die Möglichkeit verschiedene Konferenzen zu besuchen und für die finanzielle Unterstützung vor/während/nach dem Stipendium.

Prof. Dr. Horst Kessler, für die Vertretung meiner Doktorarbeit an der Fakultät für Chemie der Technischen Universität München.

Dr. Matthias Kotzsch, für die ausgezeichnete Kooperation und Mitbetreuung meiner Arbeit.

Prof. Dr. Manfred Schmitt, für die finanzielle Unterstützung vor, während und nach meinem Stipendium. Und für die Möglichkeit meine Arbeit in der Klinischen Forschergruppe der Frauenklinik des Klinikums rechts Isar durchzuführen.

Prof. Dr. Ute Reuning, für die guten Ratschläge und die Hilfe bei der ICC.

Dr. Thomas Luther, für seine guten Ideen und die tatkräftige Unterstützung der Publikationen.

Bastian Seubert und Prof. Dr. Achim Krüger für die Durchführung der Tierversuche.

Dr. Nathalie Beaufort, für Ihre fachlichen Tipps und die guten Ratschläge.

Dr. Virginia Egea und Dr. Christian Ries von der Klinischen Chemie der LMU, für die Möglichkeit Invasions-Assays und Zymogramme an Ihrem Institut zu erlernen.

Sonja Schäfer, die mich so herzlich im Labor begrüßt hat. Außerdem danke für deine Vorarbeiten.

Sabine Creutzburg, für die Hilfe bei Klonierungen, Aufreinigungen und für alles andere.

Anke Bengel, danke für die Zellkultur-Tipps und deine gute Laune.

Daniel Utschneider, für viel Kaffee, deine Motivation und die Gaudi.

Vielen Dank auch an alle anderen Mitarbeiter der Klinischen Forschergruppe der Frauenklinik, Klinikum rechts der Isar, für jegliche Hilfe und die schöne Zeit!

Der TUM für das Stipendium „Chancengleichheit für Frauen in Forschung und Lehre“, ohne das die Finanzierung meiner Arbeit am Schluss nicht möglich gewesen wäre.

Richard Huss, der immer für mich da ist, mich immer unterstützt, motiviert und mir auch fachlich eine große Hilfe ist!